The Texas Medical Center Library

DigitalCommons@TMC

The University of Texas MD Anderson Cancer Center UTHealth Graduate School of Biomedical Sciences Dissertations and Theses (Open Access)

The University of Texas MD Anderson Cancer Center UTHealth Graduate School of Biomedical Sciences

12-2014

TARGETING COX-2 AND RANK IN AGGRESSIVE BREAST CANCERS: INFLAMMATORY BREAST CANCER AND TRIPLE-NEGATIVE BREAST CANCER

Monica Elizabeth Reyes

Follow this and additional works at: https://digitalcommons.library.tmc.edu/utgsbs_dissertations

 Part of the Biology Commons, Cancer Biology Commons, Laboratory and Basic Science Research Commons, and the Translational Medical Research Commons

Recommended Citation

Reyes, Monica Elizabeth, "TARGETING COX-2 AND RANK IN AGGRESSIVE BREAST CANCERS: INFLAMMATORY BREAST CANCER AND TRIPLE-NEGATIVE BREAST CANCER" (2014). *The University of Texas MD Anderson Cancer Center UTHealth Graduate School of Biomedical Sciences Dissertations and Theses (Open Access)*. 544.
https://digitalcommons.library.tmc.edu/utgsbs_dissertations/544

This Dissertation (PhD) is brought to you for free and open access by the The University of Texas MD Anderson Cancer Center UTHealth Graduate School of Biomedical Sciences at DigitalCommons@TMC. It has been accepted for inclusion in The University of Texas MD Anderson Cancer Center UTHealth Graduate School of Biomedical Sciences Dissertations and Theses (Open Access) by an authorized administrator of DigitalCommons@TMC. For more information, please contact digitalcommons@library.tmc.edu.

TARGETING COX-2 AND RANK IN AGGRESSIVE BREAST CANCERS:

INFLAMMATORY BREAST CANCER AND TRIPLE-NEGATIVE BREAST CANCER

BY

MONICA ELIZABETH REYES, B.S.

APPROVED:

_____

Naoto T. Ueno, M.D. Ph.D. Supervisory Professor

_____

Oliver Bogler, Ph.D.

_____

Joya Chandra, Ph.D.

_____

James M. Reuben, Ph.D.

_____

Bedrich L. Eckhardt, Ph.D.

APPROVED:

_____

Dean, The University of Texas Graduate School of Biomedical Sciences at Houston

TARGETING COX-2 AND RANK IN AGGRESSIVE BREAST CANCERS: INFLAMMATORY BREAST CANCER AND TRIPLE-NEGATIVE BREAST CANCER

A

DISSERTATION

Presented to the Faculty of
The University of Texas
Health Science Center at Houston
Graduate School of Biomedical Sciences
in Partial Fulfillment

of the Requirements

for the Degree of

Doctor of Philosophy

by

Monica Elizabeth Reyes, B.S.
Houston, Texas

December, 2014

DEDICATION

This dissertation is dedicated to the memory of my mother Linda L. Linan, and to the IBC and TNBC patients and those that have lost their lives while fighting these aggressive diseases.

ACKNOWLEDGEMENTS

I am truly grateful to the support and guidance provided by the Graduate School Of Biomedical Sciences at The University of Texas at Houston, and to all of my friends, and colleagues that I had the privilege to work with during my graduate education.

To everyone who had helped to contribute to the work presented in this dissertation, I am thankful for your technical support and guidance.

I would like to thank my husband Jorge Reyes who has been supportive, understanding, and patient with me. Words cannot express how blessed I am to have him and our two children Hugo and Ainhoa in my life.

I would also like to thank my dad, sister, and brother for their continuous love and support. Thank you for having faith in me and providing encouragement during this journey.

I would like to extend a heartfelt thank you to Dr. Gayle Slaughter and Dr. Laurie Connor at the Baylor College of Medicine. Without their endless support, encouraging words and faith in my abilities, I may not have had the opportunity to embark on this path to pursue a career in the biomedical sciences.

Thank you to my supervisory committee members for their support and guidance throughout my graduate education. I would especially like to thank my mentor, Naoto T. Ueno, M.D., Ph.D. for his encouragement and support.

TARGETING COX-2 AND RANK IN AGGRESSIVE BREAST CANCERS: INFLAMMATORY BREAST CANCER AND TRIPLE-NEGATIVE BREAST CANCER

Monica Elizabeth Reyes, B.S.

Supervisory Professor: Naoto T. Ueno, M.D., Ph.D.

Inflammatory breast cancer (IBC) and triple-negative breast cancer (TNBC) are two highly aggressive breast cancer subtypes associated with a poor outcome. Despite sensitivity to current treatment, these breast cancers subtypes have a high recurrence rate and proclivity to metastasize early. The aggressiveness of IBC and TNBC have been linked to CSCs and epithelial to mesenchymal transition (EMT), which are critical features of breast cancer progression and metastasis. The clinical challenge faced in the treatment of IBC and TNBC is finding a treatment strategy to target the cancer stem-like (CSC) population to block metastasis. Cyclooxygenase-2 (COX-2) and receptor activator of nuclear factor kappa B ligand/receptor activator of nuclear factor kappa B (RANKL/RANK) pathway mediate an inflammatory response linked to breast cancer progression. However, the mechanism of how COX-2 and RANKL/RANK regulates the progression of IBC and TNBC, respectively, is unclear. Therefore, we investigated COX-2 and RANKL/RANK in IBC and TNBC. We hypothesize that targeted inhibition of COX-2 and RANK in IBC and TNBC, respectively, could eradicate CSCs to suppress tumor progression.

We observed elevated COX-2 levels in EGFR-positive IBC cells and a significant correlation between COX-2 and EGFR gene expression in IBC tumors. How

COX-2 linked to CSCs and regulates IBC progression is not well understood. We hypothesize COX-2 to be critical for IBC progression through regulation of the CSC population. Celecoxib, a selective COX-2 inhibitor, has anti-tumorigenic effects by reducing breast cancer cell migration and invasion. Celecoxib treatment in an IBC xenograft mouse model reversed EMT and downregulated expression of the embryonic stem cell regulator Nodal. We concluded COX-2 regulation of the CSCs through Nodal contributed to the progression of IBC and targeting the COX-2 has clinical relevance in blocking the progression of IBC.

RANKL/RANK pathway promotes the invasion, EMT and mammary epithelial stem cell population. We observed elevated expression in TNBC tumors and RANKL to be an independent prognostic factor for worse outcome in RANK-positive TNBC patients. How RANK promotes TNBC progression is not clear. We hypothesize that suppression of RANK inhibits TNBC progression through eradication of CSCs. We observed the suppression of RANK to reduce MDA-MB-231 cell migration and invasion, and mammosphere formation. Stem cell genes, implicated in inflammatory signaling, were down-regulated in MDA-MB-231 RANK shRNA cells.

Collectively, our findings suggest COX-2 and RANK to regulate of CSCs in IBC and TNBC potentially through mediating an inflammatory response. Future pre-clinical studies are needed to further interrogate COX-2 and RANK as novel therapeutic targets for IBC and TNBC.

TABLE OF CONTENTS

LIST OF ILLUSTRATIONS

LIST OF TABLES

LIST OF FIGURES

ABBREVIATIONS

IBC (Inflammatory breast cancer)

TNBC (triple-negative breast cancer)

EGFR (Epidermal-growth factor receptor)

EGF (Epidermal growth factor)

AR (Androgen receptor)

COX-1 (Cyclooxygenase-1)

COX-2 (Cyclooxygenase-2)

RANK (Receptor activator of nuclear factor kappa B)

RANKL (Receptor activator of nuclear factor kappa B ligand)

NFκB (Nuclear factor kappa B)

TNFα (Tumor necrosis factor α)

TGFβ (Transforming growth factor β)

BMP (bone morphogenetic protein)

MMP (matrix metalloproteinase)

ECM (extracellular matrix)

IL (interleukin)

CSCs (cancer stem-like cells)

CTCs (circulating tumor cells)

EMT (epithelial to mesenchymal transition)

ALDH1 (Aldefluor dehydrogenase 1)

qRT^{2}PCR (quantitative real-time reverse transcriptase polymerase chain reaction)

TMA (tissue microarray)

OD (optical density)

OS (overall survival)

pCR (pathological complete response)

BL1 (basal-like 1)

BL2 (basal-like 2)

IM (immunomodulatory)

M (mesenchymal)

MSL (mesenchymal stem-like)

LAR (luminal androgen receptor)

UNS (unstable)

DMEM (Dulbecco’s modified Eagle’s medium)

FBS (fetal bovine serum)

AA (antimycotic-antibiotic)

PG (prostaglandin)

PGE_2 (prostaglandin E_2)

$PGF_{2\alpha}$ (prostaglandin $F_{2\alpha}$)

15-PGDH (15-prostaglandin dehydrogenase)

HCL (hydrogen choride)

BSA (bovine serum albumin)

RIPA (radio-immunoprecipitation assay)

ALDH (aldehyde dehydrogenase)

DEAB (diethylaminobenzaldehyde)

MTT (3-4, 5-(dimethylthiazol-2-yl)-2,5-diphenyltetrazolium bromide)

GOI (gene of interest)

HKG (housekeeping gene)

C_T (threshold cycle)

AVG (average)

APPENDIX

CHAPTER 1: INTRODUCTION

1.1 BREAST CANCER

For 2014, it is predicted that about 235,000 new cases of breast cancer will be diagnosed, and about 40,000 breast cancer patients are expected to die from the disease (1). While we are making advancements in breast cancer treatments, we are still met with the challenge of finding treatments to inhibit metastasis, a leading cause of death in breast cancer patients. Breast cancer metastasis is a complex process preceded by the development of resistance to treatment or recurrence which is often associated with aggressive breast cancer subtypes. The multistage progression of breast cancer is as follows: 1) normal mammary cells, 2) atypical ductal hyperplasia, 3) ductal carcinoma in situ (DCIS) or lobular carcinoma in situ (LCIS), 4) invasive breast cancer, and 5) metastatic breast cancer (2, 3). While stage I and II breast cancer patients have a better prognosis, the locally advanced and metastatic breast cancers stage III and IV, have a poorer prognosis (4). The current treatment strategy for advanced stage breast cancers includes doxorubicin or taxane-based neoadjuvant chemotherapy followed by surgery and adjuvant chemotherapy paclitaxel and/or anthracycline. Patients may also receive radiotherapy and/or hormone receptor targeted therapy (5). Depending upon the molecular breast cancer subtype, luminal, basal-like, or normal, hormone receptor targeted therapy may be administered as part of the treatment regimen. Breast tumors associated with a particular intrinsic molecular subtype, luminal (non-HER2-positive), HER2-positive, basal-like, or triple-negative, express molecular markers, EGFR, ER and/or HER2, which can be targeted for treatment (6, 7). As a basal marker and molecular therapeutic target of interest for

aggressive breast cancers, the epidermal growth factor receptor (EGFR) is under intense investigation.

1.2 EPIDERMAL GROWTH FACTOR RECEPTOR

Since the first discovery of gene amplification of the epidermal growth factor receptor (EGFR) in breast cancer, significant progress has been made in our understanding of the EGFR signaling pathway and its role in breast cancer tumorigenesis and progression (8). The activation of the EGFR pathway may occur through different growth factor ligands that bind to the receptor to induce the downstream activation of key regulators of cell growth, proliferation, invasion, and metastasis. The PI3K/AKT and MAPK signaling pathways activated by EGFR promotes the progression of breast cancer (illustration 1.2) (9). There are several mechanisms by which EGFR-mediated tumorigenesis and metastasis can occur including, EGFR gene amplification, heterodimerization with HER2, and activating mutations, in breast cancer. Greater than 50% of breast tumors have EGFR amplification, and EGFR has been

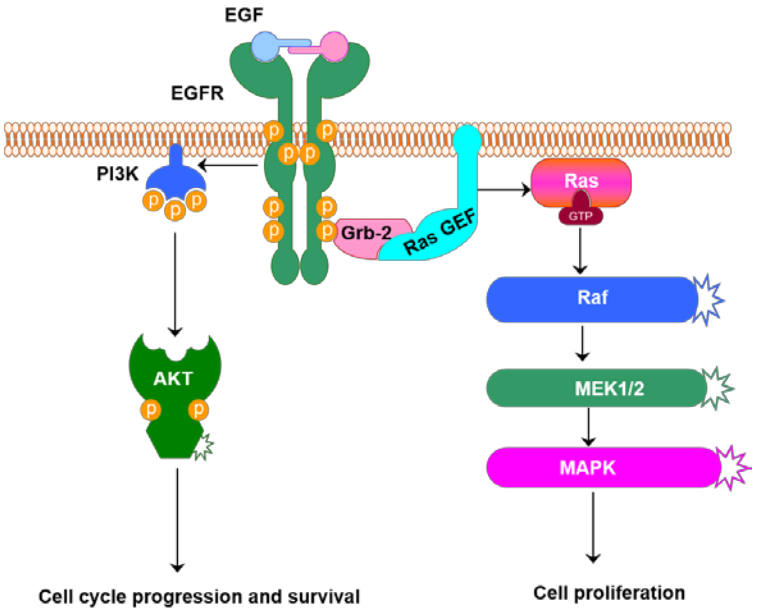

ILLUSTRATION 1.2 EPIDERMAL GROWTH FACTOR RECEPTOR SIGNALING

The process of EGF-EGFR and EGFR-EGFR interaction activates the PI3K/AKT and MAPK signaling pathways which promote malignant behavior critical to breast cancer progression.

shown to contribute to the invasiveness of breast cancers and the stem cell phenotype in breast cancer (10). In the basal-like breast cancer subtype, greater than 50% of tumors have an overexpression of EGFR (10). Highly aggressive triple-negative breast cancer (TNBC) and inflammatory breast cancer (IBC) subtypes, characterized by advanced and less-differentiated histological features associated with a poorer prognosis, have an overexpression of EGFR in approximately 30 to 50% of tumors (9, 11). Although it is unknown whether EGFR is a predictive marker for TNBC or IBC, EGFR expression levels are being utilized in treatment studies for patient selection (9), and EGFR-targeted therapies, lapatinib, erlotinib, and panitumumab, are currently being exploited in TNBC and IBC (12, 13).

1.3 TRIPLE-NEGATIVE BREAST CANCER

TNBC is an aggressive disease that is commonly diagnosed in younger women between the ages of 30-40 years, and has a high tendency to develop resistance to standard chemotherapy and metastasize (14). TNBC makes up about 30% of all breast cancers diagnosed, and about 40% of the basal-like subtype. Based on the intrinsic gene expression profile described by Bertucci F.*et al.*, approximately 80% of TNBC tumors are considered to be basal tumors (15). Both TNBC and basal tumors are described as having genetic mutations in DNA repair proteins such as, *P53*, and *BRCA1*, and amplification of oncogenes, *c-myc*, and *EGFR* (16). Although there is an overlap between TNBC and basal tumors in gene expression profiles, there is controversy surrounding the concept that all TNBC tumors are basal tumors. Histoclinical and molecular differences were detected between basal and non-basal TNBCs but not between TNBC and non-TNBC basal tumors, which implies TNBC

tumors to have a higher degree of heterogeneity than basal tumors. In a gene expression profiling study conducted by Lehmann B.D. *et al*, it was observed that TNBC can be classified based on transcriptional profiles described in the TNBC subtypes: basal-like 1 (BL1), basal-like 2 (BL2), immunomodulatory (IM), mesenchymal (M), mesenchymal stem-like (MSL), luminal androgen receptor (LAR), and unstable (UNS) (17). Masuda H*. et al.* predicted the BL1 and MSL TNBC subtypes to be the predominant subtypes in IBC because of the highly aggressive gene expression profiles inclusive of increased cell proliferative markers (i.e. Ki67), and EMT markers (17). Not only did both studies confirm the heterogeneity of TNBC but they also confirmed gene expression linked with an inflammatory response. Indeed, a signature of transforming growth factor β (TGFβ) activation was identified in the M and MSL subtypes, while the expression of growth factor signaling molecules including EGFR was up-regulated in the BL2 and MSL subtypes (12). These findings confirm the TNBC subtype to be enriched with an inflammatory and metastatic gene expression profiles which includes BMP2 and ALDH1 mesenchymal stem cell markers. (12).

Metastasis occurs in a higher proportion of TNBC patients than ER+/HER2+ breast cancer patients, at approximately 33% and 20%, respectively (18). Unlike luminal and HER2-positive breast cancers, which express ER and HER2, TNBC lacks clinically-validated, markers and targeted therapeutics. Depending upon tumor stage, size, grade, and the presence of invasive disease at diagnosis, TNBC patients may receive a treatment regimen including neoadjuvant chemotherapy, surgery, and adjuvant chemotherapy and radiation therapy (4). Initially, TNBC tumors are sensitive to chemotherapy and radiation; however, they eventually develop resistance to treatment resulting in locoregional or distant recurrence.

Patients with EGFR-positive TNBC are associated with a poor response to chemotherapy alone (19). To address this issue, there have been a number of studies that investigated a combination approach of targeting EGFR with systemic therapy to delay TNBC progression (20). In a clinical phase II study for patients with late-stage metastatic TNBC treated with cetuximab alone or in combination with carboplatin resulted in a higher response rate in those that received combination treatment. Regardless of this difference, a majority of patients had activated EGFR pathway following treatment suggesting that either cetuximab was not effective or the EGFR pathway is activated, by another pathway independently of its ligand in these tumors (21, 22). In a phase II clinical study of panitumumab, a fully humanized EGFR-specific monoclonal antibody, with anthracycline and taxane-based chemotherapy in TNBC, a higher response rate and longer progression-free survival was observed (23). Despite the findings that EGFR-targeted therapy with systemic therapy maybe a more beneficial therapeutic strategy for TNBC patients, we do not have a clear understanding of the progression of TNBC. It is likely that breast tumors that do not respond to EGFR-targeted therapy may benefit from other targeted therapy. In light of the recent discovery that TNBC heterogeneity can be classified based on molecularly defined subtypes, it is predicted that TNBC tumors belonging to one subtype may be more responsive to a particular therapy over another (12). For instance, TNBC expressing mutated BRCA1 or p53 appear to have increased sensitivity to PARP inhibitors, including those with elevated immune signaling pathways (12). Thus, there are several clinically-relevant and targetable pathways in certain types of TNBC, which may help to block progression of the disease and improve survival in TNBC patients.

1.4 INFLAMMATORY BREAST CANCER (IBC)

Inflammatory breast cancer (IBC) is an aggressive breast cancer, which makes up approximately 1-5% of all breast cancers diagnosed in the U.S. It is one of the deadliest breast cancers, and comprises approximately 8-10% of total breast cancer mortality rate in the United States (24-26). Despite the fact that IBC is diagnosed as being a locally advanced and highly invasive breast cancer with inflammatory-like symptoms including erythema and edema, a molecular mechanism of a physiologic inflammatory response has not yet been identified in IBC. The clinical manifestations presented in IBC patients include: erythema, edema, *peau d' orange*, and breast swelling with pain or tenderness (27). In addition, IBC patients may or may not present with a palpable mass (28). A majority of IBC patients have lymph node metastasis and 30% have distant metastasis at the time of diagnosis (28). Another clinical manifestation presented in IBC patients is dermal lymphatic tumor emboli, which is identified by a skin-punch biopsy (29). The current treatment strategy for IBC is a multimodality approach, which includes pre-operative standard chemotherapy and radiation therapy, surgery and adjuvant therapy, inclusive of hormone-targeted therapy (4). Treatment with adjuvant or neoadjuvant hormone receptor therapy, such as trastuzumab or tamoxifen, is provided to patients with IBC tumors that express HER2 or ER, respectively. Although some IBC tumors respond to current treatment, there is the dilemma of local and distant recurrence, which needs to be addressed by investigating molecular targeted therapies (30).

As represented in about 30% of IBC, the overexpression of EGFR is associated with high risk of recurrence and low 5-year overall survival (9, 31). The use of EGFR

inhibitors has been explored in clinical trials as potential therapeutic strategies for IBC (9). Lapatinib, an EGFR/HER2 dual-kinase inhibitor, was shown to improve clinical response in a phase II clinical trial in combination with paclitaxel in IBC patients (29, 32). On the otherhand, with about 30-40% of IBC tumors being triple-negative, the dual-kinase inhibition of EGFR and HER2 is not likely to be a suitable approach for all IBC cases. In fact, one study revealed a HER2-dependency for lapatinib in metastatic breast cancer (17, 33). As a consequence of these findings, selective EGFR inhibitors, such as erlotinib, have become a major focus for the clinical treatment of IBC. The pre-clinical studies of selective EGFR inhibitor erlotinib demonstrated suppression of IBC tumorigenicity and metastasis, but in a clinical trial erlotinib treatment had a low impact on the outcome of advanced breast cancer patients (9, 34). As a result of the confounding results for HER2 and EGFR-targeted therapies presented in pre-clinical and clinical-based studies, there is still a need to define molecular drivers of IBC progression and metastasis.

1.5 EPITHELIAL TO MESENCHYMAL TRANSITION

A cellular process often associated with breast cancer 'aggressiveness' is epithelial to mesenchymal transition (EMT). EMT is a reversible process that takes place during embryonic development in which cells acquire specific molecular and cellular features to facilitate their transition between epithelial and mesenchymal phases (35). Following EMT, cells are endowed with mesenchymal properties and a migratory phenotype involving the loss of cell-to-cell and cell-matrix adhesion with a gain in proteolytic activity. In addition to the loss of cell adhesive properties, there is a

remodeling of the cytoskeleton during cellular movement, a critical event for gastrulation during embryonic development (36).

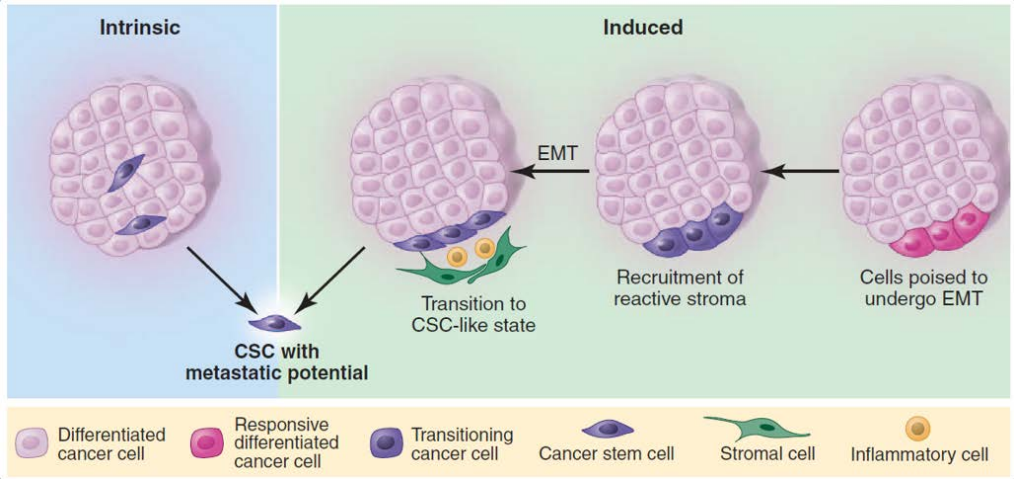

ILLUSTRATION 1.5 THE INTRINSIC AND EMT-INDUCED CSC WITH METASTATIC POTENTIAL

Cancer stem cells may be intrinsic or induced by extrinsic components, such as reactive stromal cells. In the case of an induced phenotype, epithelial to mesenchymal transition (EMT) enables the cells to transition to a CSC-like phenotype and acquire metastatic potential. From 'A Perspective on Cancer Cell Metastasis'. Christine L. Chaffer and Robert A. Weinberg. Science 25 March 2011:331 (6024), 1559-1564. [DOI:10.1126/science.1203543. Reprinted with permission from AAAS.

Although EMT is a normal process which supports embryonic development, and tissue repair, EMT can aberrantly occur in cancer cells in adult breast tissue (35). It is proposed that EMT contributes to cancer based on the concordance between the mesenchymal phenotype and the characteristics required for cancer cell metastasis. Breast cancer cells undergo molecular and cellular changes during EMT that enhance cell migratory and invasive capacity, contributing to a metastatic phenotype (35). Remarkably, EMT observed in both carcinogenesis and embryonic development is mediated by similar signaling pathways (36). EMT cellular changes are orchestrated by the release of secreted signals, such as TGF-β and WNTs, from stromal tissues which act on nearby epithelial cells (37). These signals mediate the upregulation of

mesenchymal markers, fibronectin and vimentin, N-cadherin, and transcription factors, SNAIL, TWIST, SLUG, and ZEB1, in tumor cells. Mesenchymal transcription factors suppress the epithelial phenotype and cell-to-cell adhesion through the downregulation of epithelial protein E-cadherin (38). The EMT-induced upregulation of mesenchymal markers and downregulation of E-cadherin allows cells to acquire an invasive phenotype demonstrated in an *in vitro* 2D culture and three-dimensional (3D) basement membrane extract (BME)/Matrigel assay (39) . In addition to the acquisition of an invasive phenotype, there is evidence that breast cancer cells, which undergo EMT, are endowed with stem cell characteristics (40). EMT can serve as a prerequisite for the acquisition of CSC-like traits within a cancer cell subpopulation, resulting in an increased metastatic potential of these subpopulation of cancer cells (illustration 1.5). It is this subpopulation of cancer cells that must be targeted to block metastasis.

1.6 CANCER STEM-LIKE CELLS

Cancer stem-like cells (CSCs) are characterized as a subpopulation of cancer cells endowed with properties similar to that of normal stem cells such as the ability to self-renew, migrate, invade, evade apoptosis, and give rise to a heterogeneous cell population which drives recurrence and metastasis (41). Studies imply a role for CSCs in the resistance to therapy and progression of breast cancer, but how CSCs contribute to these events is not entirely clear (42). The ability to self-renew is a critical feature of CSCs and normal stem cells (illustration 1.6) and can be partially demonstrated by an *in vitro* mammosphere assay in which clusters of breast cancer stem cells can proliferate and survive under non-adherent non-differentiating culture conditions (43). In addition to the mammosphere assay as a surrogate assay for studying the CSC

population, several stem cell marker studies have been conducted to try to identify and enrich for CSCs in breast cancer (44-47). The CD44+/CD24- cell population was identified as a CSC population that promotes metastasis of breast cancer (44). It is well-established that the basal-like subtype of breast cancers have derived or have acquired stem cell-like properties during transformation (48). Cancer stem cells originating from the basal lineage express cell surface molecules such as the hyaluronan receptor CD44 and have downregulated heat stable antigen CD24. The expression of CD44 has been linked to the epithelial-to-mesenchymal transition (EMT) phenotype by which ectopic expression of CD44 in normal human mammary cells can facilitate invasion, metastasis, and drug resistance (49). From a biological perspective, a single-cell isolation from the cell lineage lin-/CD24-/CD44+ breast cancer stem cell population can generate new tumors in immunocompromised mice, supporting a tumorigenic function of the CD44+CD24- subpopulation (13). Although the CD44 and CD24 markers may serve as a positive

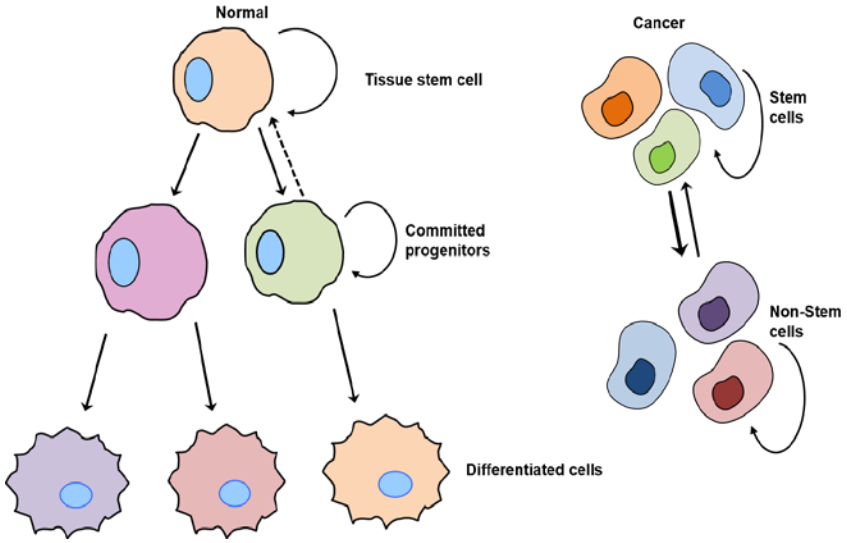

ILLUSTRATION 1.6 THE DIFFERENTIATION OF NORMAL AND CANCER STEM CELLS

In normal tissues, stem cells self-renew and give rise to committed progenitor cells which eventually differentiate. Progenitor cells have the capability to dedifferentiate under the appropriate conditions. In opposition to normal stem cells, cancer stem cells have an enhanced ability to transdifferentiate from the non-stem cell to stem cell phenotype.

indicator of stem-like characteristics in some breast tumors, CD44 and CD24 may not be expressed in all breast tumors (42).

In addition to the CD44 and CD24 markers, Aldefluor dehydrogenase 1 (ALDH1) is a putative stem cell marker associated with poorly differentiated basal-like breast cancers and resistance to therapy (42). As an enzyme that oxidizes intracellular aldehydes, it is thought that the activity of ALDH1 may play a role in the early differentiation of stem cells (13). The expression of ALDH1 was found to be upregulated in several types of carcinomas including malignant breast tissue (13, 50). It was also noted as a predictor for metastasis in IBC patients (42). Recently, it was found that a rare subpopulation of cells within the CSC population, termed side population or SP cells, have the ability to export a fluorescent dye Hoescht 33342 (46). Cells with a SP phenotype also have stem cell like characteristics including mammosphere formation capability, and the ability to initiate tumor formation in an *in vivo* mouse model. As one particular signaling pathway that promotes breast cancer progression, the inhibition of the PI3K/mTOR pathway led to a reduction in the SP cells. Another CSC marker identified as a potential marker for breast cancer stem cells is the ganglioside GD2 marker. Higher expression of GD2 level was observed in the more aggressive basal-like breast cancer cells, which included several TNBC cell lines. The GD2+ cell population in breast cancer cells demonstrated a CSC phenotype compared with GD2- cell population (47). As poorly differentiated breast cancers, IBC and TNBC are enriched with CSCs potentially driven by clinically-relevant molecular targets. As new evidence emerges supporting the concept of CSCs in the progression of breast cancer, there is growing interest in the tumor microenvironment and inflammatory signaling pathways and how they regulate breast CSCs.

1.7 CYCLOOXYGENASE-2 (COX-2)

Inflammation plays a critical role in the progression of breast cancer; however, the mechanisms are not clearly defined. There is evidence that inflammatory breast cancer is associated with inflammatory-like symptoms and activation of inflammatory response pathways (51). There are several prospective targets in IBC linked with inflammation. As an inflammatory response molecule and transcription factor, NF-kappa B induces the expression of inflammatory response genes which can facilitate breast tumor progression, including the cyclooxygenase-2 (COX-2) gene (52). Activation of NF-kappa B is elevated in the basal-like breast cancer subtype which includes the EGFR-overexpressing and ER-negative breast cancers (52). In an investigation of inflammatory response genes in IBC, one study found that about 60% of NF-kappa B-related genes were up-regulated in IBC tumors compared with non-IBC tumors (53). Interestingly, *PTGS2* (COX-2 gene) was among one of the genes upregulated by NF-kappa, which plays a critical role in cell proliferation, angiogenesis, and metastasis (53).

Unlike COX-1, which is constitutively expressed in all tissues to maintain normal tissue homeostasis, COX-2 expression is undetectable in most tissues with the exception of immune cells, vascular endothelium, and synovial fibroblasts.COX-2 is up-regulated under aberrant conditions within tissues displaying inflammation, such as in arthritic joints (54). Upon up-regulation of its expression and activation by inflammatory cytokines or induction via hypoxic conditions (55), COX-2 catalyzes the conversion of arachidonic acid to PGs, including its major products, PGE_2 and $PGF_{2\alpha}$ (54). In addition to its role in maintaining normal tissue homeostasis, PGE_2 and $PGF_{2\alpha}$ have a pro-tumorigenic effect in contrast to other PGs produced by COX-2 (13). In tumors, where there is a down-regulation of the enzyme 15-hydroxyprostaglandin dehydrogenase (15-PGDH) which normally degrades PGE_2 to a 15-keto metabolite, there is an accumulation of the active PGE_2 which leads to a pro-tumorigenic effect (13). PGE_2 contributes to tumor progression through binding to the EP4 receptor and the subsequent transactivation of EGFR through the Arrestin/Src complex, leading to

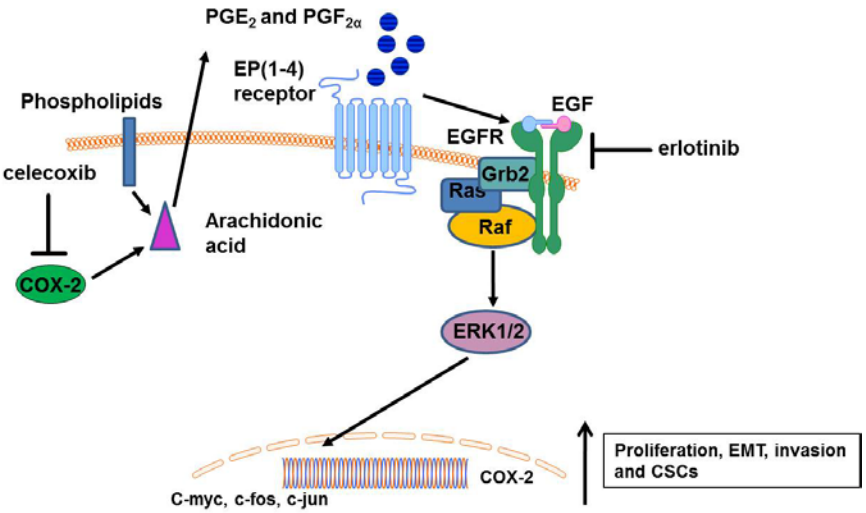

ILLUSTRATION 1.7 CROSS-TALK BETWEEN EGFR AND COX-2

Stimulation of the EGFR pathway via PGs can activate the translocation of ERK1/2 to the nucleus where expressions of its target genes, including PTGS2, are up-regulated. Erlotinib or celecoxib can block the overproduction of COX-2 metabolites, PGE_2 and $PGF_{2\alpha}$, and thereby, inhibit EGFR/COX-2-mediated cell proliferation, EMT, invasion and CSC phenotype.

activation of the PI3K/AKT pathway. In addition, activation of the MAPK/ERK1/2 pathway can occur as a result of PG-transactivation of the EGFR signaling cascade (13). Cross-talk between EGFR and COX-2 leads to an overstimulation in cell proliferation, and promotes EMT, invasion and CSC phenotype in breast cancer cells (illustration 1.7). The link between PGs and pro-tumorigenic effects revealed COX-2 as a prospective target for the treatment of inflammatory-associated conditions.

In early studies, COX-2 inhibitors and non-steroidal anti-inflammatory drugs (NSAIDs) were efficacious in the treatment of rheumatoid arthritis through inhibition of pain and inflammation. However, the use of NSAIDs was associated with gastrointestinal and cardiovascular side effects (56). To minimize the side effects associated with pan-COX inhibition, selective COX-2 inhibitors, celecoxib and rofecoxib, were synthesized. These drugs were designed specifically to block the enzymatic activity of COX-2 by binding to a site that is accessible in COX-2 but not COX-1 in order to suppress pain and inflammation while minimizing side effects (54). In patients with familial adenomatous polyposis (FAP), the use of the first FDA-approved selective COX-2 inhibitor, celecoxib, reduced the occurrence of sporadic colorectal adenomas (57). Although treatment with celecoxib in arthritis and colorectal cancer has been successful, the therapeutic efficacy of celecoxib in breast cancer remains to be seen.

Highly invasive and advanced breast cancers including IBC overexpress COX-2 (58). High COX-2 expression in breast cancer prompted investigation of the correlation between COX-2 expression and the CSC phenotype of breast cancer (58). There is evidence that suggests that COX-2 can regulate the CSC phenotype of breast cancer cells, however the mechanism remains unknown (59). The overexpression of COX-2 in

a breast cancer cell line or its transient suppression in a TNBC cell line model showed that COX-2 can regulate the EMT phenotype including the expression of genes important for motility, invasion, and metastasis (60). COX-2 can mediate the expression of MMP-2, a molecule critical for cell motility and invasion, but also those critical for tumor immunosuppression such as IL-10 (61, 62). It was recently found that the cytokine IL-17 can induce COX-2/PG signaling in cancer cells to indirectly regulate tumor-associated macrophages (TAMs) to modulate the microenvironment in favor of an immunosuppressive tumor microenvironment (63). Induction of the COX-2/PG signaling pathway, via cytokine stimulation, contributes to the progression of breast cancer by up regulating the aforementioned PI3K/AKT, MAPK, and NFKB downstream targets. Studies using celecoxib revealed a role for COX-2 in the tumorigenicity of IBC cells and regulation of breast cancer stem cells (64). By targeting the COX-2 inflammatory pathway, IBC metastasis could be inhibited through the suppression of inflammatory molecules which may regulate the stem cell phenotype, leading to a novel treatment strategy for IBC patients (34, 42).

1.8 NODAL A STEM CELL REGULATOR AND ITS ROLE IN BREAST CANCER

It is thought that cancer stem cells may arise as a result of the uncontrolled expression of molecules that control stem cell-fate during embryogenesis. These embryonic stem cell regulators, which are down-regulated in adult tissues, are aberrantly re-expressed in tumors.(65). Nodal, an embryonic morphogen and regulator of normal mammary gland development and stem cells, is down-regulated in adult tissues but re-expressed in malignant breast tumors (65, 66). During embryogenesis, the function of Nodal is to direct meso-endoderm formation and the specification of the left-right axis in germ layer formation and patterning (67). Nodal is a ligand member of the TGFβ superfamily. The canonical signaling of Nodal activates the SMAD2/3/4 signaling pathway through binding to an upstream receptor complex CRIPTO/EGF-CFC/Activin-like type I and II

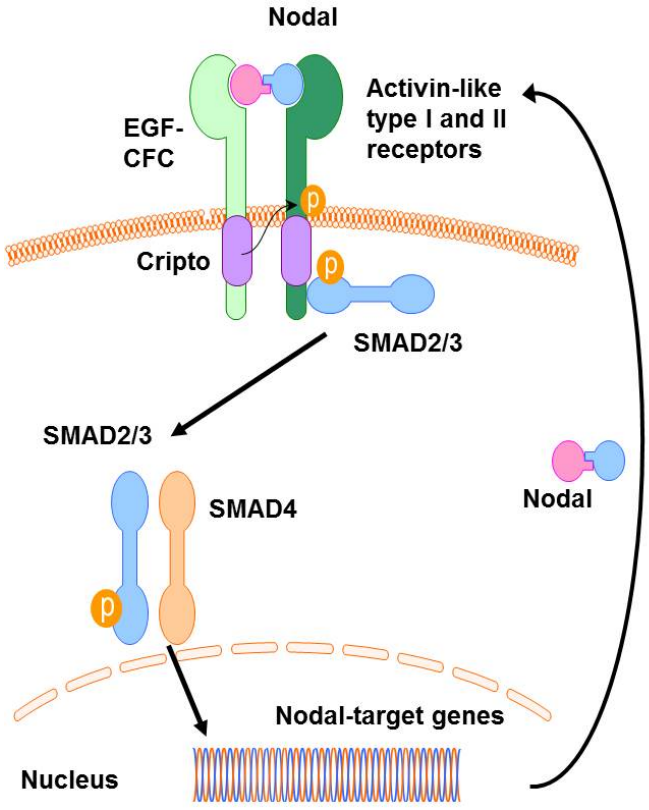

ILLUSTRATION 1.8 NODAL SIGNALING IN BREAST CANCER CELLS

As a member of the TGFβ superfamily, Nodal binds to the heterodimer ALK type I and II receptor complex activating SMAD2/3 transcription factors which complex with SMAD4 and translocates to the nucleus to induce Nodal gene transcription. In the absence of antagonist Lefty, breast cancer cells have an up-regulated positive feedback loop for Nodal expression.

receptors. Upon Nodal binding, SMAD2 is phosphorylated and activated to form a complex with SMAD3/4. The SMAD2/3/4 complex translocates to the nucleus where it binds with transcription factors, foxh1, Mixer, or P53 to activate the transcription of ld1, Nodal, and its inhibitor lefty1/2 (67). The absence of the Nodal antagonist lefty1/2 can induce a positive feedback mechanism for the overexpression of Nodal in breast tumor cells (illustration 1.8).

Nodal signaling in breast cancer highly complex due to post-transcriptional and post-translational modifications, and potential interactions with other TGFB ligands, which can all regulate Nodal signaling (68). In hypoxia-induced breast cancer progression, Nodal expression in breast cancer cells facilitates angiogenesis and metastasis (69). Hypoxic or low oxygen conditions can promote the expression of Nodal and activation of pro-angiogenic pathways critical to breast tumor progression (69). In breast cancer cells, the HIF1-4 transcription factors are induced under low-oxygen conditions. Through Notch1 stabilization, HIF1 transcription factors are able to bind to the NDE promoter site on the Nodal gene to activate the transcription of Nodal. However, the interaction between HIF1 and Notch in transcriptional activation of Nodal has not been investigated in breast cancer cells (69).

Another study observed Nodal to promote tumorigenesis and metastasis of breast cancer cells via EMT linked to the activation of the MAPK signaling pathway (66). This finding suggested that MAPK activation of Nodal via phosphorylation of the linker region in SMAD2, promotes SMAD2 activation and subsequent binding to SMAD3/4 and translocation to the nucleus for transcription of Nodal. Activation of the Nodal signaling pathway can up-regulate mesenchymal markers, down-regulate

epithelial markers, and increase cell motility and invasion, which are all prerequisites of breast cancer progression and metastasis (66).

1.9 RECEPTOR ACTIVATOR OF NUCLEAR FACTOR KAPPA B

It is known that about 70% of advanced breast cancer patients develop metastases and between 65-75% of patients with metastatic breast cancer develop bone metastases (70, 71). The occurrence of bone metastasis disrupts normal bone remodeling, a tightly regulated balance between osteolytic (bone resorption) and osteoblastic (bone formation) activity, causing skeletal-related events and pain (71). Uncontrolled regulation of receptor activator of nuclear factor kappa B (RANK), a key regulator of normal bone remodeling and mammary gland development, promotes metastasis.

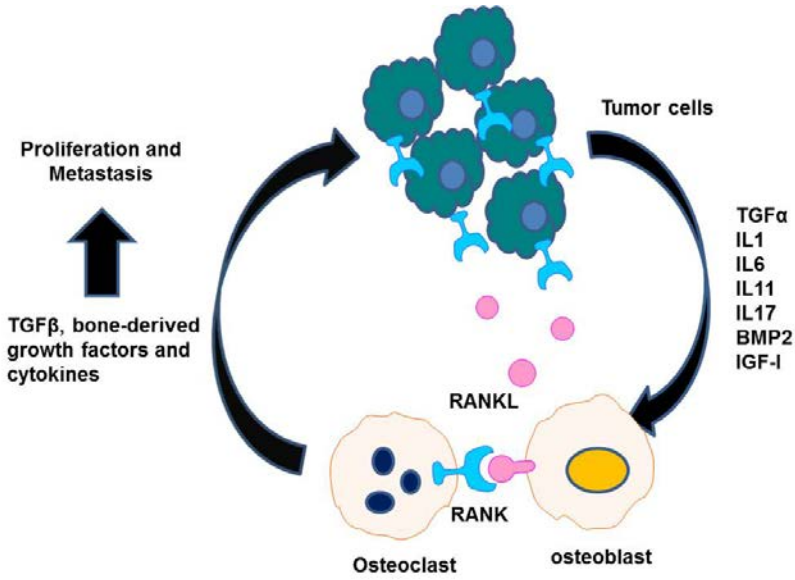

ILLUSTRATION 1.9 RANKL/RANK AND THE 'VICIOUS' CYCLE

Tumor cells may release cytokines and growth factors that act on osteoblasts. The osteoblasts produce RANKL which bind to RANK expressed at the surface of osteoclasts and tumor cells. Tumor cell proliferation occurs in response to growth factors released by osteoclasts.

RANK and its ligand the receptor activator of nuclear factor kappa B ligand (RANKL) play a major role in osteoclast differentiation, activation and survival. RANKL/RANK regulates lymphogenesis, and mammary gland development. RANKL binds to its cognate

receptor RANK expressed on mammary epithelial cells. Normal mammary gland development of lobulo-alveolar structures and lactation morphogenesis are dependent upon the function of RANKL/RANK signaling and disruption of this signaling either through deletion of RANKL or RANK can lead to underdeveloped mammary glands with an inability to secrete milk (72). RANKL expression can be regulated by several hormones including parathyroid hormone-related protein (PTHrP) and progesterone. During breast cancer progression, it has been demonstrated that RANK-positive cancer cells have a higher propensity to metastasize to the bone, an environment enriched with pro-tumorigenic RANKL, amongst other growth factors and cytokines that can facilitate the formation of metastasis (71). A model that best describes the tumor- bone microenvironment interaction is the 'vicious cycle' model. During tumor-bone interaction, tumor cells overstimulate the production of RANKL in osteoblasts through secreting growth factors and hormones (i.e. PTHrP, and interleukins). The mechanism of action for RANKL/RANK is initiated as RANKL binds to RANK expressed on the surface of osteoclasts and breast tumor cells. RANKL-induced osteolytic activity promotes the proliferation and invasion of tumor cells through the release of tumor-promoting growth factors, cytokines, and bone matrix components (illustration 1.9) (73-75).

Tumor-promoting factors, which promote proliferation and invasion, include matrix metalloproteinases (MMPs), bone morphogenetic proteins (BMPs), and tumor growth factor β (TGFβ) (71, 74, 76). MMP promoters contain a *cis* element which can be bound by the NFκB transcription factor, a downstream molecule activated by RANKL/RANK signaling (77). The matrix metalloproteinase 1 (MMP1) activity induces bone matrix degradation as a consequence of bone metastases (78). Under normal

conditions, BMPs play a role in osteoblast differentiation and positively regulate bone formation. However, as a result of tumor cells invading the bone microenvironment, BMPs are able to stimulate the production of pro-osteolytic and osteoblastic factors as part of the 'vicious cycle' (76). In fact, activated BMPs have also been linked with cancer stem cells based upon their regulation of EMT in breast cancer cells (79). As a result of RANKL/RANK signaling, another growth factor secreted by osteoclasts and tumor cells to stimulate tumor proliferation is TGFβ. TGFβ released by activated osteoclasts can directly bind to its receptor expressed on the surface of tumor cells and increase production of PTHrP which can act on osteoblasts or stromal cells in surrounding visceral tissue to stimulate RANKL production and release. This mechanism of action generates a positive-feedback loop that leads to further cancer cell growth in bone (80).

The aggressive phenotype promoted by RANKL is dependent upon RANK expression in tumor cells. Indeed, RANK-expressing breast cancer cells were observed to undergo EMT (81). Knockdown of RANK expression in an *in vivo* mouse model had reduced the tumorigenesis and self-renewal ability of breast cancer cells indicating a potential role for RANK signaling in the regulation of CSCs (82). In line with the potential role of RANK in regulating the tumorigenesis and CSC phenotype in breast cancer, another study demonstrated that overexpression of RANK increased the CD44+CD24- subpopulation and expression of stem cell markers, SOX2, NANOG and OCT4 (81).

In maintaining the physiologic balance between RANKL and RANK in the bone matrix, osteoprotegerin (OPG), expressed by osteoblasts, functions as a soluble decoy receptor that binds to RANKL, blocking its ability to bind and activate the RANK

pathway. In breast tumor cells, there is suppression of OPG expression, resulting in an uncontrolled positive feedback loop for RANKL production and activation of the RANK pathway (74). As a potential therapeutic strategy to block overstimulated osteolytic activity and breast tumor progression, a soluble recombinant form of OPG, OPG-Fc, has been studied in breast cancer. OPG-Fc has demonstrated to reduce bone lytic disease in breast cancer patients (83). However, due to the potential health risks associated with the use of OPG-Fc in humans and its short half-life, a fully-humanized antibody, denosumab, was investigated as a potential treatment for targeting RANKL. The use of denosumab for osteoporosis treatment has shown efficacy in a phase II clinical trial of denosumab treatment in post-menopausal women (84). The proven efficacy of denosumab in reducing osteoporosis led to clinical investigations of denosumab as a potential therapy for metastatic breast cancer patients. The use of denosumab demonstrated a reduction in SREs and pain-associated with metastatic breast cancer in patients (76). More studies are needed to elucidate the mechanism of RANK in the metastatic phenotype of TNBC cells and whether targeting the stem cell population can inhibit the progression of TNBC.

1.10 STATEMENT OF PROBLEM

TNBC and IBC are considered to be the most aggressive and poorly characterized breast cancer subtypes. Their high rate of recurrence and metastasis, there is an urgent need to identify molecular targets that will help reduce IBC and TNBC metastasis and improve clinical outcome (9). There is emerging evidence linking CSCs with IBC and TNBC progression. However, it is unknown which molecular pathways can be therapeutically exploited to suppress the progression of TNBC and IBC.

1.11 HYPOTHESIS

We hypothesize that targeted inhibition of COX-2 and RANK in IBC and TNBC, respectively, could eradicate CSCs to suppress tumor progression. By targeting COX-2 and RANK, we can help to eliminate breast cancer metastasis, an inevitable and deadly outcome associated with these aggressive diseases. Our findings will advance our understanding of how inflammatory mediators, COX-2 and RANK, regulate the breast cancer progression and unveil novel potential for COX-2 and RANK as therapeutic targets.

CHAPTER 2: TARGETING THE RANK PATHWAY AS A NOVEL THERAPEUTIC APPROACH IN TNBC

2.1 INTRODUCTION

Triple-negative breast cancer (TNBC) accounts for approximately 25-30% of all breast cancers and is characterized as lacking ER, PR, and HER2 receptors. Although, TNBC patients are more likely to respond to neoadjuvant chemotherapy compared with non-TNBC patients, metastasis following treatment is more likely to occur in TNBC (85). It is thought that breast CSCs contribute to the development of resistance to standard therapy and subsequent metastasis (86). Studies demonstrated that the RANKL/RANK pathway can regulate the 'stemness' of breast cancer cells via EMT, a process linked to tumor initiation, progression, and metastasis (81, 82, 87), however, it is unclear whether targeted inhibition of the RANKL/RANK pathway could eradicate CSCs in TNBC. Since TNBC cells are enriched with stem-like features and demonstrate RANKL-stimulated invasion and metastasis, we hypothesized that suppressing RANK will eradicate CSCs in TNBC. We investigated RANK in TNBC as a potential prognostic marker and predictor for clinical outcome by using statistical methods to assess both RANKL and RANK expression in a TNBC patient cohort. In addition, we investigated the effects of RANK suppression in TNBC cell migration, invasion, and CSC phenotype.

2.2 MATERIALS AND METHODS

2.2.1 cDNA MICROARRAY ANALYSIS

We first performed a statistical analysis to compare the gene expression levels of RANK between three different patient cohorts derived from the MDACC cohort (n=57) of the GEO database: 1) ER+/HER2- (n= 22), 2) HER2+ (n= 17), and 3) ER-/HER2- (n=18; 17/18 negative for PR). The platform used in which samples were constructed on was the Affymetrix U133a GeneChip. Cases with normalized ESR1 mRNA expression (probe set 205225_at) were defined as ER-positive for ESR1 > 10.18, cases with HER2 (216836_s_at) were considered HER2 amplified for HER2 > 12.54, and cases with PgR (208305_at) > 2.907 were considered PR positive (17). The probe set for RANK mRNA (TNFRSF11A: 207037_at) was obtained from the 'gene card' website (http://www.genecards.org/). RANK mRNA expression levels were log2 transformed and normalized using MAS5 algorithm and the P-values were calculated using Wilcoxon test. $P > 0.05$ was considered to be statistically significant.

2.2.2 CELL LINES AND TISSUE CULTURE REAGENTS

Human TNBC and non-TNBC cell lines (Table 2.1) were screened for endogenous levels of RANK expression. MDA-MB-231, MDA-MB-468, BT20, BT474, KPL4 and MCF7 cell lines were maintained in DMEM/F12 Medium (catalog #12634-010; Life Technologies, Grand Island, NY) supplemented with 10% fetal bovine serum (FBS) (catalog #10438-026; Life Technologies, Grand Island, NY) and 1% antimycotic-antibiotic (AA) (catalog #15240-062; Life Technologies, Grand Island, NY), and SUM149, SUM159 and SUM190 cell lines were maintained in Ham's F12 Nutrient Mix (catalog #11765-054; Life Technologies, Grand Island, NY) supplemented with 5%

FBS, 1% AA, 5 µg/mL insulin (catalog #I9278; Sigma-Aldrich, St.Louis, MO), and 1 µg/mL hydrocortisone (catalog #H0888; Sigma-Aldrich, St. Louis, MO) in a humidified atmosphere containing 5% CO_2 at 37°C. SKBR3 cell line was maintained in McCoy's 5a (Modified) Medium (catalog #16600-082; Life Technologies, Grand Island, NY) supplemented with 10% FBS, and 1% AA. HCC70, HCC38, and HCC1954 cell lines were maintained in RPMI 1640 medium (catalog #11875-119; Life Technologies, Grand Island, NY) supplemented with 10% FBS and 1% AA.

Table 2.1 Human TNBC and non-TNBC cell lines

TNBC	Non-TNBC
MDA-MB-231	SUM190 (ER-/HER2+)
MDA-MB-468	KPL-4 (ER+/HER2+)
SUM159	SKBR3 (ER-/HER2+)
BT20	BT474 (ER+/HER2+)
HCC70	HCC1954 (ER-/HER2+)
HCC38	MCF7 (ER+/HER2-)
SUM149	

2.2.3 LENTIVIRAL-BASED EXPRESSION OF RANK SHRNA

To generate MDA-MB-231 cells with stable knockdown of RANK protein, we produced lentiviral particles from HEK293T cells transfected with the pGIPZ lentiviral plasmid expressing short-hairpin RNA (shRNA) against RANK (mature anti-sense 3'-TATCTTCTTCATTCCAGCT- 5'; mature sense 5'- ATAGAAGAAGTAAGGTCGA-3') or a non-silencing sequence (scrambled shRNA) (GE Healthcare, Dharmacon). HEK293T cells were co-transfected via Lipofectamine (Invitrogen) with lentiviral packaging vectors DR82, and VSV-G along with the target plasmid (pGIPZ-Scrambled shRNA or

pGIPZ-RANK shRNA). MDA-MB-231 cells were seeded at 5 x 10^4 cells/well into a 24-well plate 24h prior to infection with lentiviral infected medium. A 5-fold serial dilution (dilution factors of 5, 25, 125, 625, 3125, 15625) of viral particles diluted 1/10 in serum-free media were used to infect the 231 cells at 5 x 10^4 cells/well in a 24-well plate and 293T cells were infected in parallel as a control. At 6 hours post-infection, 1 mL of complete media was added per well. Cells were cultured for 48h prior to observing GFP expression seen by light microscope.

GFP-positive colonies were counted and the transducing unit per milliliter (TU/mL) or multiplicity of infection (MOI) was calculated using the following formula: (average number of GFP-positive colonies calculated for 4 wells) x (dilution factor) x 40. The lowest MOI was 0.17 for the 125-fold dilution factor. The MDA-MB-231 cells infected at the lowest MOI were treated with selection antibiotic puromycin (1 µg/mL) and expanded in culture. Following selection for 2 weeks in 1 ug/mL puromycin diluted in complete media, the MDA-MB-231 cells infected with pGIPZ-Scrambled shRNA, or RANK shRNA, were screened for RANK protein expression via flow cytometry analysis.

2.2.4 FLOW CYTOMETRY ANALYSIS

To analyze the level of RANK in MDA-MB-231 Scrambled shRNA and MDA-MB-231 RANK shRNA cells, we stained for the following: DAPI (cell viability), APC + IgG_1 (negative control), RANK (APC + N2-B10) (Table 2.2). MDA-MB-231 parental cells were stained as a control only.

Table 2.2 FACS samples	
Cell lines	**Samples**
MDA-MB-231 parental	**Unstained**
	DAPI
	DAPI + APC
	DAPI + APC + IgG_1 isotype
	DAPI + APC + N2-B10
MDA-MB-231 Scrambled shRNA	**Unstained**
	DAPI + APC + IgG_1 isotype
	DAPI + APC + N2-B10
MDA-MB-231 RANK shRNA	**DAPI + APC + IgG_1 isotype**
	DAPI + APC + N2-B10

Cells were blocked in FACS blocking buffer (3-5% goat serum + 0.005% sodium azide + PBS) for 20 minutes at 4°C with rotation then spun down at 4°C for 4 minutes at 4 x 10^3 rpm. Cells were re-suspended in FACS buffer (2% fetal bovine serum + 0.005% sodium azide + PBS) with primary RANK antibody (N2-B10) or purified mouse IgG_1 isotype antibody and incubated under the same conditions as in the blocking step. Cells were washed 2X with FACS buffer prior to incubation with the secondary antibody (APC) for 30 minutes. For the final wash step, cells were washed 2X with FACS buffer prior to re-suspension in 1 mL FACS buffer, and analyzed using Gallios flow cytometry instrument (MDACC Flow Cytometry Core Facility). Histograms were generated using FlowJo_V10 software (figure 1).

2.2.5 CELL MIGRATION AND INVASION ASSAYS

MDA-MB-231 scrambled shRNA and RANK shRNA cells were serum starved for 24 hours prior to stimulation with 25 ng/mL human soluble RANKL (product #R138; Leinco Technologies, Inc. St. Louis, MO) for 24 hours. For Boyden chamber trans-well migration assay (n=3), 1.5×10^5 cells in serum-free medium were layered in the top chamber of 24-well trans-well plates with serum-free media containing RANKL (25 ng/mL) in the lower chamber and incubated at 37°C for 6 hours. Cells in the top chamber (non-migrated) were removed, and cells in the bottom chamber (migrated) were fixed with 0.1% crystal violet/20% methanol solution. For the invasion assay (n=3), 1.5×10^5 cells were plated in serum-free medium in the upper chamber of a Boyden chamber coated with BD Matrigel Basement Membrane Matrix Growth Factor Reduced Phenol Red Free (catalog #356231; BD Biosciences) with serum-free media containing RANKL (25 ng/mL) in the lower chamber. Twenty-four hours later, non-invading cells were removed from the upper chamber, and the underside membranes were fixed and stained as above in the cell migration assay. Migrated and invaded cells were quantitated by dissolving stained cells in a solution of 4% sodium deoxycholate and performing colorimetric reading of optical density at 595 nm. Results were analyzed using unpaired Student's *t*-test with a $*P$ value < 0.05 considered significant.

2.2.6 MAMMOSPHERE ASSAY

MDA-MB-231 scrambled shRNA and RANK shRNA cells were plated into an ultra-low attachment 6-well plate at a density of 5×10^3 cells/well containing Mammocult Basal Medium (catalog #05621; STEMCELL Technologies, Inc.) supplemented with 1% Proliferation Supplement (catalog #5622; STEMCELL

Technologies, Inc.), 2 µg/mL heparin (catalog #07980; STEMCELL Technologies, Inc.), and 0.12 µg/mL hydrocortisone (catalog #07904; STEMCELL Technologies, Inc.). On day 5 following incubation, cells from primary mammospheres (P_0) were counted and re-plated for secondary mammosphere (P_1) formation. Under both primary and secondary mammosphere conditions, each group was tested in triplicate. Mammospheres were quantitated on day 5 by staining with MTT reagent (0.4 mg/mL) for 2 hours and enumerated using GelCount software (Oxford Optronix). Results were analyzed using unpaired Student's *t*-test with a $*P$ value < 0.05 considered statistically significant.

2.2.7 HUMAN STEM CELL RT^2 PCR ARRAY ANALYSIS

Using the human stem cell RT^2 PCR array (catalog #PAHS405Z; Qiagen) we analyzed the gene expression levels of several stem cell markers in MDA-MB-231 scrambled shRNA and RANK shRNA cells. We purified total RNA from each cell line using the RNeasy Mini prep kit (catalog #74104; Qiagen). The total RNA samples were reverse transcribed to cDNA using the RT^2 First-strand Kit (catalog #330401; Qiagen), followed by mixing of the synthesized cDNA with the RT^2 SYBR Green Mastermix (catalog #330513; Qiagen) then samples were aliquoted (25 µL/well) into the human stem cell PCR array 96-well assay plate. The 96-well assay plate included 84 wells containing primers specific for 84 genes of interest (GOI) and the remaining 12 wells were control wells including 5 wells for housekeeping genes, 3 wells for reverse-transcription controls, and 1 well for control DNA genomic contamination, and 3 wells for positive PCR controls (Table 2.3).

Table 2.3 Human stem cell PCR array genes

Gene of interest			Housekeeping gene
ABCG2	COL2A1	KAT2A	GAPDH
ACAN	COL9A1	KAT7	HRT1
ACTC1	CTNNA1	KAT8	RPLP0
ADAR	CXCL12	KRT15	HGDC
ALDH1A1	DHH	MME	RTC
ALDH2	DLL1	MSX1	RTC
ALPI	DLL3	MYC	RTC
APC	DTX1	MYOD1	PPC
ASCL2	DTX2	NCAM1	PPC
AXIN1	DVL1	NEUROG2	PPC
BGLAP	EP300	NOTCH1	
BMP1	FGF1	NOTCH2	
BMP2	FGF2	NUMB	
BMP3	FGF3	PARD6A	
BTRC	FGF4	PDX1	
CCNAD2	FGFR1	PPARD	
CCND1	FOXA2	PPARG	
CCND2	FRAT1	RB1	
CCNE1	FZD1	S100B	
CD3D	GDF2	SIGMAR1	
CD4	GDF3	SOX1	
CD44	GJA1	SOX2	
CD8A	GJB1	T	
CD8B	GJB2	TERT	
CDC42	HDAC2	TUBB3	
CDH1	HSPA9	WNT1	
CDH2	IGF1	ACTB	
CDK1	ISL1	B2M	
COL1A1	JAG1		

The 96-well plate reactions were generated using a real-time PCR cycler (Bio-Rad CFX 96 model) with cycling conditions compatible with the Bio-Rad CFX96 cycler (Table 2.4)

Table 2.4 Human stem cell RT^2 PCR cycle conditions		
Cycles	**Duration**	**Temperature**
1	10 minutes	95ºC
40	15 seconds	95ºC
	1 minute	60ºC

The results were analyzed using the C_T method available through the SABiosciences PCR data array analysis Web Portal. The C_T value for each reaction was determined as < 35 or > 35 in which the < 35 values were reported as negative. To normalize the C_T value for each gene of interest (GOI) to the average housekeeping genes the following formula was used: $C_T = C_T^{GOI} – C_T^{AVG\ HKG}$.

2.2.8 Correlative analysis of RANK, RANKL, and ALDH1 expression with clinical outcome in TNBC

We performed an analysis to correlate the expression of human RANK with overall survival and time to first metastases in TNBC patients. Core samples (n = 96) from formalin-fixed paraffin-embedded (FFPE) MDACC TNBC patient tumors were constructed on TMAs (88) and stained by immunohistochemistry (IHC) with anti-human RANK (N-1H8 or N2-B10; Amgen, Inc., Seattle, WA) and RANKL (M366; Amgen, Inc., Seattle, WA) monoclonal antibodies as described in (89), and interpreted and scored by pathologist D.B. blinded to clinical characteristics and outcome.

RANK and RANKL expression was quantitated based on the histoscore (H score) formula defined as the sum of intensity (0, 1, 2, 3) x percentage of intensity; (percentage of 0 intensity) * 0+ (percentage of 1 intensity) * 1 + (percentage of 2 intensity) * 2 + (percentage of 3 intensity) * 3. H scores range from 0-300 where

intensity of staining was defined as 0 = negative, 1 = weak, 2 = moderate, 3 = high, relative to RANK staining in tumor-associated macrophages as an internal control.

Using the median (RANK H score = 10) as the cut-off value, RANK IHC staining results were categorically defined as: high RANK (H score > or = 10) or low RANK (H score < 10), and clinicopathological parameters: age (median = 50 years), race, tumor size, lymph nodes, pathological stage (pStage), nuclear grade (NG), and lymphovascular invasion (LVI), were tabulated and compared between the high RANK and low RANK groups using the Fisher's exact test; $P < 0.05$ statistically significant. The Kaplan-Meier survival curve analysis was used to estimate the survival of each group: high RANK (n = 49) and low RANK (n= 47) and were compared using a log-rank test; $P < 0.05$ statistically significant. SPSS statistic software (version 20.00; IBM corporation, Armonk, NY) was used to estimate the association between each RANK group and 'Overall survival 'defined as from date of surgery to date of death or loss of follow-up and 'Time to first metastases' defined as from date of surgery to date of first metastases detected. The median follow-up time was 2025 days (range 346-5906).

TNBC patient tumors (n=91) were stratified as RANK positive (RANK >0; n=66) or RANK negative (RANK =0; n=25). A correlative analysis was performed for RANKL expression with clinicopathological parameters (appendix D) and statistically analyzed using fisher's exact test, *P*-value > 0.05 considered to be significant. Kaplan-Meier curves for OS and RFS was performed for both RANK positive and RANK negative cohorts, and a log-rank test was performed to determine the p-value. SPSS statistic software (version 20.00; IBM corporation, Armonk, NY) was used to estimate the association between RANKL > 0 and RANKL = 0 in both RANK cohorts.

IHC staining of ALDH1 was performed on proximal TMA sections of TNBC tumor specimens (MDACC Histology Core Facility) as described in (42) and interpreted and scored by pathologist S.K. blinded to clinical characteristics and outcome. ALDH1 scores were determined based on the average percentage of intensity in either tumor cells and/or stroma.

2.2.9 STATISTICAL ANALYSIS FOR CLINICAL AND NON-CLINICAL DATA

Patients with histologically defined TNBC were divided into two groups based on H scores: RANK positive (H score > 0) and RANK negative group (H score =0). Baseline patients' characteristics include age, race, menopausal status, pathological stage, nuclear grade, lymphovascular invasion, and estrogen receptor expression and they were tabulated. For the comparison of continuous variables, we used Wilcoxon rank sum test. Associations between two groups were assessed by using Fisher's exact test. Overall Survival (OS) was defined from the date of surgery to that of death and Recurrence Free Survival (RFS) was defined from the date of surgery to that of first local or distant metastasis or lost follow-up whichever comes earlier. Patients who died before having a recurrence event were censored at the date of death. The Kaplan-Meier survival curves were used to estimate the survival of each group and two groups were compared by using log-rank test. Chi-square test or Fisher's exact test was used to assess the correlation among categorical variables depending on their expected values. Multivariate Cox proportional hazard models were used to evaluate the association of covariates with survival. Covariates with p-value < 0.3 in univariate analysis were included in multivariate analysis.

A p-value < 0.05 was considered statistically significant. All statistical analyses were performed by STATA version 13 (STATA Corp, College Station, TX). This study was approved by the Internal Review Board at the University of Texas MD Anderson Cancer Center.

For cDNA microarray analysis, cases were normalized with MAS5 algorithm and RANK mRNA gene expression was log2 converted and the P-value was calculated by the wilcoxon test. For all other *in vitro* studies, student t-test was performed to determine the p-value. P-value > 0.05 considered significant.

For all other data, results were presented as mean ± SD except where otherwise stated. When two groups were compared, Student's *t*-test was used ($P < 0.05$ was considered significant).

2.3 RESULTS

2.3.1 RANK IS HIGHLY EXPRESSED IN HUMAN TNBC PRIMARY TUMORS

Since the study of RANK expression in breast tumors has resulted in discrepancies in RANK expression in breast tumors and its prognostic value, and has not yet been studied in TN breast tumors (90), we evaluated the clinical relevance of RANK expression in TNBC by first interrogating the expression of RANK and RANKL amongst TNBC patients. We analyzed the level of RANK mRNA expression in patient tumors from the MDACC IBC data set. ER-/HER2- (n=18) was compared with other breast cancer cohorts, ER+/HER2- (n=22) and HER2+ (n=17) by statistical analysis of patient tumor-derived RANK mRNA constructed on an Affymetrix U133a GeneChip array. We found the ER-/HER2- cohort to have a statistically significant higher level of RANK expression compared to the ER+/HER2- breast tumor cohort ($P = 0.034$) while there was not a statistically significant difference in RANK mRNA expression between ER+/HER2- and HER2+ cohorts (Figure 2.1). In addition, we looked at RANK mRNA expression in TNBC and non-TNBC primary tumors and observed RANK mRNA levels to be higher in the TNBC compared to non-TNBC tumors (Figure 2.2).

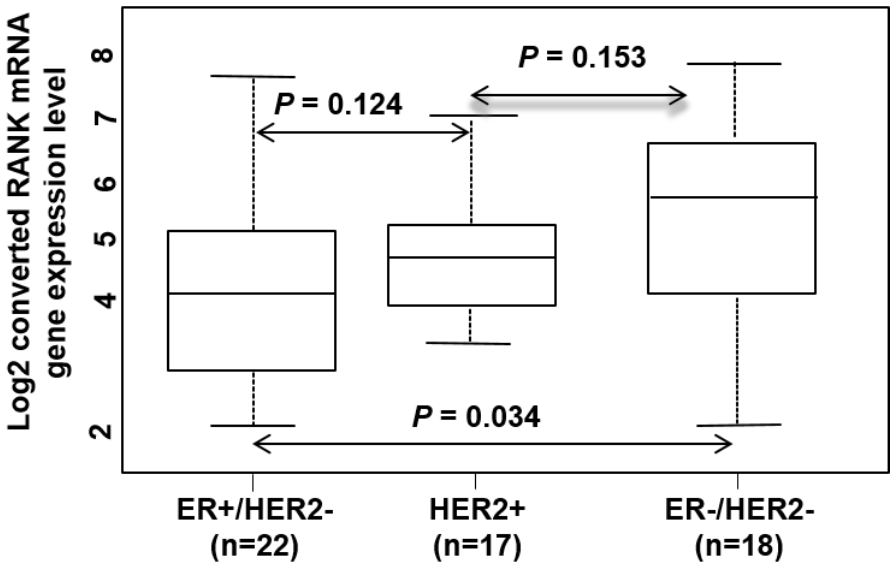

Figure 2.1 RANK mRNA expression is significantly higher in ER-/HER2- breast tumors than ER+/HER2- tumors. We analyzed RANK gene expression using an Affymetrix U133a GeneChip array containing mRNA from breast tumors taken from the following cohorts: ER-/HER2- (n= 18) cohort, HER2+ (n=17), and ER+/HER2- (n=22). Results were normalized with MAS5 algorithm and log2 transformed and p-values were calculated by Wilcoxon test (P-value = 0.034).

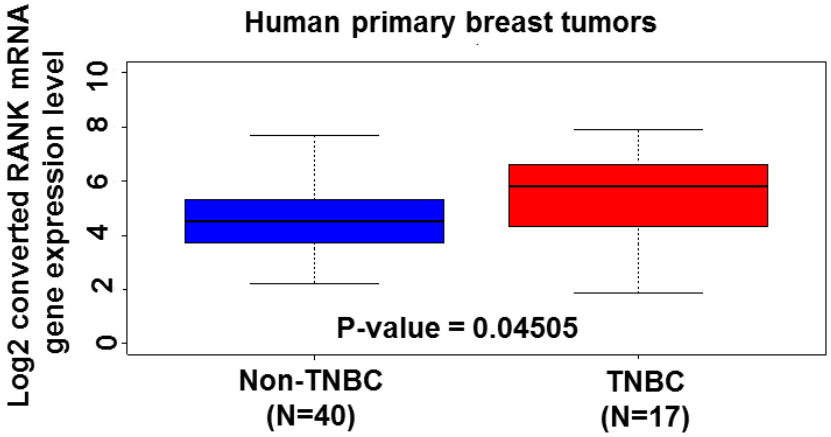

Figure 2.2 RANK mRNA expression is significantly higher in TNBC compared to non-TNBC tumors. We analyzed RANK gene expression using an Affymetrix U133a GeneChip array containing mRNA from breast tumors (n=57) taken from the following cohorts: TNBC (n=17) and non-TNBC (n=40). Results were normalized with MAS5 algorithm and log2 transformed and p-values were calculated by Wilcoxon test (P-value = 0.045).

2.3.2 RANKL IS A PREDICTOR OF WORSE CLINICAL OUTCOME IN RANK-POSITIVE TNBC

Previous retrospective studies have shown that RANK expression can predict the occurrence of skeletal-related events (SREs), bone disease progression, and death (75). As effective RANK signaling requires the presence of RANKL, we sought to find out if associated RANK and RANKL expression in TNBC tumors could better delineate clinical outcome. TMAs constructed with core biopsies from TNBC patients (n=91) and tumor-associated macrophages (TAMs) were stained as an internal control for RANK and RANKL positivity (data not shown) with anti-human RANK monoclonal antibody (N-1H8 or N2-B10; Amgen, Inc.) and RANKL antibody (M366; Amgen, Inc.). RANK and RANKL expression was semi-quantitated by H score method. The cut-off value for positive RANKL/RANK was H score > 0. Based upon our initial analysis that a univariate analysis of RANK expression did not correlate with clinicopathological parameters and was not associated with a lower RFS or OS (data not shown), we performed statistical analyses for RANKL expression in both RANK negative and RANK positive cohorts. According to a Fisher's exact test (*P* –value > 0.05 significant) to correlate clinicopathological parameters (age, race, menopause, NG, pStage, and LVI) in the whole cohort (n=91) (Table 2.5), 55.4% (n=41) of RANKL-negative TNBC patients correlated with pStage II disease (p-value = 0.551; not significant). There was a significant correlation between nuclear grade III and RANKL negativity, 94.6% (n=69) of RANKL negative tumors were nuclear grade III (p-value < 0.01). Lymphovascular invasion did not significantly correlate with RANKL expression (p-value = 0.705). In a univariate and multivariate analysis for 5-year recurrence and overall survival in the RANK positive TNBC cohort (n=66), RANKL expression was found to be an independent predictor for worse survival outcome (Table 2.6). A Kaplan-Meier survival

curve analysis was performed to determine if RANKL associated with a poorer relapse-free survival and overall survival. We did not observe RANKL associated with survival outcome in RANK negative cohort (Figure 2.3), but we did observe RANKL associated with a worse survival outcome (Figure 2.4).

Table 2.5 Clinicopathological parameters by RANKL expression in TNBC patients

	RANKL negative no. (%) (n=74)	RANKL positive no. (%) (n=16)	All patients no. (%) (n=90)	*P* -Value
Age				
<=50	34 (45.9)	5 (31.3)	39 (43.3)	
>50	40 (54.1)	11 (68.7)	51 (56.7)	0.282*
Menopausal status				
Pre	22 (29.7)	6 (37.5)	28 (31.1)	
Post	52 (70.3)	10 (62.5)	62 (68.9)	0.543*
Pathologic stage				
I	28 (37.8)	8 (53.3)	36 (40.4)	
II	41 (55.4)	6 (40)	47 (52.8)	
III	5 (6.8)	1 (6.7)	6 (6.8)	0.551
Nuclear grade				
I	2 (2.7)	2 (12.5)	4 (4.5)	
II	2 (2.7)	5 (31.3)	7 (7.9)	
III	69 (94.6)	9 (56.2)	78 (87.6)	<0.01
Lymphovascular invasion				
Negative	49 (83.1)	11 (78.6)	60 (82.2)	
Positive	10 (16.9)	3 (21.4)	13 (17.8)	0.705

* chi-square test

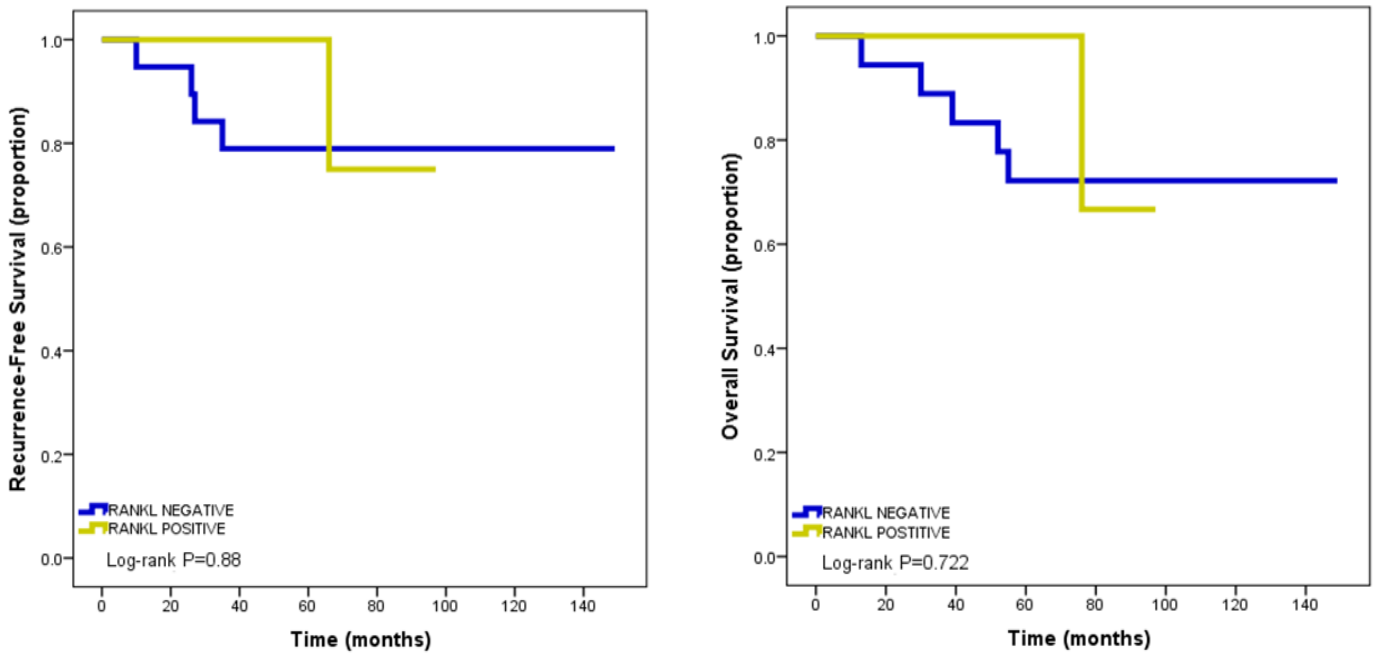

Figure 2.3 RANKL expression is not associated with poor clinical outcome in RANK-negative TNBC. Kaplan-Meier curve analysis of TNBC patients with primary breast tumors negative for RANK expression (RANK = 0) including RANKL positive (n= 16) or negative (n=74) was performed for recurrence-free survival (left), and for overall survival (right). A log-rank test was performed between RANKL positive and negative groups in each analysis to determine the p-value.

Table 2.6 Univariate and Multivariate analysis for 5-year recurrence and survival in RANK positive TNBC cohort												
	Univariate Analysis						Multivariate Analysis*					
	RFS			OS			RFS			OS		
	HR	95%CI	*P* Value	HR	95%CI	*P* Value	HR	95%CI	*P* Value	HR	95%CI	*P* Value
Age (relative to <=50)	2.67	0.30-3.88	0.38	3.3	0.39-28.26	0.28				2.91	0.34-25.22	0.33
Pathologic stage I (relative to stage III)				0.20	0.02-2.20	0.19				0.09	0.007-1.28	0.08
Pathologic stage II (relative to stage III)	0.28	0.031-2.53	0.26	0.29	0.30-2.81	0.29	0.16	0.02-1.78	0.14	0.16	0.01-1.93	0.15
Nuclear grade II (relative to grade III)	3.06	0.34-7.37	0.32	2.62	0.31-22.47	0.38						
Lymphovascular invasion (relative to negative)	2.00	0.21-9.25	0.55	2.93	0.27-32.35	0.38						
RANKL (relative to negative)	3.54	0.59-1.23	0.17	5.32	1.07-26.37	0.04	6.91	0.97-9.43	0.05	7.81	1.29-47.24	0.03

*Covariates with P-value < 0.3 in univariate analysis were included in multivariate analysis.

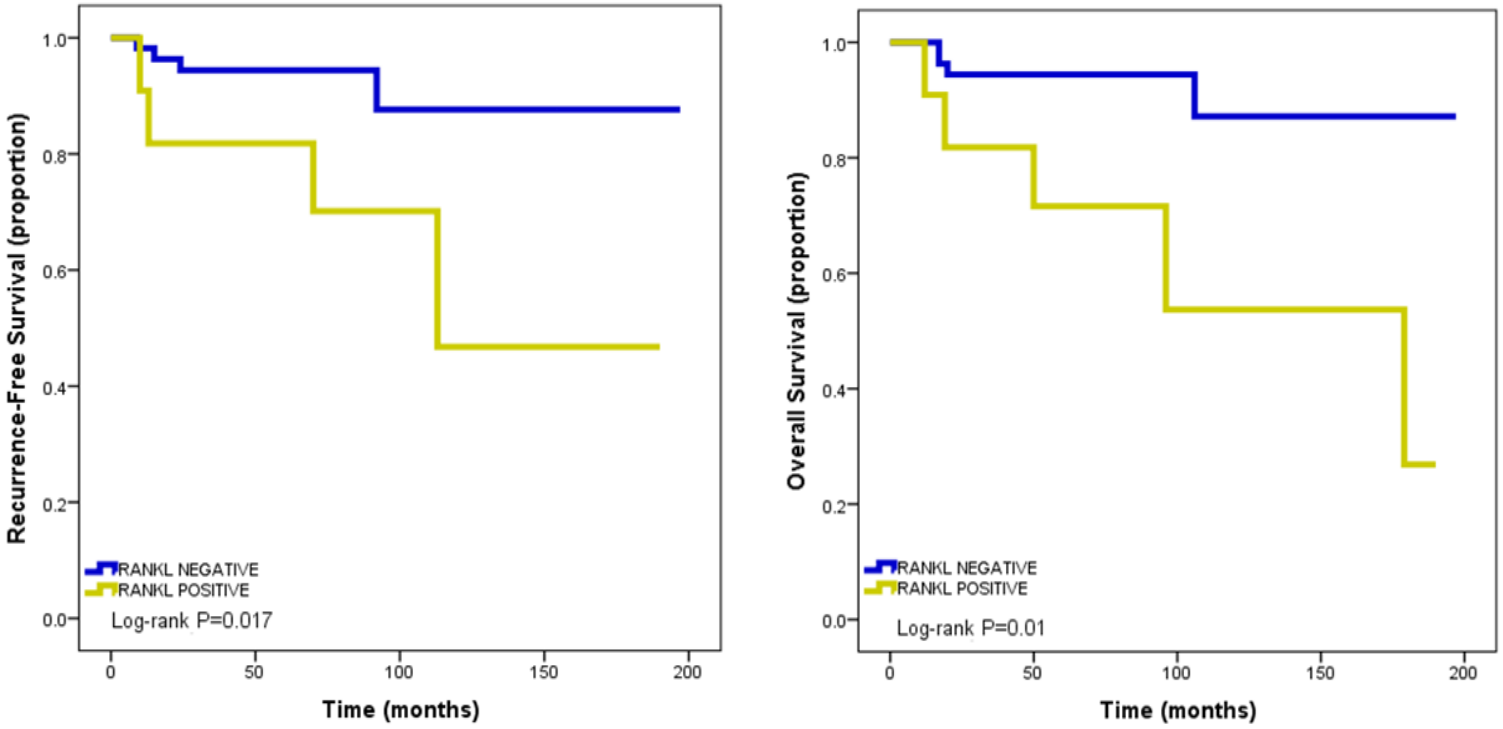

Figure 2.4 RANKL expression is associated with poor clinical outcome in RANK-positive TNBC. Kaplan-Meier curve analysis of TNBC patients with primary breast tumors positive for RANK expression (n=66) were stratified as RANKL positive (n=11) or negative (n=55) was performed for assessment of recurrence-free survival (left) and overall survival (right). A log-rank test was performed between RANKL positive and negative groups to determine the p-value.

2.3.3 HUMAN TNBC CELL LINES HAVE HIGHER EXPRESSION OF RANK THAN NON-TNBC CELL LINES

Based on our clinical findings that RANK expression was higher in the TNBC cohort compared to non-TNBC, we screened a panel of human TNBC and non-TNBC cell lines for RANK protein expression by flow cytometry analysis. By immunostaining of endogenous RANK with an anti-human RANK monoclonal antibody (N2-B10) and APC secondary antibody, followed by detection using flow cytometry analysis, we observed higher APC-RANK expression levels in the majority of TNBC cell lines compared to non-TNBC cell lines (Figure 2.5). We calculated the median difference between the isotype control peak (red) and APC-RANK peak (blue). We found the TNBC cell lines to have a higher median difference and averaged median difference compared to the non-TNBC cell lines (Appendices A and B). The MDA-MB-231 TNBC cell line had high levels of RANK expression that was comparable to that of other TNBC cell lines (HCC70, MDA-MB-468, and HCC38). Due to its high tumorigenicity and metastatic ability, we used the MDA-MB-231 cell line for subsequent experiments to investigate the role of RANK in TNBC cells. We investigated the effects of RANK suppression in MDA-MB231 to characterize the role of RANK and determine if RANK is a potential therapeutic target for inhibiting the progression of TNBC.

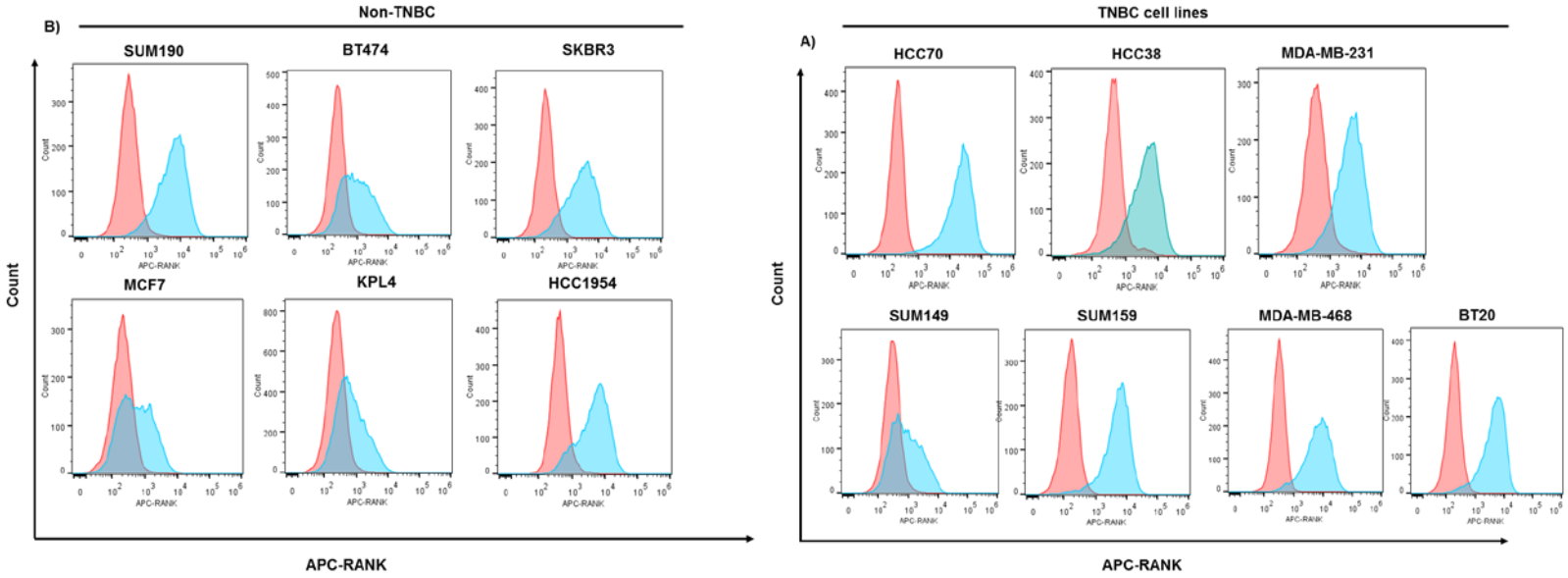
B)
Non-TNBC
SUM190
BT474
SKBR3
MCF7
KPL4
HCC1954
Count
APC-RANK
A)
TNBC cell lines
HCC70
HCC38
MDA-MB-231
SUM149
SUM159
MDA-MB-468
BT20
Count
APC-RANK

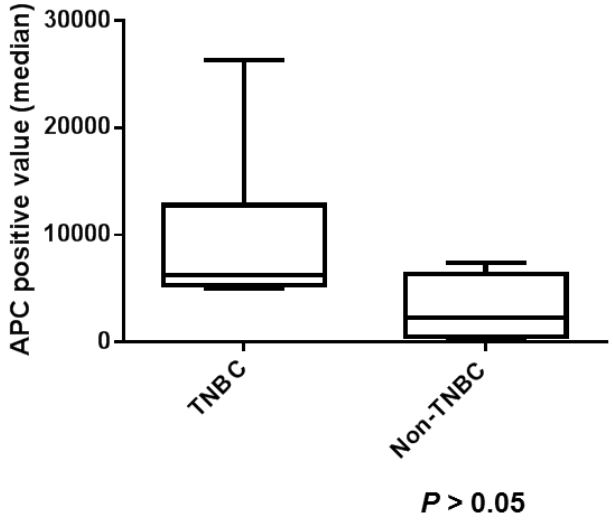
APC positive value (median)
30000
20000
10000
0
TNBC
Non-TNBC
P > 0.05

Figure 2.5 RANK expression is higher in TNBC cell lines compared to non-TNBC cell lines. A panel of human A) TNBC and B) non-TNBC cell lines were screened by flow cytometry for endogenous RANK expression. Isotype control (red peak), and APC-RANK positive (blue peak). Y-axis = Count (number of cells); X-axis = APC-RANK signal intensity. Flow cytometry results were analyzed by FlowJo version VX software. The APC positive value medians for TNBC and non-TNBC were calculated and graphed using Graphpad Prism version 6.01 (boxplot graph).

2.3.4 SUPPRESSION OF RANK DECREASED MDA-MB-231 CELL MIGRATION AND INVASION

Evidence suggests RANK/RANKL to promote breast cancer metastasis, but the role of RANKL/RANK in breast cancer metastasis is not well understood. Using MDA-MB-231 cells, we investigated the effects of RANK suppression in TNBC cell migration and invasion. In consensus with another study conducted by Tang ZN *et al*. (91), after we observed suppression of RANK to have little effect on the migration and invasion of MDA-MB-231 cells in the absence of RANKL-stimulation (data not shown), we pre-stimulated MDA-MB-231 scrambled shRNA and RANK shRNA cells with 25 ng/mL human soluble RANKL for 24 hours prior to seeding cells for 6-hour Boyden chamber transwell cell migration and 24-hour cell invasion assay. We observed MDA-MB-231 RANK shRNA cells to have significantly decreased cell migration (figure 2.6A) and invasion (figure 2.6B).

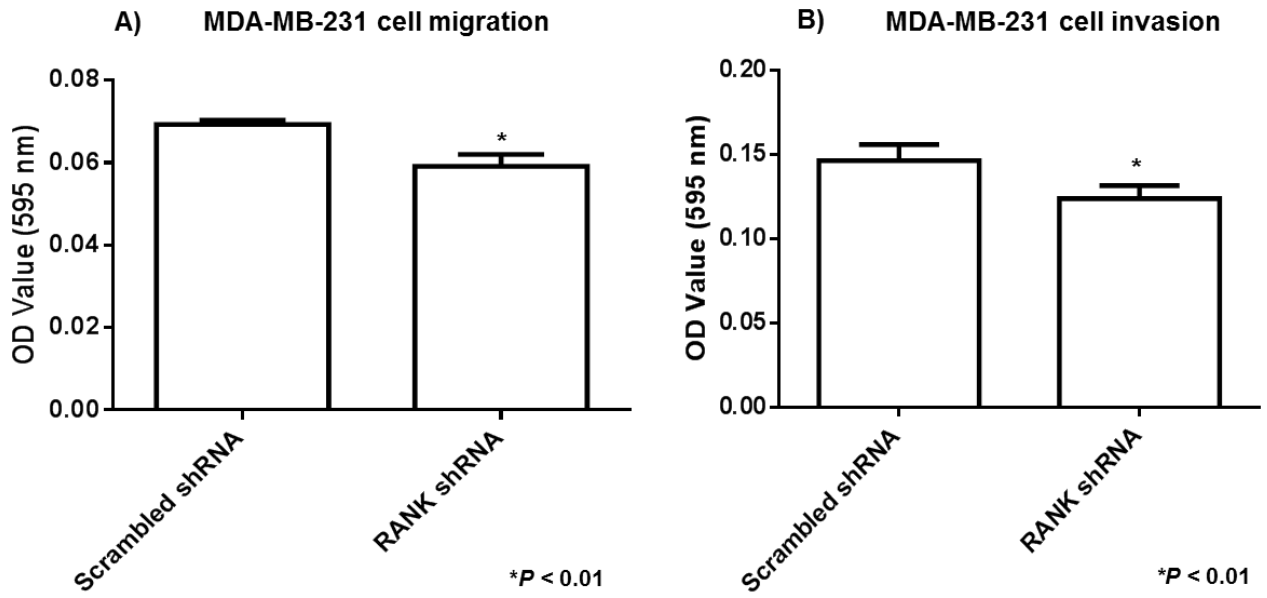

Figure 2.6 Suppression of RANK reduced RANKL-stimulated MDA-MB-231 cell migration and invasion. MDA-MB-231 scrambled shRNA and MDA-MB-231 RANK shRNA cells were pre-stimulated with human soluble RANKL (25 ng/mL) for 24 hours prior to a Boyden chamber transwell cell migration (6-hour) and invasion assay (24-hour). A) Cells migrated for 6 hours, B) cells invaded growth factor-reduced Matrigel for 24 hours. Migrated and invaded cells were quantitated by fixing and staining with 0.1% crystal violet/20% methanol solution followed by resuspension in 4% sodium deoxycholate and quantification using Perkin-Elmer Microplate reader at 595 nm. *P > 0.01 statistically significant.

2.3.5 SUPPRESSION OF RANK DECREASED SELF-RENEWAL ABILITY

The RANKL/RANK pathway plays an important role in the progression of breast cancer, but the CSC phenotype which contributes to the invasiveness of TNBC, had not been well-studied (91).To determine if RANK can regulate the CSC phenotype, we performed a mammosphere assay in which MDA-MB-231 RANK shRNA, or MDA-MB-231 Scrambled shRNA cells were cultured under low adherence conditions in mammosphere media. Following a 6-day incubation period, we observed a reduction in the number of primary mammospheres (P_0) formed and the number of secondary mammospheres (P_1) formed which is associated with a reduction in the self-renewal ability of MDA-MB-231 cells (Figure 2.7).

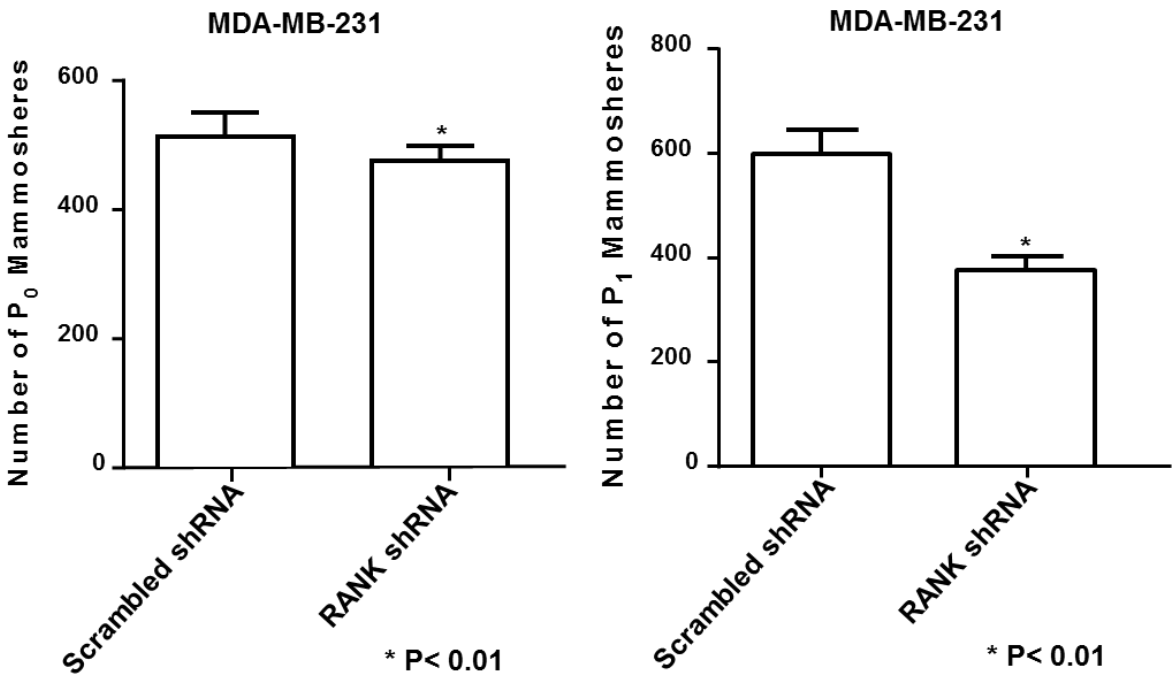

Figure 2.7 Mammosphere formation and self-renewal ability of MDA-MB-231 cells was reduced by the suppression of RANK. MDA-MB-231 scrambled shRNA and MDA-MB-231 RANK shRNA cells were seeded into ultra-low attachment 6-well plates in mammosphere media and cultured for 6 days for primary (P_0) mammosphere formation followed by re-plating of cells for secondary (P_1) mammosphere formation (self-renewal ability) for an additional 6 days. P_0 and P_1 mammospheres were stained with 5 mg/mL MTT reagent for 1 hour then quantitated by GelCount software. *$P < 0.01$ statistically significant.

2.3.6 STEM CELL GENES ARE MODULATED BY THE SUPPRESSION OF RANK IN MDA-MB-231 CELLS

Previous studies have found that the RANKL/RANK pathway regulates EMT and CSC phenotype of breast cancer cells (81, 92). To determine which stem cell pathways are regulated by RANK in TNBC cells, we analyzed stem cell gene expression levels of MDA-MB-231 RANK shRNA cells using a human stem cell RT^2 PCR array. We observed several stem cell genes downregulated in MDA-MB-231 RANK shRNA cells when normalized to the MDA-MB-231 scrambled shRNA cells (Figure 2.8). The top five stem cells genes that had the greatest reduction in expression based on the fold-regulation were: 1) BMP2, 2) CCND2, 3) FOXA2, 4) SOX2, and 5) BMP3 (Table 2.3).

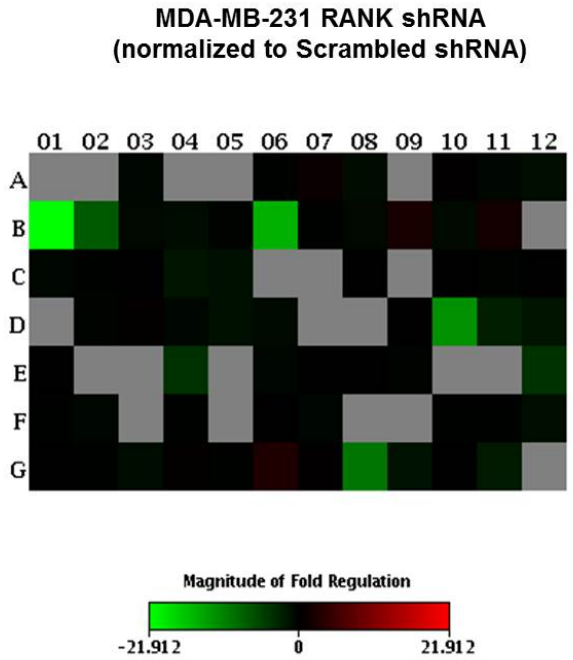

Table 2.3 Top-5 genes down-regulated in MDA-MB-231 RANK shRNA cells

Position	Gene of interest	Fold-regulation
B01	BMP2	-22.91
B06	CCND2	-16.28
D10	FOXA2	-13.55
G08	SOX2	-11.17
B02	BMP3	-8.72

Figure 2.8 Human stem cell genes in MDA-MB-231 cells are modulated by the suppression of RANK. A qRT PCR array (Qiagen PAHS405A) was used to analyze stem cell gene expression in MDA-MB-231 RANK shRNA normalized to MDA-MB-231 Scrambled shRNA. A heat map was generated showing the log 2 fold-change in stem cell gene expression for MDA-MB-231 RANK shRNA normalized to MDA-MB-231 scrambled shRNA. The negative inverse of the fold-change (data not shown) was calculated to obtain the fold-regulation and the top 5 stem cell genes of interest were selected based on the greatest magnitude of fold-regulation (Table 2.3).

2.4 DISCUSSION

TNBC is one of the most aggressive and deadliest breast cancer subtypes without any clinically-defined molecular targets for treatment. There is a critical need for finding a therapeutic target to prevent the relapse and progression of TNBC. RANKL/RANK pathway is critical to the metastasis of breast cancer. Although RANK expression is associated with increased metastasis and poor prognosis in breast cancer, RANK has not been investigated in the progression of TNBC. In determining whether RANK expression is associated with the more aggressive TNBC subtype, we analyzed the basal levels of RANK gene expression in primary breast tumors constructed on an Affymetrix cDNA GeneChip array. Stratified by hormone receptor status, our results indicated RANK expression to be higher in the ER-/HER2- breast tumors compared to ER+/HER2- breast tumors (Figure 2.1). Despite the significantly higher RANK gene expression in the ER-/HER2- breast tumors compared to ER+/HER2- breast tumors, ER-/HER2- breast tumors did not have significantly higher level of RANK expression compared to the HER2+ breast tumors. When we had analyzed RANK expression in breast tumors stratified as TNBC or non-TNBC, we found RANK expression was significantly higher in TNBC tumors (Figure 2.2). This finding is in concordance with another study conducted by Santini D. *et al*. in which ER- breast tumors were found to have significantly higher RANK expression compared to hormone receptor-positive breast tumors (93). Thus, this finding suggests RANK expression to be elevated in TNBC tumors compared to non-TNBC tumors, and provides a rationale to investigate RANK protein expression and its prognostic value in TNBC patient tumors.

Generally, the more aggressive breast cancer subtypes are associated with a poorer prognosis. To investigate whether RANKL or RANK expression in TNBC associated with a poorer clinical outcome, we analyzed IHC staining of RANK and RANKL proteins in TNBC TMAs. In the whole cohort of TNBC patients (n=91), we performed a correlative analysis to look at RANKL expression and clinicopathological parameters. We found a significant correlation between RANKL negative tumors and nuclear grade (NG) III clinical factor (Table 2.1). This suggests that in the absence of RANK expression (n=25), RANKL does not predict an advanced and poorly differentiated TNBC tumor. In a Kaplan-Meier curve analyses for RANK negative cohort stratified by RANKL, we observed RANKL did not have an association with the recurrence-free survival or overall survival in TNBC patients (Figure 2.3). This finding supports the results of our initial analysis that RANK expression alone, irrespective of RANKL, is not a predictor of clinical outcome in TNBC patients (data not shown). Alternatively, we analyzed RANKL expression in the RANK positive cohort (n= 66) performing univariate and multivariate analyses using clinicopathological parameters that were obtainable for up to 5 years post-diagnosis. In both analyses, we observed RANKL positive tumors to be associated with a worse 5-year recurrence and overall survival compared to RANKL negative tumors (Table 2.2). This suggests RANKL to be an independent predictive factor for the 5-year recurrence and overall survival in TNBC patients. In the Kaplan-Meier curve analysis for recurrence-free survival and overall survival, we observed an association between RANKL positive and a shorter recurrence-free survival and overall survival (Figure 2.4). In relation to other studies which have indicated RANK to be associated with a poor breast cancer prognosis (94), our results indicate RANK expression to be essential for the RANKL association with

poor prognosis of TNBC. In contrast to our study, Santini D. *et al*. reported low expression of RANK in primary breast tumors and concluded RANK to be a predictive marker for bone metastasis in breast cancer patients (93). The discordance between our study and the study by Santini D. *et al*. of RANK expression associated with overall survival could be explained by the different methods used to define the cut-off for RANK expression, and the variability in IHC staining of RANK protein, which can result in detected RANK-positive events in tumor samples across both studies. Owen S. *et al.* observed a breast cancer cohort with reduced RANK mRNA expression to have a significantly poorer overall survival compared to those with higher RANK mRNA expression (95). In contrast to this, an investigational study of RANK protein in primary breast tumors found RANK did not correlate with clinical factors while high RANK expression associated with a poorer outcome compared to low RANK expression (94). In addition, Park *et al*. observed RANK protein expression to associate with a poorer disease-free survival and RANKL to significantly correlate with primary breast tumors with a lower Ki67 proliferative index (96). In comparison, we also did not observe RANK to correlate with clinical factors but did find RANKL negativity to correlate with a higher nuclear grade. We speculate that depending upon the breast tumor cohort, RANK is associated with a poorer clinical outcome and RANKL is a predictive factor for a clinically aggressive TN breast tumor in the presence of RANK. This could indicate that activated RANKL/RANK pathway promotes an aggressive TNBC phenotype and poorer outcome.

Upon observing an association between the co-expression of RANK and RANKL and poorer outcome in TNBC patients, we investigated whether endogenous RANK expression in a TNBC cell line can recapitulate an aggressive behavior in *in vitro*

studies. We performed flow cytometry analysis to compare endogenous RANK protein levels between a panel of TNBC and non-TNBC cell lines. Endogenous RANK protein expression was observed to be higher in TNBC cell lines compared to non-TNBC cell lines (Figure 2.5). Interestingly, the TNBC cell line SUM149 was observed to have a lower amount of RANK protein expression relative to the other TNBC cell lines. Within the non-TNBC cohort, ER-/HER2+ cell lines SUM190, SKBR3, and HCC1954, were observed to have relatively higher amount of RANK protein level compared to all other non-TNBC ER+ cell lines. These results confirm that ER- breast cancer tends to have higher levels of RANK expression compared to ER+ breast cancers. However, there is a general consensus that there is discordance in RANK expression in breast tumors and breast cancer cell lines at the transcriptional and protein level (90, 91). TNBC is a heterogeneous disease and that RANK expression varies across breast cancer subtypes as we had observed that not all TNBC cell lines have high RANK expression. Possible reasons for discordance between the reported RANK expression level in cell lines may be due to the variation in post-transcriptional regulatory mechanisms and immunohistochemistry staining for RANK protein (74). Nevertheless, our findings warrant a comparative study of RANK expression between TNBC molecular subtypes (BL1, BL2, IM, LAR, M, MSL, and UNS). By applying this strategy, we may be able to determine if RANK expression in TNBC tumors or cell lines is significantly associated with a particular TNBC molecular subtype.

To study the biological role of RANK in the invasive and CSC phenotype of TNBC cells, we knocked down RANK in MDA-MB-231 using a lentiviral-based shRNA system. We observed the suppression of RANK, following stimulation with and in the presence of RANKL as a chemo attractant, to significantly reduce MDA-MB-231 cell

migration and invasion. This result is comparable to what was observed in other studies of RANKL-stimulated MDA-MB-231 cell migration and invasion (91, 97). Jones D.H. *et al.* reported RANKL-independent signaling through CXCR4 chemokine signaling pathway in MDA-MB-231 cell migration and invasion (97). CXCR4 chemokine receptor expression is upregulated by the NFkB pathway. Tang Z. *et al.* reported the inhibition of Src to abrogate RANKL-stimulated MDA-MB-231 cell migration and invasion, and concomitantly suppressed downstream activity of ERK1/2, P38, and JNK (91). Other studies have shown that these same pathways were activated following RANKL stimulation in ER-negative and ER-positive breast cancer cell lines, SKBR3 and T47D, respectively (82, 97). Although our *in vitro* migration and invasion assays confirmed the suppression of RANK significantly reduced RANKL-stimulated TNBC cell migration and invasion, we do not know which signaling pathways downstream of RANK mediate MDA-MB-231 cell migration and invasion. Further studies are required to investigate potential signaling pathways downstream of RANK, including JNK, P38 MAPK, and the activation of NFκB, as mediators of TNBC cell migration and invasion.

Since CSCs are associated with breast cancer cell motility and invasion and are features of an aggressive phenotype, we investigated whether the suppression of RANK negatively regulates the self-renewal ability of TNBC cells by performing an *in vitro* mammosphere assay. In the mammosphere assay, we observed the knockdown of RANK to significantly reduce primary and secondary MDA-MB-231 mammospheres. Thus, we concluded RANK to positively regulate the CSC phenotype of TNBC cells. Our findings are in concordance with other studies, which demonstrated RANK regulation of breast CSCs in TNBC cells. It was observed in a study by Pelligrini P*. et al.* that overexpression of RANK promoted the repopulation of differentiated breast tumor cells and cancer stem cells in an *in vivo* mouse model (98).

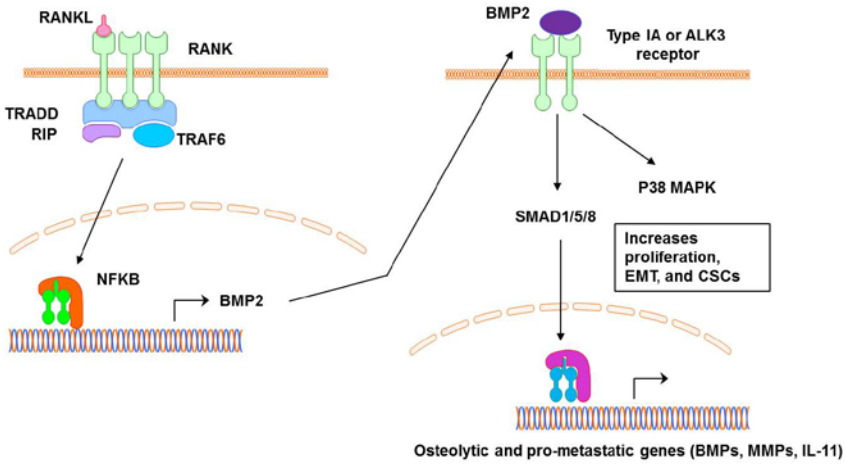

ILLUSTRATION 2.4 A PROPOSED MODEL FOR RANKL/RANK-MEDIATED BMP2 SIGNALING IN TNBC CELLS

RANKL binds to RANK expressed on the surface of TNBC cells and induces the transcription of BMP2 which then the secreted form binds to its receptor to activate the SMAD1/5/8 signaling cascade to activate transcription of several pro-metastatic and inflammatory genes such as other BMPs, MMPs, and IL-11. This chain of events supports a proliferative and pro-metastatic state including EMT and CSC phenotype.

To find out if the suppression of RANK modulated stem cell genes in MDA-MB-231 cells, we performed a RT^2 PCR human stem cell array analysis to compare the

expression levels of stem cell genes between MDA-MB-231 RANK shRNA and MDA-MB-231 Scrambled shRNA cells. Based on our findings, we concluded RANK regulates breast CSCs through stem cell genes implicated in cell proliferation and differentiation. Bone morphogenetic protein 2 (*BMP2*) had the greatest magnitude in fold-regulation (-22.91), followed by *CCND2* (-16.28), *FOXA2* (-13.55), *SOX2* (-11.17) and *BMP3* (-8.72). The bone morphogenetic proteins (BMPs) are growth factors which regulate cell proliferation and differentiation. BMP2 in particular is considered a mesenchymal stem cell-specific marker which regulates cell differentiation (12), while BMP3 is an antagonist for the BMP receptor (99). *FOXA2* and *SOX2* are both stem cell regulators involved in cancer metastasis. *CCND2* (cyclin D2), a proliferative marker and regulator for G1/S phase cell cycle transition, can increase malignancy through enrichment of the stem cell population (100). However, there is no evidence suggesting that RANKL stimulation of RANK in breast tumor cells regulates the expression of cyclin D2. As opposed to BMP3, which has anti-tumorigenic effects, BMP2 harbors oncogenic activity to promote tumor cell invasion and metastasis. In a study by Blake M.L. *et al.,* RANKL stimulation of MDA-MB-231-RANK cells up-regulated pro-metastatic genes MMPs (MMP1, 3, 7, and 9) and IL-11 (55). In addition, another study found metastatic genes up-regulated in a bone-metastatic derivative subpopulation of MDA-MB-231 cells (101). Transcription factors *FOXA2* and *SOX2* play a critical role in regulating progenitor cell development, differentiation, and migration (102). The link between *SOX2* and breast cancer progression is that it's found to be primarily expressed in early-stage breast cancers rather than in the later-staged or invasive breast cancers, indicative of a functional role in tumor initiation (103). The mechanism underlying the dedifferentiation of breast cancer cells by *SOX2* expression is unknown, however, one study indicated

NFkB to indirectly regulate *SOX2* (103). NFkB is a target downstream of the RANKL/RANK pathway and therefore, it is logical to conclude that the stem cell genes in the PCR array screen are possibly indirectly modified by the suppression of RANK. In addition, the methods used to investigate gene expression regulated by RANK, including stimulation with or without RANKL stimulation, are likely to vary the outcomes in expression of these stem cell genes. Therefore, our study warrants an investigation into the modification of stem cell genes (*BMP2, BMP3, SOX2, FOXA2,* and *CCND2*) by RANKL stimulation.

In summary, the observation of higher RANK expression in TNBC tumor samples merits an investigation into the prognostic value of the RANK pathway in a clinical cohort of TNBC. Our findings suggest that there is a positive correlation between RANK and RANKL protein expression which is associated with poor prognosis of TNBC patients. Based on *in vitro* studies, we conclude that targeting the RANK pathway could be a potential strategy for reducing the progression of TNBC. We will investigate molecular pathways downstream of RANK, including regulators of the stem cell phenotype to elucidate the mechanism of TNBC progression through RANKL stimulation. We will perform experimental and spontaneous metastasis mouse models using a TNBC cell line expressing luciferase-tagged RANK shRNA in mice, we will generate experimental and spontaneous metastasis models to monitor the effects of RANK suppression on TNBC metastasis and expression of metastatic and stem cell markers.

From a clinical perspective, targeting RANKL to block RANKL/RANK activity in TNBC is a suitable approach because there is evidence of improved breast cancer patient survival and reduced bone metastases following denosumab treatment. A

Phase II Clinical study in ER-positive breast cancer patients, in which denosumab has already been described to reduce bone metastases, we will investigate the effects of denosumab on the presence of CTCs and DTCs. Since the use of denosumab has not been studied in a TNBC patient population, we may also conduct a pilot study in TNBC patients treated with neoadjuvant denosumab in which the presence of CTCs and DTCs will be evaluated before and after denosumab treatment.

CHAPTER 3: COX-2 PROMOTES TUMORIGENESIS OF IBC THROUGH THE REGULATION OF NODAL

3.1 INTRODUCTION

IBC is one of the most aggressive breast cancers accounting for approximately 8-10% of all breast cancer-related deaths in the U.S. Despite the fact that IBC is a locally advanced breast cancer associated with inflammatory-like symptoms, a physiologic mechanism of inflammatory response has not yet been found in IBC. There is evidence that implicates a role or COX-2 in enrichment of CSCs in breast cancer. However, the mechanism of COX-2-regulated breast CSCs is not clearly defined. Suppression of the CSC phenotype in IBC may have anti-tumorigenic and anti-metastatic potential. It was reported in IBC that the EGFR pathway promotes EMT, a requisite of breast cancer metastasis and an observed invasive-like phenotype associated with CSCs. In this study, we not only observed a positive correlation between EGFR and COX-2 expression in IBC tumors, but we found COX-2 to regulate EMT in IBC cells. Furthermore, in our investigation, treatment with COX-2 selective inhibitor, celecoxib, downregulated Nodal expression, a potential stem cell marker regulated by COX-2. Thus, we evaluated the Nodal stem cell pathway as a potential target for eradicating CSCs in IBC.

3.2 MATERIALS AND METHODS

3.2.1 cDNA MICROARRAY ANALYSIS

For this study, we used an Affymetrix U133a GeneChip array constructed with cDNA derived from human IBC (n = 25) and non-IBC (n = 57) tumor specimens from The University of Texas MD Anderson Cancer Center IBC database. Gene expression obtained from the microarrays was normalized with the MAS5 algorithm, mean-centered to 600 and log 2-transformed. Statistical analyses were performed by using BRB-ArrayTools version 3.9.0 alpha (http://linus.nci.nih.gov/BRB-ArrayTools.html) and R statistical software version 3.0.0 (http://www.r-project.org/). The correlation between the mRNA expression levels of EGFR (211551_at) and COX-2 (204748_at) was analyzed using the Spearman's rank correlation coefficient analysis.

3.2.2 CELL LINES AND TISSUE CULTURE REAGENTS

Human non-IBC breast cancer cell lines, BT-474, SK-BR-3, MDA-MB-231, purchased from American Type Culture Collection, were grown in Dulbecco's modified Eagle's medium/F12 medium supplemented with 10% FBS (GIBCO/BRL) in a humidified atmosphere containing 5% CO_2 at 37°C. IBC cell lines, SUM149 and SUM190, were purchased from Asterand (Detroit, MI) and were grown in Ham's F12

medium supplemented with 5% FBS, 5 µg/mL insulin, 1 µg/mL hydrocortisone, and 1% antibiotic-antimycotic. The human IBC cell line KPL-4 (104) was kindly provided by Dr. Junichi Kurebayashi (Kawasaki Medical School, Japan) and maintained in Dulbecco's modified Eagle's medium/F12 medium supplemented with 10% FBS and 1% antibiotic-antimycotic. Non-IBC and IBC human breast cancer cell lines were validated using a short term tandem repeat method based on a primer extension to detect single base derivations in October 2010, and July 2013, respectively, by the Characterized Cell Line Core Facility at M.D. Anderson Cancer Center. Cells used for experiments were grown in culture for no longer than 2 months. All cell lines were confirmed to be mycoplasma free using a MycoAlert Mycoplasma Detection Kit (Lonza Cologne AG). For prostaglandin (PG) treatment, cells were serum-starved for 24 hours prior to adding PGE_2 (catalog #14010; Cayman Chemical) or $PGF_{2\alpha}$ (catalog #16010; Cayman Chemical) was added to the cells cultured in serum-free medium. Celecoxib (Selleck Chemicals, Houston, TX) was reconstituted in dimethyl sulfoxide (DMSO). Recombinant human Nodal (R&D Systems, Inc., Minneapolis, MN) was reconstituted in 4 mM HCl and 0.1% bovine serum albumin solution.

3.2.3 WESTERN BLOT ANALYSIS

Cell lysates were prepared as follows: 1) Cells were washed 1X with cold 1X PBS, 2) On ice, 1 mL of cold 1X PBS was added/plate or well and cells were scraped with a cell lifter and collected in 1.5 mL Eppendorf tubes, 3) cells were centrifuged for 4 minutes at 4°C at 4 x 10^3 rpm, 4) cell pellets were lysed on ice in 30-40 uL 1X RIPA cell lysis buffer containing 1:100 phosphatase and protease inhibitors, and finally, cell lysates were cleared by centrifugation for 30 minutes at 4°C at maximum speed (13.2 x

10^3 rpm). See 'Bradford Protein Assay' methods section for determination of total protein concentrations.

Western blot analysis was performed as previously described (105) using the following antibodies (table 3). anti-EGFR (catalog # sc-03; Santa Cruz Biotechnology, Inc.), anti-Phospho-EGFR (Y1173) (catalog #sc-12351; Santa Cruz Biotechnology), anti-COX-2 (catalog #160112; Cayman Chemical), anti-E-cadherin (catalog #610182; BD Biosciences), anti-fibronectin (catalog # 610077; BD Biosciences), anti-vimentin (catalog #AB-1620; Chemicon International), anti-N-cadherin (catalog #4061S; Cell Signaling), and anti-β-actin (catalog #A-5441; Sigma-Aldrich).

3.2.4 SIRNA TRANSFECTION

Using Invitrogen Oligofectamine 2000 reagent (catalog # 12252-001), SUM149 cells were transfected with COX-2 or EGFR-targeted siRNA. The COX-2 siRNA oligonucleotide sequences # 1 (forward 5'GAAUCAUUCACCAGGCAAA-3' and reverse 5'-UUUGCCUGGUGAAUGAUUC-3') and #2 (forward 5'-CUCCAAACACAGUGCACUA-3' and reverse 5'-UAGUGCACUGUGUUUGGAG-3') were transfected into SUM-149 cells at 200 nM final concentration per well. Into a 6-well plate containing 3 x 10^5 SUM149 cells/well. At the 4h time point, complete medium was added at 1 mL/well. At 48h post-transfection, cells were harvested and lysed with 1:10 dilution of 10X RIPA cell lysis buffer (125 mL 1M Tris-HCL PH 7.4, 25 mL NP-40, 12.5 mL SDS, 5 mL 0.5 M EDTA, 12.5 g NaDOC, 75 mL 5M $NaCl_2$, and 7.5 mL distilled H_2O).

3.2.5 PROSTAGLANDIN EXTRACTION AND ANALYSIS

Endogenous PGE_2 and $PGF_{2\alpha}$ were extracted from IBC and non-IBC cells, and PG levels were analyzed by using quantitative high-performance liquid chromatography tandem mass spectrometry (HPLC-MS/MS) according to the protocol of Yang *et al*. (3). Briefly, cell pellets were suspended in 0.5 mL of PBS, 40 µL of 1 N citric acid, and 5 µL of 10% (w/v) butylated hydroxytoluene. PGs were extracted by liquid-liquid extraction using 2 mL of 1/1 ethyl acetate/hexanes (v/v), three times. The organic layers were separated, pooled, and evaporated to dryness under nitrogen. The samples were reconstituted in 100 µL of 50/50 methanol/0.1% acetic acid (v/v). Prostaglandins were detected using an Agilent 6460 triple quadrupole mass spectrometer (Agilent Technologies, Palo Alto, CA) equipped with an Agilent HP 1200 binary HPLC pump. PGE_2 and $PGF_{2\alpha}$ were separated using a 2 × 100-mm Kinetex 3 µm C18 analytical column (Phenomenex, Torrance, CA). Mobile phase A consisted of 0.1% formic acid, and mobile phase B was acetonitrile with 0.1% formic acid. Compounds were eluted with a gradient starting at 20% B and ramped to 90% B over 14 minutes. The column temperature was maintained at 40°C, and samples were kept at 4°C during the analysis. For the detection and quantification of PGE_2 and $PGF_{2\alpha}$ levels in SUM149 xenograft tumors from mice, following tumor extraction the tissue samples were processed and reconstituted prior to analysis by liquid chromatography tandem mass spectrometry (LC-MS/MS) as follows in Pirman D.A. *et al* (55).

3.2.6 qRT^{2}PCR

Total RNA was extracted using the RNeasy Mini kit (Qiagen). Real-time quantitative RT-PCR was performed using the Bio-Rad iScript One-Step RT-PCR kit.

7S rRNA was used as a housekeeping gene. The relative quantitation value for each target gene compared to the calibrator for that target was expressed as $2^{-(Ct-Cc)}$ (Ct and Cc are the mean threshold cycle differences after normalization to 7SL rRNA). 7SL primers were as follows: forward 5'-ATCGGGTGTCCGCACTAAGTT-3'; reverse 5'-CAGCACGGGAGTTTTGACCT-3'.

The relative expression levels of samples were presented using a semi log plot. The sequences of the primers used in this study were as follows: E-cadherin: forward 5'-AGTGCCAACTGGACCATTCA-3', reverse 5'-TCTTTGACCACCGCTCTCCT-3'; N-cadherin: forward 5'-ACTCGCAGACGCTCACACGC-3', reverse 5'-GCGGGACTCGCACCAGGAGT-3'; fibronectin: forward 5'-CCATCACTGTGTATGCTGTC-3', reverse 5'-TGGTTTGTCAATTTCTGTTCGG-3'; Snail: forward 5'-TCCAGGCTCGAAAGGCCTTCAAC-3', reverse 5'-GCAGCGTGTGGCTTCGGATGT-3'; Slug: forward 5'-GGGTGACTTCAGAGGCGCCG-3', reverse 5'-GGCGGTCCCTACAGCATCGC-3'; vimentin: forward 5'-CAAGGGCCAAGGCAAGTCGCG-3', reverse 5'-ACGCGGGCTTTGTCGTTGGTTA-3'; and Nodal forward 5'-AGCATGGTTTTGGAGGTGAC-3', reverse 5'-CCTGCGAGAGGTTGGAGTAG-3'.

3.2.7 FLOW CYTOMETRY ANALYSIS

For the detection of CSC markers, SUM149 cells were collected by trypsinization and stained with anti-CD44 and anti-CD24 antibodies and analyzed by multicolor flow cytometry. Briefly, combinations of fluorochrome-conjugated monoclonal antibodies against human CD44 (fluorescein isothiocyanate; catalog #555478; BD Biosciences) and CD24 (phycoerythrin; catalog #555428; BD Biosciences) or their

respective isotype controls were added to the cell suspension at concentrations recommended by the manufacturer and incubated at room temperature in the dark for 30 minutes. The labeled cells were washed and resuspended in FACS buffer (PBS + 1% FBS) and then analyzed on a FACSVantage flow cytometry system (BD Biosciences). Cell populations with high aldehyde dehydrogenase (ALDH) enzymatic activity were identified using an ALDEFLUOR fluorescent reagent system according to the manufacturer's method (STEMCELL Technologies Inc., Vancouver, Canada). Briefly, 1×10^6 SUM149 cells were collected following trypsinization, and 2.5×10^5 cells were resuspended in Aldefluor assay buffer containing ALDH substrate. As a negative control, we used di-ethylaminobenzaldehyde, a potent inhibitor of ALDH activity. Cells were then incubated at 37°C for 30 minutes with Aldefluor, washed with Aldefluor assay buffer, and stained with 1 µg/mL propidium iodide (Sigma) to discriminate viable cells from dead cells before detection in the green fluorescence channel (520-540 nm) on the flow cytometer (Beckman Coulter Gallios Instrument).

3.2.8 CELL MIGRATION AND INVASION ASSAYS

MDA-MB-231 scrambled shRNA and RANK shRNA cells were serum starved for 24 hours prior to stimulation with 25 ng/mL human soluble RANKL (product #R138; Leinco Technologies, Inc. St. Louis, MO) for 24 hours. For Boyden chamber trans-well migration assay (n=3), 1.5×10^5 cells in serum-free medium were layered in the top chamber of 24-well trans-well plates with serum-free media containing RANKL (25 ng/mL) in the lower chamber and incubated at 37°C for 6 hours. Cells in the top chamber (non-migrated) were removed, and cells in the bottom chamber (migrated)

were fixed with 0.1% crystal violet/20% methanol solution. For the invasion assay (n=3), 1.5×10^5 cells were plated in serum-free medium in the upper chamber of a Boyden chamber coated with BD Basement Membrane Matrigel Growth Factor Reduced Phenol Red Free with serum-free media containing RANKL (25 ng/mL) in the lower chamber. Twenty-four hours later, non-invading cells were removed from the upper chamber, and the underside membranes were fixed and stained as above in the cell migration assay. Migrated and invaded cells were quantitated by dissolving stained cells in a solution of 4% sodium deoxycholate and performing colorimetric reading of optical density at 595 nm. Results were analyzed using unpaired Student's *t*-test with a $*P$ value < 0.05 considered significant.

3.2.9 MAMMOSPHERE ASSAY

SUM149 or KPL-4 cells were plated into a 6-well plate at a density of 3×10^5 cells/well and pretreated for 24 hours with 10, 25, or 50 µM celecoxib. As a control, cells were pretreated with DMSO. For generation of primary mammospheres, SUM149 cells were seeded at 2×10^4 cells/well or KPL-4 cells were seeded at 2.5×10^3 cells/well into an ultra-low-attachment 6-well plate containing Mammocult Basal Medium (catalog #05621; STEMCELL Technologies, Inc.) supplemented with 1% Proliferation Supplement (catalog# 05621; STEMCELL Technologies, Inc.), 2 µg/mL Heparin (catalog #07980; STEMCELL Technologies, Inc.), and 0.12 µg/mL hydrocortisone (catalog #07904; STEMCELL Technologies, Inc.) with celecoxib or DMSO. On day 5, primary mammospheres were passaged to secondary mammospheres. Both primary and secondary mammosphere conditions were tested in triplicate. Mammospheres were quantitated on day 5 by staining with MTT reagent (0.4 mg/mL) for 2 hours and enumerated using GelCount software (Oxford Optronix).

Results were analyzed using unpaired Student's *t*-test with a *P* value < 0.05 being considered significant.

3.2.10 THREE-DIMENSIONAL (3D) MATRIGEL ASSAY

As a surrogate model for the invasive-like epithelial-to-mesenchymal (EMT) phenotype, the three-dimensional (3D) Matrigel assay was created to allow for the assessment of the 'invasiveness' of cells in a basement layer-like substrate. During the migratory process of breast cancer cells, the cells must invade the surrounding stroma which encapsulates the luminal and basal layers of the mammary tissue. The cells ability to transverse the basal layer is represented in the cells' ability to invade the basement membrane and help organize communication between cells embedded within the matrix as in the 3D-Matrigel assay. Matrigel is an enriched substance composed of key growth factors found in the basement membrane of tissue including factors found in the extracellular membrane (ECM) (106). The Matrigel used was derived from Engelbreth-Holm-Swarm (EHS) mouse sarcoma and contained the components laminin, collagen IV, heparin sulfate proteoglycans, and entactin/nidogen. Corning Basement Membrane Matrix (catalog #356234; BD Biosciences) was thawed on ice, and a bottom layer consisting of 65 µL of Matrigel solution was added per well into a four-well chamber slide (Lab-Tek II; Nalge Nunc International, Rochester, NY) then incubated at 37°C for 30 minutes to allow for solidification. Then 5×10^4 cells were resuspended in 500 µL of culture medium supplemented with 2% Matrigel on ice and added to the solidified bottom layer. At 24-hours post-incubation at 37C, images of the cell projections were captured and tube formation (invasive structures) was quantitated using S.CORE (S.CO LifeSciences GmbH, Munich, Germany) or Wimasis (GmbH, Munich, Germany) analysis software.

3.2.11 IBC XENOGRAFT MODEL

All animal experiments were approved by the Institutional Animal Care and Use Committee (IACUC protocol 02-03-02134) of MD Anderson Cancer Center. A total volume of 0.15 mL of SUM149 cell suspension containing 2×10^6 cells with 50% Matrigel was injected into the fourth inguinal mammary gland of 8-week old female *nu*/*nu* mice. The mice were fed *ad libitum* with a regular diet for 3 weeks, at which time the tumors were well established. The mice were then randomly allocated (n=8 per group) to control diet (regular food pellets) or to one of two treatment diets, 250 ppm or 500 ppm celecoxib, for the following 5 weeks. Mice were weighed and estimated to be about 25 g/mouse and food intake per mouse was estimated to be about 3 g/day. The diet dose was calculated based on the formula: diet dose (DD) = Single daily dose (SD) x body weight (BW) x daily food intake (FI) (www.researchdiets.com/resource-center/diet-dose-calculator.com; Research Diets, Inc. New Brunswick, NJ). The 250 and 500 ppm (mg/kg of mouse body weight/day) diet dose translated to approximately 2083 mg of celecoxib/kg BW, and approximately 4167 mg of celecoxib/kg BW, respectively. Tumor volumes were determined by calculating weekly caliper measurements using the following formula: tumor volume (V) = ($L \times W^2$) × 0.5, where L is the length and W is the width of the tumor. Tumor growth inhibition (%) was calculated as 1 - (tumor volume change of treatment group / tumor volume change of control group) × 100%.

3.2.12 STATISTICAL ANALYSIS

Data are presented as mean ± SD except where otherwise stated. When two groups were compared, Student's *t*-test was used ($P < 0.05$ was considered significant).

3.3 RESULTS

3.3.1 *IN VITRO* TARGETING OF COX-2 AND EGFR IN IBC CELLS

We proposed EGFR to regulate the expression of COX-2 in IBC cells since we initially found a positive correlation between EGFR and COX-2 expression levels in IBC tumor samples (Figure 3.1). In determining if this correlation existed in IBC cell lines at the protein level, we immunoblotted for COX-2, and activated EGFR in IBC and non-IBC cell lines. We observed the IBC cell line SUM149 to co-express both COX-2 and activated EGFR (Figure 3.2). We observed EGF stimulation to increase COX-2 protein expression in SUM149 cells (Figure 3.3), and EGFR-targeted siRNA to suppress COX-2 expression (Figure 3.4). In addition, we observed erlotinib treatment in SUM149 cells to decrease COX-2 expression (Figure 3.5). The occurrence of decreased COX-2 levels subsequent to suppressed EGFR expression and activity indicated that EGFR positively regulates COX-2 expression in SUM149 cells. This finding supports our hypothesis that EGFR positively regulates COX-2 in IBC cells. As previous findings suggested that COX-2-activated expression is regulated through the EGFR pathway (34), we investigated the levels of PGs to assess COX activity following treatment with celecoxib and erlotinib and vehicle-treated SUM149 cells at 24h and 48h time points (Figure 3.6). Basal levels of PGs (PGE_2 and $PGF_{2\alpha}$) were checked in a panel of IBC and non-IBC cell lines (Figure 3.7), in which we found PGs to be higher in the IBC cell lines compared to the non-IBC cell lines. Collectively, these findings suggest EGFR to regulate the expression and activity of COX-2 in IBC cells and that pharmacological intervention with COX-2 or EGFR-targeted therapy may reduce the tumorigenicity of IBC cells as observed by the downregulation of PGE_2, the most tumorigenic byproduct

of COX-2 activity. In determining whether COX-2 plays a functional role in the tumorigenicity and progression of IBC cells, we investigated the biological function of COX-2 in *in vitro* studies and an *in vivo* study.

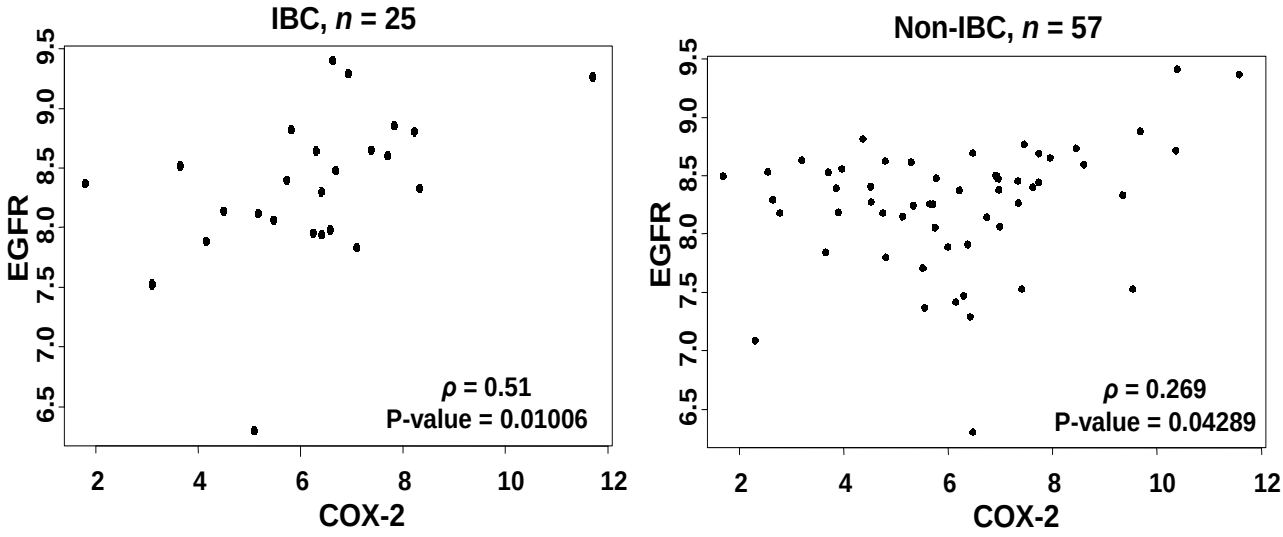

Figure 3.1 EGFR correlates with COX-2 gene expression in breast cancer. We correlated EGFR and COX-2 gene expression in IBC (n=25) and non-IBC (n=57) tumor samples constructed on an Affymetrix cDNA microarray. The correlative analysis was performed using the Spearman's Rank Correlation Coefficient analysis. IBC data (*P*-value = 0.01; rho = 0.51); non-IBC data (*P*-value = 0.04; rho = 0.269).

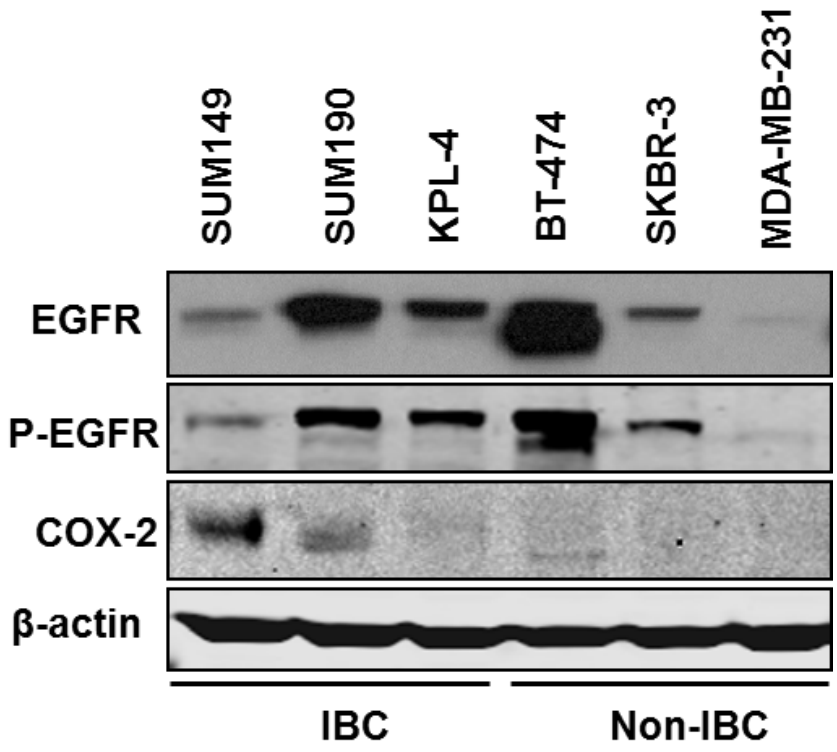

Figure 3.2 COX-2 and EGFR expression in IBC and non-IBC cell lines.

SDS-PAGE was performed using total protein lysate samples collected from IBC and non-IBC cell lines cultured under normal conditions. A western blot was performed to immunoblot for basal level expression of COX-2, EGFR, and p-EGFR in IBC and non-IBC cell lines. B-actin was used as a loading control.

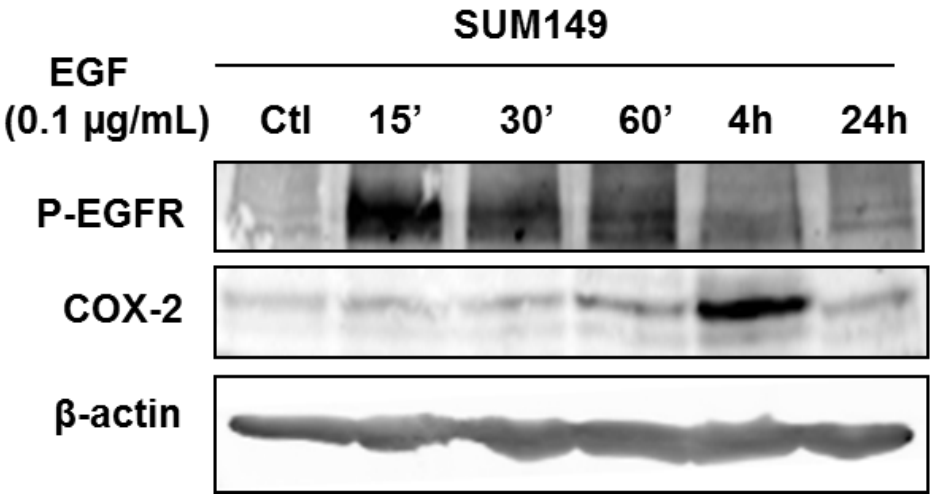

Figure 3.3 EGF stimulates COX-2 expression in SUM149 cells.

SUM149 cells were serum-starved then stimulated with 0.1 µg/mL of EGF in serum-free medium for the time points as indicated (15, 30, or 60 minutes and 4 or 24 hours). Ctl; untreated control. COX-2, EGFR, and p-EGFR proteins were immunoblotted. B-actin was used as a loading control. Odyssey imager was used to detect the protein.

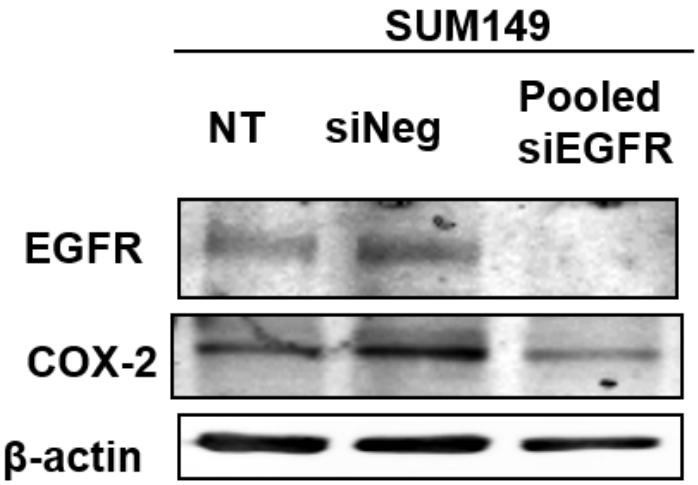

Figure 3.4 Suppression of EGFR expression reduced COX-2 expression in SUM149 cells. SUM149 cells were transiently transfected with pooled EGFR-targeted siRNAs, negative siRNA, or not transfected as a control for 48 hours prior to harvesting and lysing cells to collect and isolate total protein lysate. A total of 30 µg of protein was loaded/well for SDS-PAGE on a 8% resolving gel and transferred to a PVDF membrane. The membrane was immunoblotted with primary antibodies for pEGFR, total EGFR, and COX-2. β-actin was immunoblotted as a loading control. Samples were probed with AlexaFluor (680 nm) secondary antibody. The membrane was scanned using the LI-COR imager. NT; non-transfected, neg; negative, and si; siRNA.

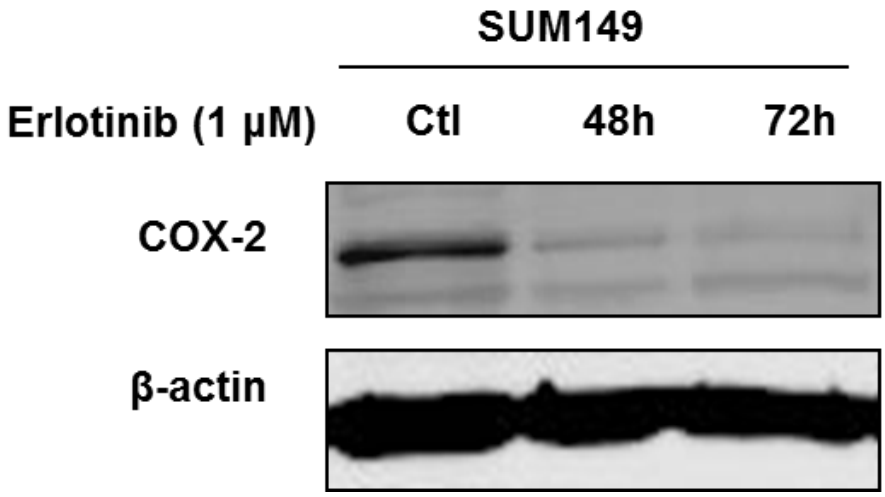

Figure 3.5 Erlotinib reduced COX-2 levels in SUM149 cells.

SUM149 cells were treated with EGFR-specific tyrosine kinase inhibitor, erlotinib, for 48 and 72 hours prior to immunoblotting for COX-2 and β-actin as a loading control. Ctl; untreated control.

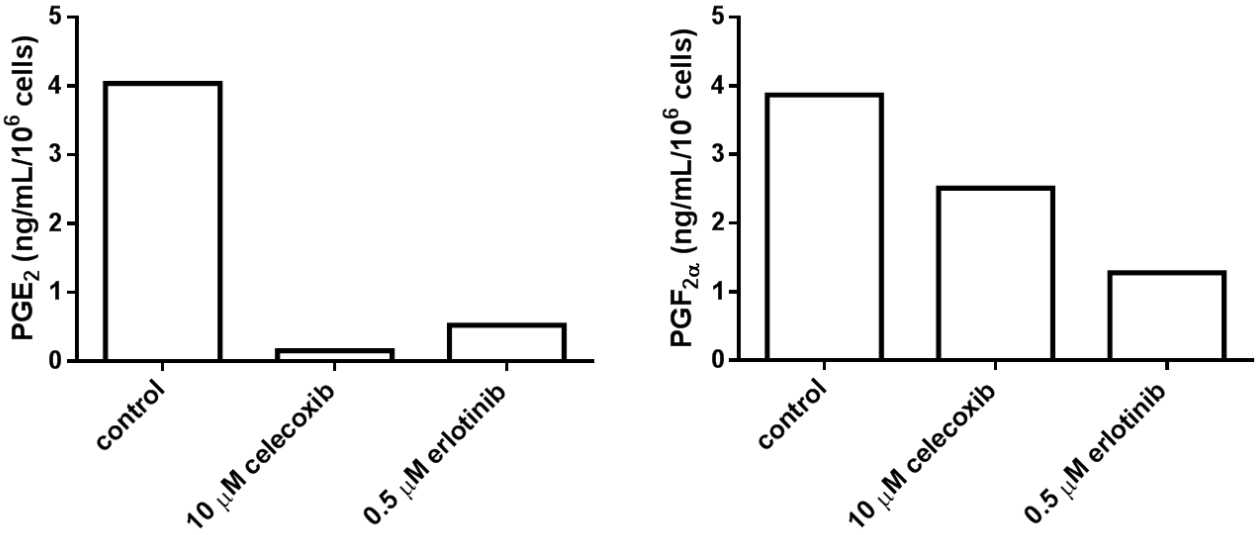

Figure 3.6 Celecoxib and erlotinib reduced PGE_2 and $PGF_{2\alpha}$ levels in SUM149 cells. SUM149 cells were treated with celecoxib (10 µM), erlotinib (0.5 µM), or DMSO (control) for 48 hours prior to collecting cells and cell media for analysis. Each sample contained 3 x 10^6 cells/mL of 1X PBS for HPLC/MS analysis of insoluble PGE_2 (measured from cells collected at 48 hours post-treatment) and soluble $PGF_{2\alpha}$ (measured from media collected at 48 hours post-treatment). Quantitated PGE_2 and $PGF_{2\alpha}$ levels were calculated as ng/mL/10^6 cells and results were graphed using GraphPad Prism version 6.01 software.

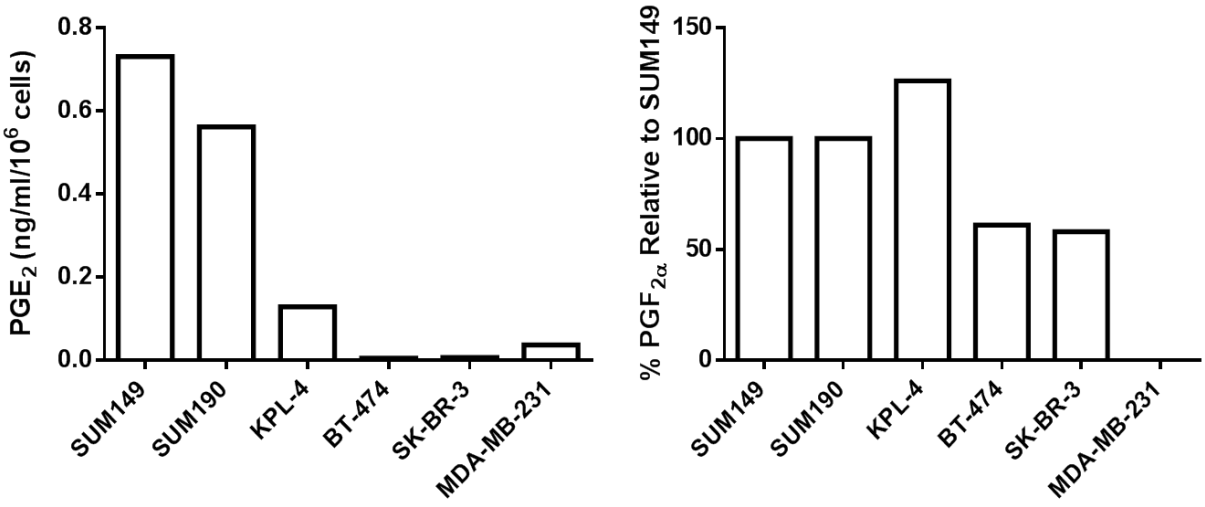

Figure 3.7 IBC cell lines have higher levels of COX activity compared to non-IBC cell lines. Under normal culture conditions, a panel of human IBC and non-IBC cell lines were analyzed for soluble PGE_2 and $PGF_{2\alpha}$ levels at 1 x 10^6 cells/mL of 1X PBS by HPLC/MS analysis. Quantitated soluble PGE_2 concentrations (ng/mL/10^6 cells) and $PGF_{2\alpha}$ (% relative to SUM149) were graphed using GraphPad Prism version 6.01software.

3.3.2 COX-2 REGULATES IBC CELL MIGRATION AND INVASION

Previous studies have found COX-2 to regulate the tumorigenicity and invasiveness of breast cancer cells, however, the mechanism by which COX-2 promotes IBC tumorigenicity and invasiveness has not been well studied in IBC (58, 64). PGE_2 is known to have tumorigenic effects, and to promote a stem cell-like phenotype, however, this link remains to be elucidated in IBC. In finding out whether the COX-2 pathway is required for IBC cell migration and invasion, we performed a cell migration and invasion assay using SUM149 cells. Cells were serum-starved for 24 hours prior to stimulation with 0.5 µM PGE_2 or $PGF_{2\alpha}$ or untreated as a control for 24 hours. We observed SUM149 cell migration and invasion significantly increased by PGs (Figure 3.8), while celecoxib decreased SUM149 cell migration and invasion (Figure 3.9).

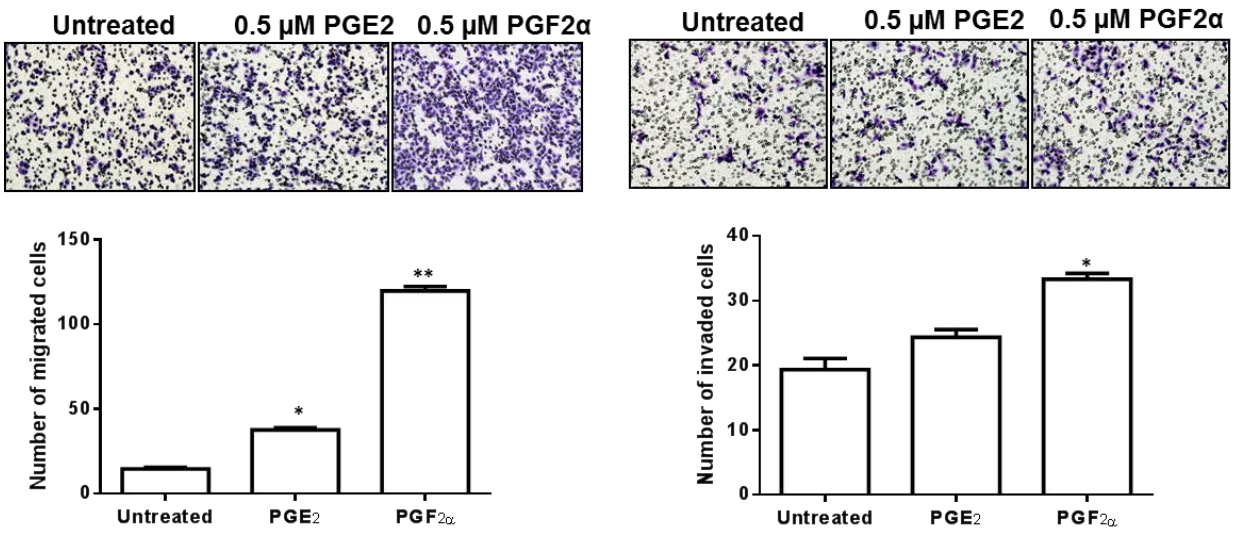

Figure 3.8 Prostaglandin stimulation increased SUM149 cell migration and invasion. SUM149 cells were serum-starved for 24 hours then either left untreated as a control or treated with PGE_2 or $PGF_{2\alpha}$ (0.5 µM) in triplicate for 24 hours. Cells were seeded at 2.5 x 10^5 cells/well in which cells were incubated with serum-free media containing PG or without PG (untreated) for A) 6-hour cell migration assay (n=3) or B) 24-hour cell invasion assay (n=3). Migrated and invaded cells were stained with 0.1% crystal violet/20% methanol solution for 5 minutes and under a light microscope cells were counted and averaged per well. Results were graphed using GraphPad Prism version 6.01 software. *P= 0.002; **P < 0.0001.

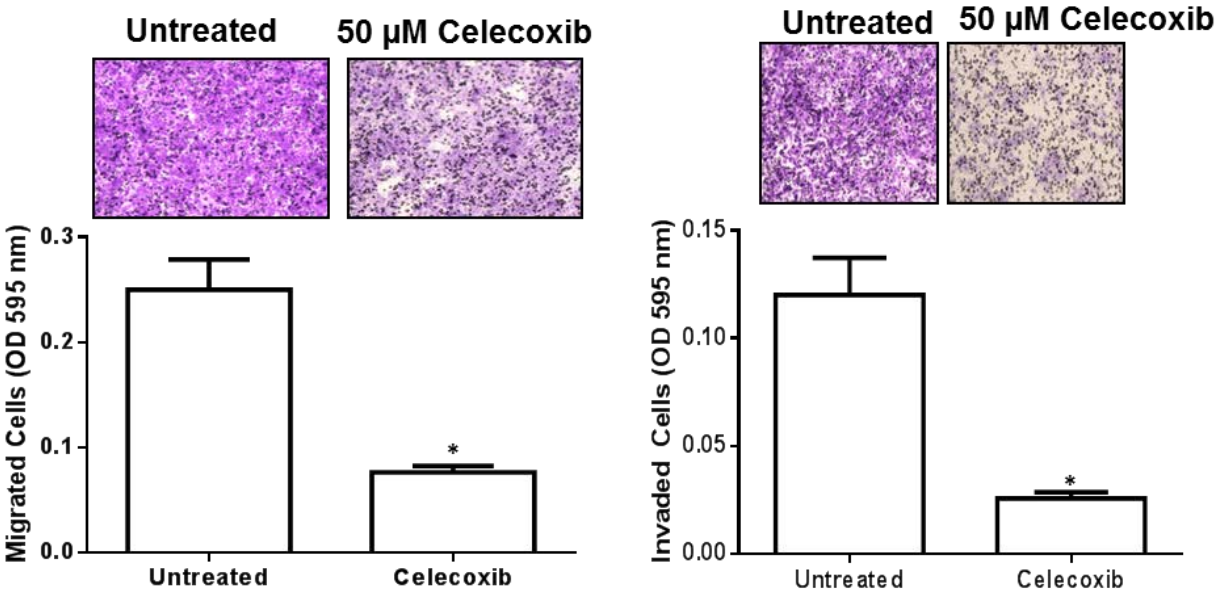

Figure 3.9 Celecoxib inhibited the migration and invasion of SUM149 cells. SUM149 cells were pre-treated with 50 µM of celecoxib or untreated in triplicate for 24 hours prior to seeding at a density of 2.5 x 10^5 cells/well for A) 6-hour cell migration assay (n=3), or B) 24-hour cell invasion assay (n=3). Migrated and invaded cells were stained with 0.1% crystal violet/20% methanol solution for 5 minutes then dissociated from the membrane by incubation with 4% sodium deoxycholate for 20 minutes. Samples were quantitated by luminescence (595 nm) using Perkin-Elmer Victor X microlabel plate reader. Results were graphed using GraphPad Prism version 6.01 software. *$P < 0.01$.

3.3.3 THE EMT AND CANCER STEM-LIKE CELL PHENOTYPE IN IBC CELLS IS REGULATED BY THE COX-2 PATHWAY

The reversible process of EMT allows cells to acquire molecular features such as upregulation of mesenchymal markers Fibronectin, Vimentin, N-cadherin, and transcription factor Twist, and downregulation of epithelial marker E-cadherin. Whether through PG stimulation or treatment with a selective COX-2 inhibitor, the COX-2 pathway is shown to play a role in EMT in breast cancer cells. The link between the COX-2 pathway, EMT and stem-like properties has not been elucidated in IBC cells. To investigate whether the COX-2 pathway regulates EMT and stem-like properties in IBC cells, we treated SUM149 cells with PGs (0.5 μM) or celecoxib (10 or 25 μM) and immunoblotted for EMT markers. We observed PGs to down-regulate E-cadherin, while up-regulate mesenchymal markers, Fibronectin, Vimentin, and Twist (Figure 3.10 left panel). In celecoxib-treated SUM149 cells, E-cadherin was up-regulated, while mesenchymal markers, Fibronectin, Vimentin, and N-cadherin were down-regulated (Figure 3.10 right panel). In addition, we observed celecoxib-treated SUM149 and KPL-4 IBC cells to demonstrate a reduction in projection formation in 3D matrigel culture (Figure 3.11). PG-stimulation increased the CSC population, CD44+/CD24- subpopulation, in SUM149 cells (Figure 3.12). Aldefluor (ALDH1) activity in SUM149 cells were increased by PGs, but decreased by celecoxib (Figure 3.13). The formation of SUM149 primary and secondary mammospheres was decreased by celecoxib (Figure 3.14).

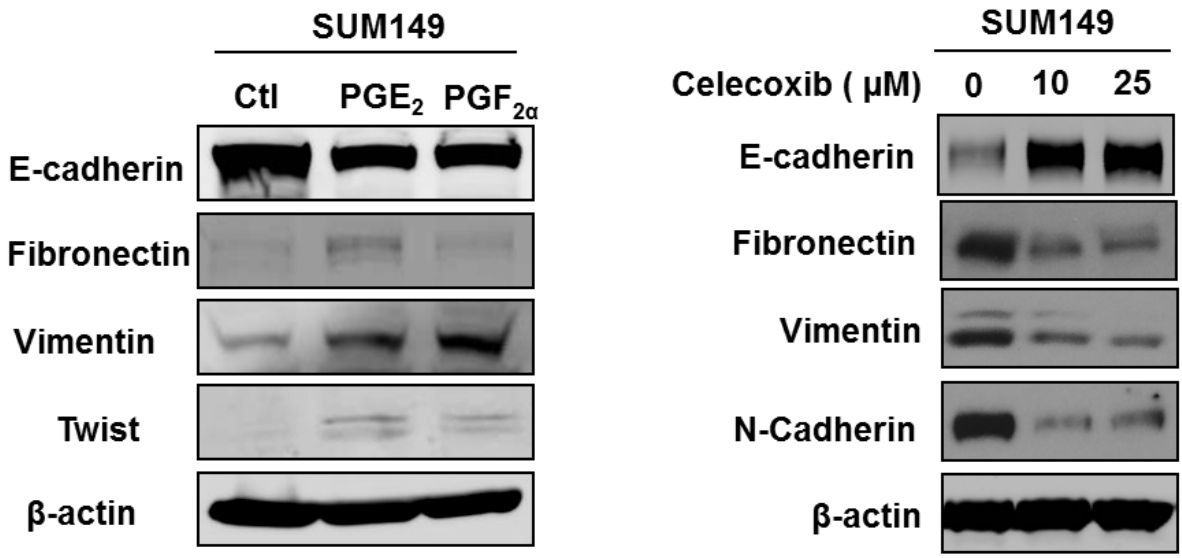

Figure 3.10 The expression of EMT markers are regulated by COX-2 activity in SUM149 cells. SUM149 cells were stimulated with PGE_2 or $PGF_{2\alpha}$ (0.5 μM) or unstimulated as a control (Ctl) for 72 hours under serum-free conditions following a 24 hour starvation and lysate was immunoblotted for EMT markers (left panel). SUM149 cells were treated with vehicle control (0), or celecoxib (10 or 25 μM) for 48 hours and cell lysate was immunoblotted for EMT markers (right panel). B-actin was immunoblotted as a loading control.

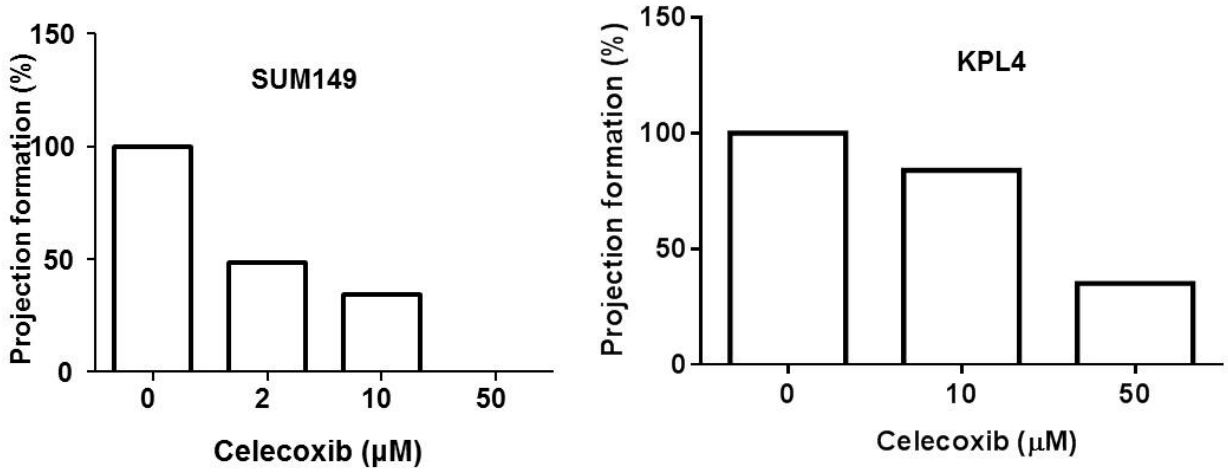

Figure 3.11 Celecoxib suppressed the EMT-like phenotype in 3D Matrigel culture. SUM149 cells and KPL-4 cells were treated with celecoxib (2, 10, and 50 µM) or untreated (0) in triplicate for 24 hours in 2D culture and under Matrigel culture conditions for another 24 hours. Images of the projections or tube formations (not shown) were taken using a light microscope connected to a Nixon camera. Projections were quantitated and averaged by S.Core for SUM149 EMT assay and Wimasis for KPL-4 EMT assay. Using GraphPad Prism version 6.01 software, results were calculated as a percentage of projections formed relative to untreated cells.

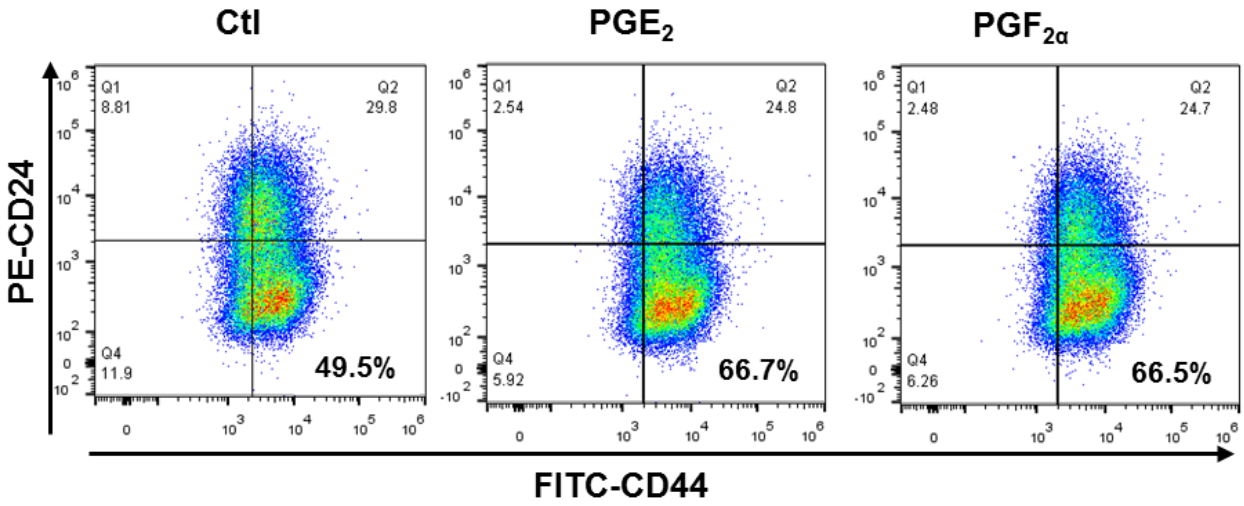

Figure 3.12 Prostaglandins increased the CD44+CD24- cell population in SUM149 cells. SUM149 cells were stimulated with PGE_2 or $PGF_{2\alpha}$ (0.5 µM) for 24 hours prior to staining with FITC-CD44 and PE-CD24 antibodies. Untreated control SUM149 cells had a 49.5% CD44+CD24- subpopulation, while PGE_2 and $PGF_{2\alpha}$ stimulated SUM149 cells had a CD44+CD24- subpopulation of 66.7% and 66.5%, respectively.

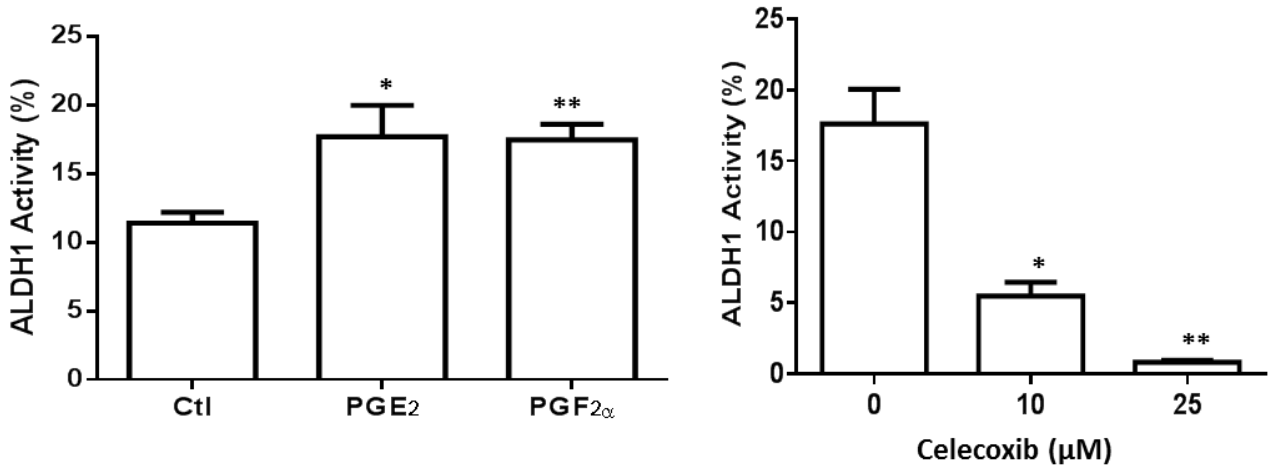

Figure 3.13 COX-2 increased the Aldefluor activity of SUM149 cells. SUM149 cells were stimulated with PGE_2 or $PGF_{2\alpha}$ for 6 days and the aldefluor activity was detected by flow cytometry after treatment. **P* = 0.0109; ***P* = 0.0016 (left panel), or treated with celecoxib for 4 days and detected for Aldefluor activity by flow cytometry, **P* = 0.0013; ***P* = 0.0003 (right panel).

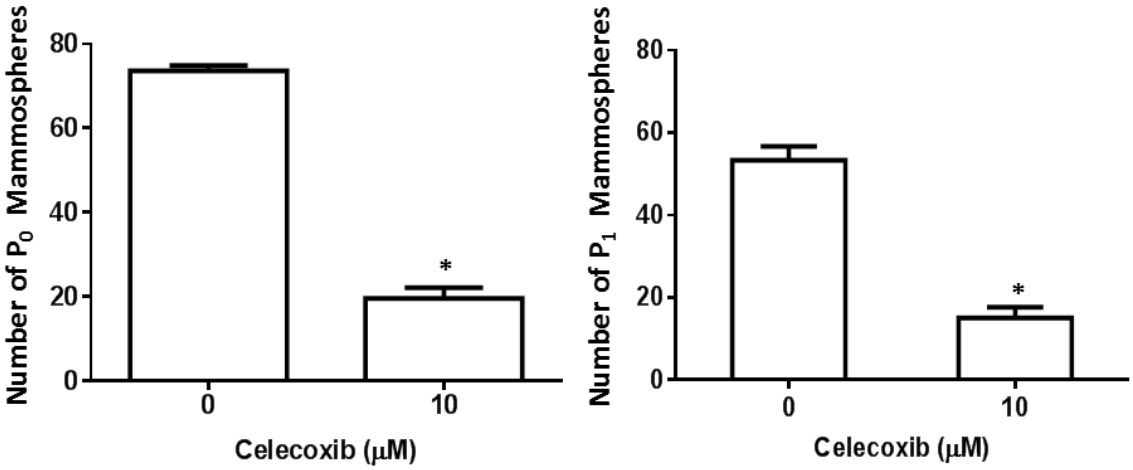

Figure 3.14 Celecoxib reduced SUM149 mammosphere formation. SUM149 cells were plated at a density of 3 x 10^4 cells/well and treated with DMSO as a control (n=3) or celecoxib (10 μM) (n=3) for 5 days under mammosphere conditions in a low-attachment plate. Live cells dissociated from primary (P_0) mammospheres were stained with trypan blue solution and counted using the Cellometer prior to re-plating and culturing for secondary (P_1) mammospheres. Mammospheres were stained with 5 mg/mL MTT reagent and enumerated after 5 days using GelCount plate reader and software. *P < 0.005.

3.3.4 THE TUMORIGENICITY OF IBC IS SUPPRESSED BY CELECOXIB

The aggressiveness of IBC is likely due to the stem cell-like phenotype which promotes tumorigenicity (64). As observed with other breast cancer subtypes, COX-2 activity has tumorigenic effects, which can be inhibited by the selective COX-2 inhibitor celecoxib. In a previous study, we had observed erlotinib, an EGFR inhibitor, to suppress IBC tumorigenicity and metastasis (34). To determine whether celecoxib has anti-tumorigenic effects in an IBC xenograft mouse model, we treated an orthotopic SUM149 xenograft mouse model with celecoxib. We investigated the effects of celecoxib on IBC tumorigenicity by the measurement of tumor growth and the levels of PGE_2 and $PGF_{2\alpha}$ in the tumors. We observed celecoxib treatment to significantly reduce tumor growth compared to control (untreated) mice (Figure 3.15). In addition, we found PG levels to be lower in tumors derived from celecoxib-treated mice compared to control mice (Figure 3.16). Since EMT is a stem cell-like characteristic associated with the invasiveness and CSC population in breast cancer, we analyzed the expression of epithelial and mesenchymal markers including Nodal, an embryonic stem cell regulator found to be highly expressed in invasive breast cancers. Relative to the control tumors, we found epithelial marker, E-cadherin, up-regulated in celeocoxib-treated tumors, while mesenchymal markers, Fibronectin, N-cadherin, Snail, Slug, Vimentin, and stem cell regulator, Nodal, down-regulated in celecoxib-treated tumors (Figure 3.17).

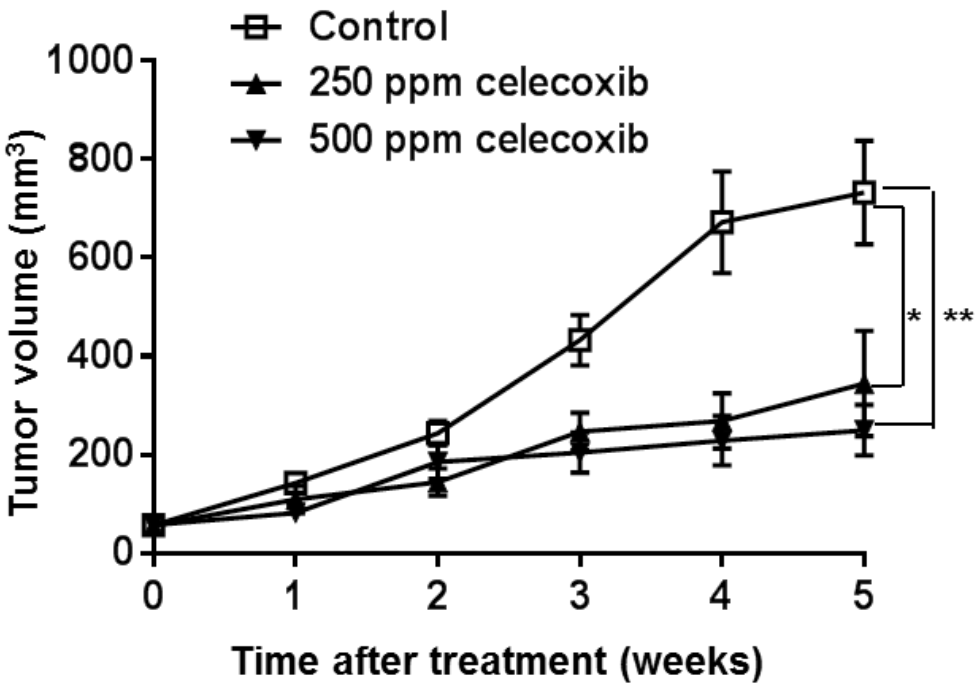

Figure 3.15 Celecoxib reduced SUM149 tumor growth in mice. A solution of 50% Matrigel/ 2 x 10^6 SUM149 parental cells were orthotopically injected into the fifth inguinal mammary fat pad of 8 week old female nu/nu mice (n=24) and treated with 250 ppm (n=8) or 500 ppm (n=8) celecoxib diet or control (normal) diet (n=8) following initial tumor formation by week 3. Tumor volumes were measured twice/week using calipers over a period of five weeks. The inhibition of tumor growth rate was calculated and results were graphed using GraphPad Prism version 6.01 software. P-value was determined by student t-test; *P = 0.0215, **P = 0.0011.

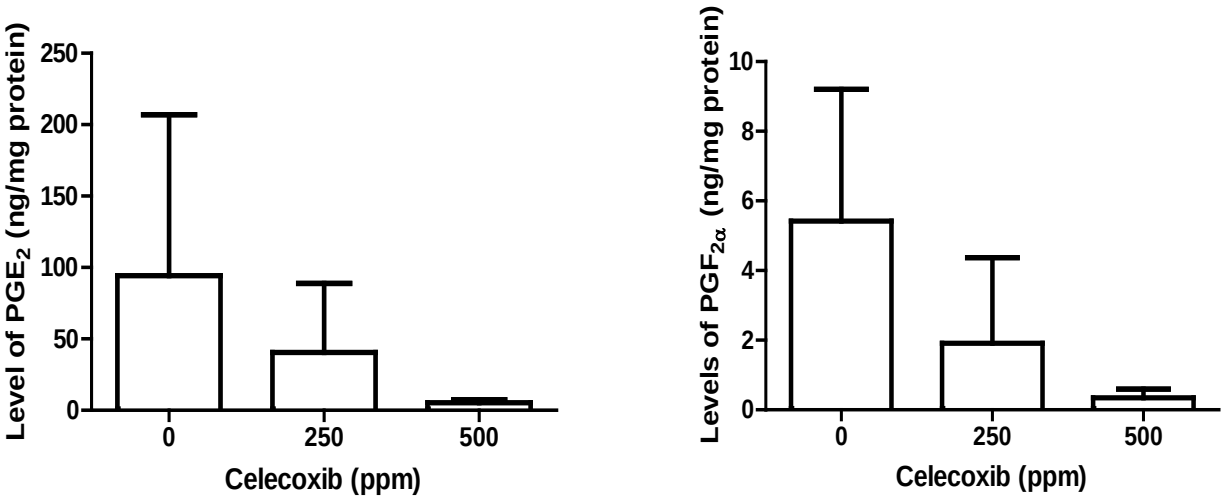

Figure 3.16 Celecoxib reduced the levels of PGE_2 and $PGF_{2\alpha}$ in orthotopic tumors in mice. Resected tumors from the mice were homogenized and cells were resuspended and lysed prior to analysis by LC-MS/MS for PGE_2 and $PGF_{2\alpha}$ levels (ng) relative to total protein (mg) determined by Bradford Assay.

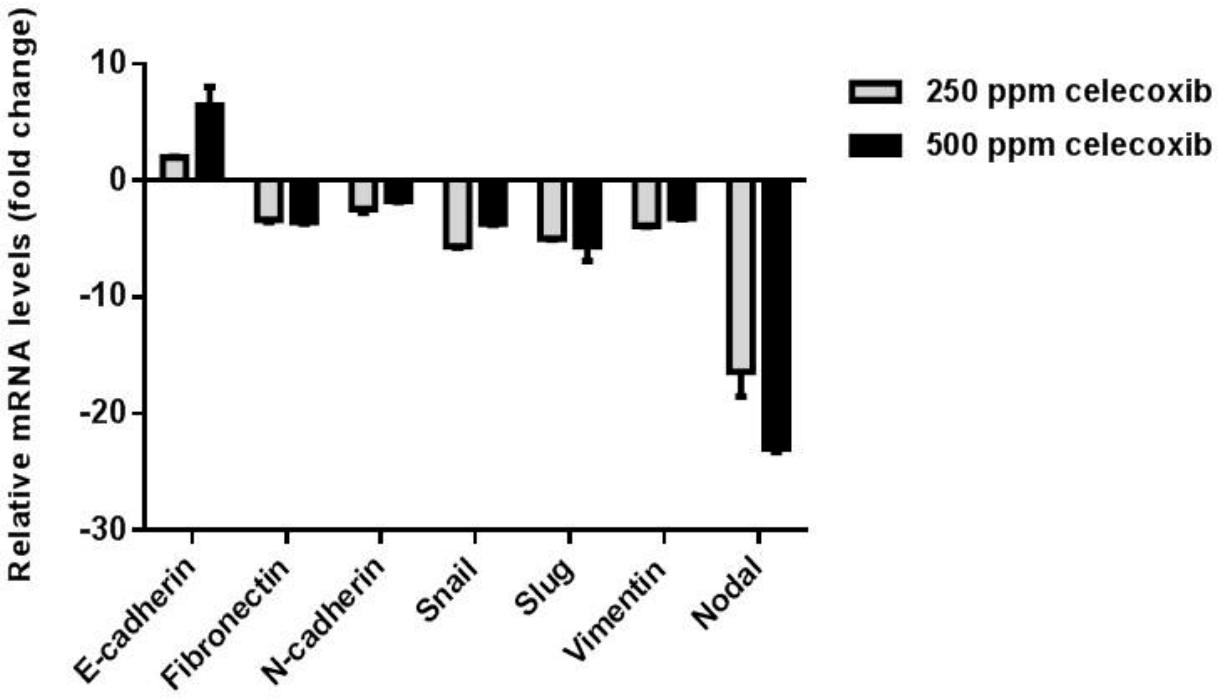

Figure 3.17 EMT markers were modulated by celecoxib treatment in SUM149 xenograft tumors. Epithelial marker E-cadherin and mesenchymal markers (Fibronectin, N-cadherin, Snail, Slug, and Vimentin) including stem cell marker, Nodal, were measured in SUM149 xenograft tumors by qRT PCR. Celecoxib-treated (250 ppm and 500 ppm) mice had increased E-cadherin and reduced mesenchymal markers relative to control treated mice. Expression of stem cell regulator, Nodal, was reduced in tumors from celecoxib-treated mice.

3.3.5 RECOMBINANT HUMAN NODAL MITIGATES THE EFFECTS OF CELECOXIB IN IBC CELLS

Following our observation that celecoxib treated mice with xenograft SUM149 tumors downregulated Nodal gene expression, we predicted that the inhibition of COX-2 in IBC cells has anti-tumorigenic effects by suppressing the Nodal pathway. To further investigate COX-2 regulation of Nodal, we investigated the *in vitro* effects of celecoxib on Nodal expression in SUM149 cells by analyzing Nodal gene expression in cells cultured *in vitro* in 3D Matrigel. We observed PGE_2 and $PGF_{2\alpha}$ stimulation to increase Nodal expression while celecoxib decreased Nodal expression in SUM149 cells (Figure 3.18). To determine the potential anti-metastatic effects of celecoxib in IBC and regulation of the CSC phenotype, we tested the combination treatment of celecoxib with recombinant human Nodal (rhNodal) on the migration, invasion, and mammosphere formation of SUM149 cells. We observed celecoxib to reduce SUM149 cell migration and invasion (Figure 3.19), and mammosphere formation (Figure 3.20) and rhNodal to mitigate celecoxib-mediated inhibition of SUM149 cell migration, invasion, and mammosphere formation.

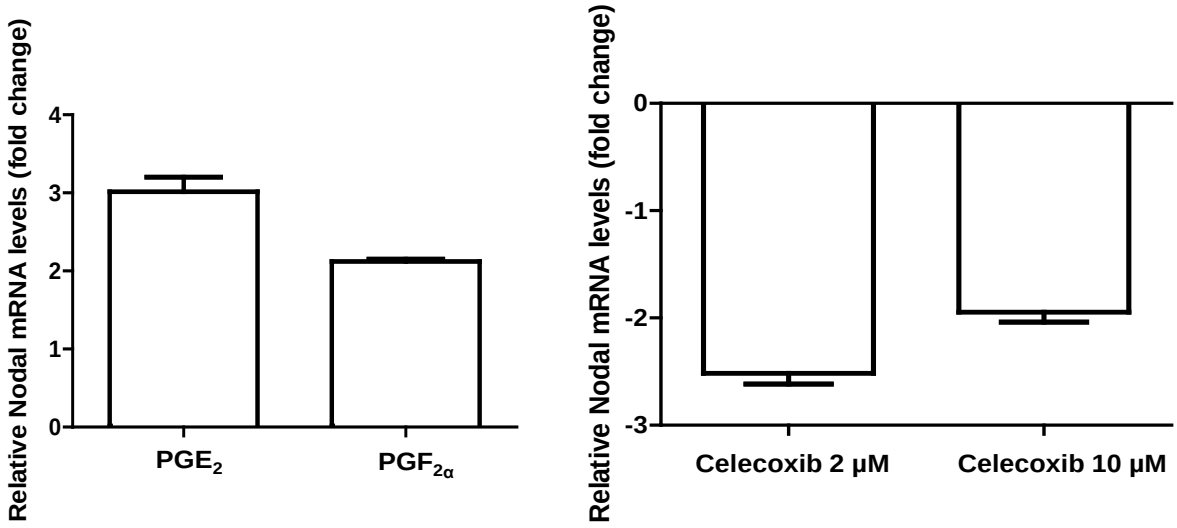

Figure 3.18 COX-2 regulates Nodal expression in SUM149 cells in 3D Matrigel culture. SUM149 cells were treated with 0.5 μM PGE_2 or $PGF_{2\alpha}$ for 48 hours (right panel) or treated with celecoxib for 24 hours under 3D Matrigel culture conditions (left panel) prior to qRT PCR analysis for Nodal expression levels (n=3). Fold-change in Nodal expression was measured relative to control (untreated) SUM149 cells in 3D Matrigel culture.

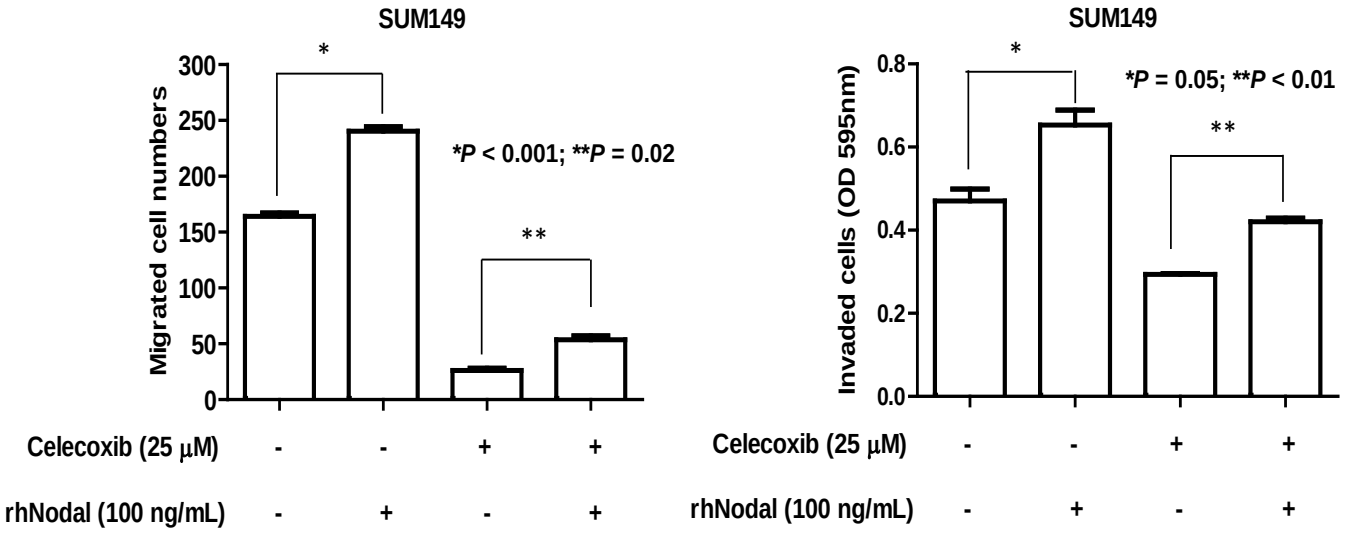

Figure 3.19 Recombinant human Nodal mitigated celecoxib-mediated inhibition of SUM149 cell migration and invasion. SUM149 cells were pre-treated with celecoxib (25 μM) or rhNodal (100 ng/mL), or in combination prior to a 6 hour cell migration and 24 hour cell invasion assay (n=3). Cells were stained with 0.1% crystal violet/20% methanol solution for 5 minutes then dissolved using 4% sodium deoxycholate. Migrated or invaded cells were quantified by luminescence imaging using a Perkin-Elmer multilabel plate reader (595 nm).

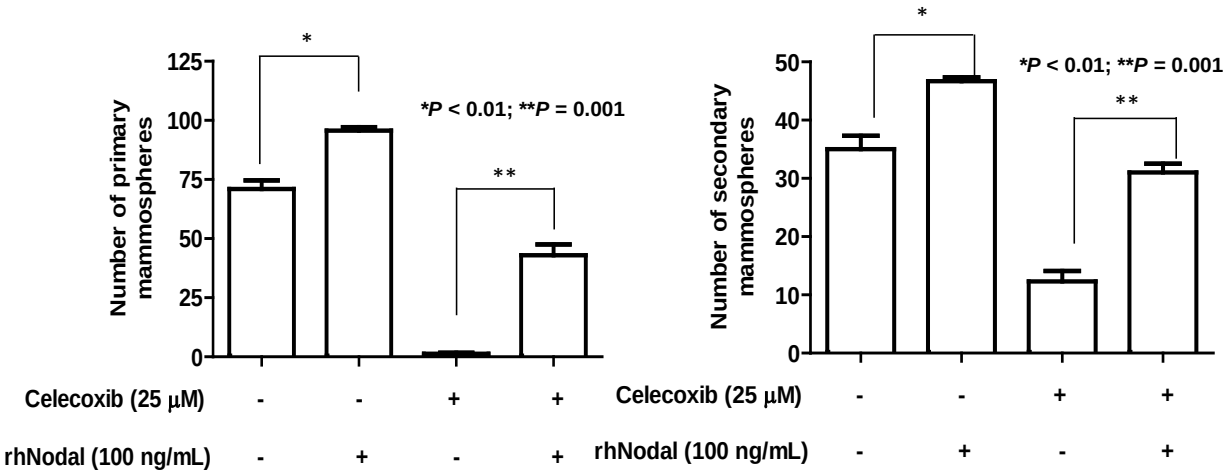

Figure 3.20 Recombinant human Nodal mitigated the effects of celecoxib in SUM149 mammosphere formation. SUM149 cells were treated with celecoxib or rhNodal alone, or in combination under mammosphere assay conditions. Primary mammospheres were passaged following cell counting to re-plate 3 x 10^4 cells/well for secondary mammosphere formation prior to staining with 5 mg/mL MTT reagent and quantification by GelCount software.

3.4 DISCUSSION

To determine if there was a correlation between EGFR and COX-2 in IBC, we performed a cDNA microarray analysis using IBC and non-IBC patient cohorts. Based upon the observation of a significantly tighter correlation between EGFR and COX-2 gene expression in IBC primary compared to non-IBC tumors, and IBC cell lines with higher levels of PGE_2 and $PGF_{2\alpha}$, it is conceivable that EGFR-positive IBC cells may elicit an increased sensitivity to COX-2 inhibition. Our observation of EGFR and COX-2 correlation in IBC and non-IBC is in accordance with other reported links between COX-2 and HER family members, such as EGFR and HER2/*neu*. In a study reported by Subbaramaiah *et al*. the overexpression of HER2 was associated with increased levels of COX-2 in human breast cancers, and COX-2 is the functional intermediate linking HER2 and aromatase, suggesting that inhibitors of PGE_2 synthesis may suppress estrogen biosynthesis in breast tissue (107, 108). The significance of COX-2 in IBC has not been thoroughly investigated and the biological role of COX-2 in EGFR-expressing IBC is unknown. Our study is the first one to find a correlation between EGFR and COX-2 gene expression in an IBC cohort, which suggests the importance of COX-2 in EGFR regulation in IBC. IBC is a heterogeneous breast cancer subtype, which has not been molecularly differentiated from non-IBC. By gene expression profiling, it was reported that IBC is composed of several TNBC molecular subtypes described in non-IBC tumors by Lehmann B.D. *et al.*; however, IBC was not found to be specific for either one of the molecular subtypes (9, 17). The pathological complete response (pCR) rate was observed to be lower in TN-IBC compared to HR+ and HER2+ IBC patients suggesting poorer prognosis in TN-IBC patients (109). By

stratifying IBC tumors by TNBC molecular subtypes, we may be able to identify EGFR and COX-2 expressing IBC tumors with a specific TNBC molecular subtype.

Upon observing a correlation between COX-2 and EGFR expression in IBC tumors along with elevated PGE_2 and $PGF_{2\alpha}$ levels in a panel of IBC cell lines compared to non-IBC cell lines, we investigated EGFR-regulation of COX-2 expression and activity via EGFR-targeted siRNA or erlotinib treatment with erlotinib. Based on our findings, we concluded that the EGFR pathway regulates COX-2 expression and activity in IBC cells. It was reported that the regulation of COX-2 expression in breast cancer cells may occur through activation of the PI3K/AKT and MAPK pathways by EGFR (110). The regulation of COX-2 could potentially occur through the MAPK pathway, which transcriptionally activates expression of COX-2 in addition to several other proteins involved in breast tumor invasion and migration. Our hypothesized model implicates the extracellular

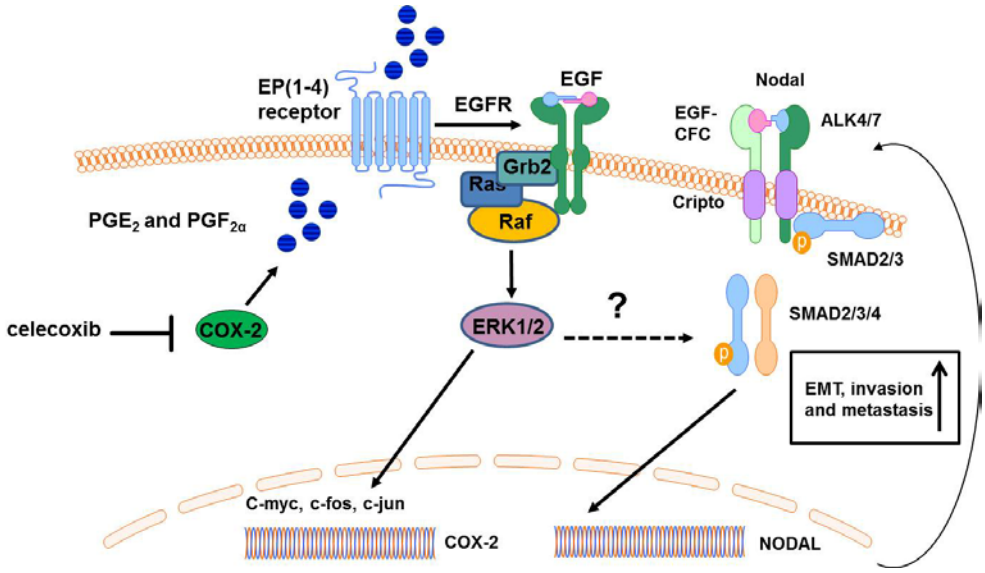

ILLUSTRATION 3.4 A PROPOSED MODEL FOR EGFR/COX-2-MEDIATED NODAL SIGNALING IN IBC CELLS

Cross-talk signaling between EGFR and COX-2 may activate ERK1/2 signaling and stimulate transcription of the NODAL gene through phosphorylation of SMAD2 linker region and maintaining a positive feedback loop enhancing Nodal signaling in the cell. Deregulation of the Nodal pathway leads to enhanced cell motility and invasion.

signal-regulated kinase 1/2 (ERK1/2) pathway downstream of EGFR (illustration 3.4).

Our rationale for speculating that the ERK1/2 pathway may be the key mediator for EGFR/COX-2 activity is also based on a prior investigation in our laboratory in which inhibition of ERK1/2 but not PI3K/AKT resulted in a synergistic outcome in combination with erlotinib treatment of IBC cells (34). Determining whether EGFR/COX-2 regulates Nodal in an ERK/1/2 dependent manner remains to be determined in future studies.

We observed that in *in vitro* studies the COX-2 pathway promoted IBC cell migration and invasion, and the invasive-like EMT phenotype. In an *in vivo* SUM149 xenograft mouse model, the inhibition of tumor growth by celecoxib occurred concomitantly with the down-regulation of EMT-associated events, including decreased Nodal expression. Our study demonstrated that the COX-2 pathway regulated the CSC population in SUM149 cells as suggested by our results from surrogate cancer stem cell assays, mammosphere formation assay, Aldefluor assay, and $CD44^{+}/CD24^{-/low}$ staining and flow cytometry analysis. Based on our findings, we concluded the suppression of COX-2 to block the progression and metastatic potential of IBC cells through down-regulation of the CSC population. Recent studies have linked the progression of breast cancer to CSCs and that targeting CSCs might be an effective strategy to circumvent drug resistance and reduce tumor recurrence (111). IBC is considered to be a highly aggressive breast cancer subtype with a CSC phenotype (112), and a poor long-term outcome associated with a high risk of relapse. In addition, prior studies have demonstrated a functional role for COX-2 in EMT and breast cancer stem cells. It was reported by Bocca C. *et al*. that hypoxia induced HIF1α expression which in turn elevated COX-2 expression and promoted an EMT phenotype in breast

cancer cells (60). Relevant to this study, EMT in IBC cells can potentially be triggered by elevated COX-2 expression under hypoxic conditions in the presence of growth factors and cytokines in the microenvironment.

We sought to elucidate the mechanism of COX-2-mediated EMT in celecoxib treated SUM149 cells. By performing data analysis of celecoxib-modulated gene expression using a human EMT RT PCR array kit, we observed down-regulation of embryonic stem cell regulator Nodal in SUM149 cells treated with celecoxib for 72 hours. This result indicated Nodal to be a potential downstream mediator of COX-2-mediated IBC cell progression (data not shown). We confirmed Nodal regulation by COX-2 through *in vitro* studies and in a SUM149 xenograft mouse model. There is evidence that Nodal is highly expressed in aggressive breast cancers, such as poorly differentiated breast cancers (113). The potential role of Nodal in the progression of IBC was further validated by our observation that recombinant Nodal promoted the migration and invasion of IBC cells and the CSC phenotype. These results suggest the therapeutic importance of targeting the COX-2 pathway in patients with IBC. However, it is not clear if Nodal is a mediator of EGFR-induced COX-2 signaling or is a target of COX-2 signaling pathway. We speculate that EGFR regulation of COX-2 in IBC cells promotes the CSC phenotype while Nodal signaling, via SMAD or a non-canonical pathway, provides positive feedback to COX-2. There is the possibility that EGFR/COX-2 regulation of Nodal occurs through MAPK ERK1/2 signaling since ERK1/2 is activated downstream of EGFR and has been shown to phosphorylate SMAD2 to regulate its nuclear translocation and transcriptional activity (113). A study showed that inhibition of ERK1/2 pathway mitigated the activity of the Nodal pathway in breast cancer cells. A more in-depth look at the mechanism of EGFR/ COX-2/Nodal in

IBC progression will be addressed in future studies to help enhance our understanding of how EGFR/COX-2 axis regulates the CSC phenotype in IBC. Overall, our results suggest an important role for COX-2 in promoting EMT and the CSC phenotype in IBC. As such, targeting of the COX-2 inflammatory pathway may represent an effective therapeutic approach for inhibiting the progression of IBC.

In summary, we conclude that there is a functional relationship between EGFR and COX-2, while a correlative relationship exists between COX-2 and Nodal in IBC cells. Further studies are required to determine if COX-2-mediated regulation of Nodal is only correlative or if it is causative. This finding could lend to the concept of Nodal as a pivotal target or biomarker for COX-2-induced CSC phenotype in IBC cells. SB431542, an inhibitor of the canonical Nodal receptors ALK4 and ALK 7, could be utilized to block the Nodal pathway and determine whether canonical signaling provides a positive feedback to promote COX-2 activity and subsequent release production of inflammatory mediators.

From a clinical perspective targeting COX-2 is efficacious, however there is a dilemma of potentially harmful side-effects (e.g. cardiotoxicity and gastrointestinal effects) resulting in the long-term use of selective COX-2 inhibitors. Alternatively, the EGFR pathway can be inhibited with an EGFR-specific monoclonal antibody, panitumumab. In an ongoing clinical study of panitumumab in IBC patients, biomarkers (e.g. COX-2, EGFR, and Nodal) will be assessed and pathological complete response will also be evaluated at the completion of the study. The use of panitumumab could reduce EGFR-mediated COX-2 activity without the harmful side-effects associated with a selective COX-2 inhibitor, leading to an improved response and clinical outcome for IBC patients.

CHAPTER 4: THE FUTURE OF TARGETED THERAPY IN AGGRESSIVE BREAST CANCERS: IBC AND TNBC

From our translational studies, we conclude that the tumorigenicity and invasiveness driven by the CSC population in IBC and TNBC can be modulated by COX-2 and RANK signaling. By eradicating the CSC population through inhibition of one of these two pathways, we can potentially block the progression of IBC and TNBC helping to reduce metastasis and prolong survival in IBC and TNBC patients.

This is the first study in which RANKL was found to be an independent prognostic factor in RANK positive TNBC patients. The basis of RANK-mediated TNBC progression may rely on its interaction with RANKL. Unlike RANK, RANKL is expressed at relatively low levels in breast tumor cells, while it is highly expressed in breast tumor stroma (114). In TNBC MDA-MB-231 cells, we found the CSC phenotype to be regulated by RANK. Our RT^2 PCR array analysis revealed stem cell genes modulated by the suppression of RANK in MDA-MB-231 cells, which provides us insight into which inflammatory pathways might be involved in the RANK-mediated CSC phenotype in TNBC. Interestingly, BMP2 and BMP3 were observed to be among the top five stem cell genes downregulated by the suppression of RANK. BMPs are members of the TGFβ superfamily, which function to regulate CSCs. The downregulation of BMP2 and BMP3 gene expression in MDA-MB-231 RANK shRNA cells suggests that RANK is a potential target for reducing the invasion and progression of TNBC cells. BMPs modulate the breast cancer cellular cytoskeleton and adhesive structures at the cell surface to mobilize the cell during migration and invasion (115). The role of BMPs in cancer stem cells is not clear, however, it has been documented that BMPs can

promote a CSC phenotype, including EMT, through stimulation of the SMAD1/5/8 pathway. An *in vivo* TNBC spontaneous metastasis mouse model will allow us to investigate the effects of RANK suppression on the invasion and metastasis of TNBC cells, and detect stem cell markers modulated downstream of RANKL/RANK in primary and metastatic tumors.

Preventing the metastasis of TNBC is of high clinical priority for patients and by targeting the RANKL/RANK pathway we can potentially block the progression of TNBC. From our analysis of RANK and RANKL expression in clinical specimens of TNBC, we observed that RANK expression is not a poor prognostic indicator and therefore, we need to evaluate RANK and RANKL in a prospective clinical trial. An ongoing phase II clinical trial (NCT01952054) at MD Anderson Cancer Center has been initiated to study the effects of the RANKL inhibitor, denosumab, on bone metastasis in breast cancer patients by monitoring for circulating tumor cells (CTCs) and disseminated tumor cells (DTCs) and identifying bone metastasis-relevant biomarkers including RANK and RANKL. In this particular clinical trial, the patient cohort will be estrogen receptor (ER)-positive advanced breast cancer patients. ER-dependent breast tumors have a tendency to develop bone metastases at a two-fold higher rate compared to non-ER breast tumors (116). Although this particular clinical trial is not targeted at TNBC patients, findings from this study may elude to whether the co-expression of RANK and RANKL in breast tumors is a predictive indicator for poorer outcome and if denosumab-treated patients have improved skeletal-disease free survival and reduced bone metastases. To evaluate RANK and RANKL expression and the efficacy of denosumab in a TNBC subtype-specific (BL1, BL2, M, MSL, LAR, and IM) cohort, patients would be randomly assigned to receive either denosumab or placebo (control) treatment. By

stratifying TNBC patients, based on the six gene expression profiles described by Lehmann BD *et al*.(12), we can determine if there is an association between TNBC subtype and favorable response to denosumab therapy. Findings from this clinical study will provide insight into whether targeting the RANKL/RANK pathway in TNBC is clinically relevant and if blocking the RANKL/RANK pathway will result in reduced metastasis and improved clinical outcome.

In IBC, we observed a positive regulation of COX-2 by EGFR in IBC, and made a novel finding that the COX-2 pathway regulates the expression of Nodal and the CSC phenotype of IBC cells. To this end, we conclude that inhibition of the Nodal pathway could be an effective strategy to eradicate CSCs in COX-2 expressing tumors. However, the mechanism of Nodal regulation by COX-2 is yet to be validated and whether targeting the Nodal pathway will suppress IBC tumorigenicity and metastasis remains unknown. We will further investigate the requirement for COX-2 and Nodal in tumor progression by assessing the efficacy of a combined celecoxib and SB431542 (an inhibitor of canonical Nodal signaling) therapy in IBC cells. EGFR, COX-2, and Nodal are linked with inflammation in breast cancer as they each are upstream regulators of transcription activators that promote the gene expression of several inflammatory molecules involved in breast cancer progression. To study the role of inflammation in IBC, a future clinical trial for the treatment of IBC patients will investigate the effects of targeting the COX-2 pathway via EP4 receptor inhibitor, and identify novel inflammatory markers modulated by the inhibition of the EP4 receptor. This study will allow us to investigate a novel therapeutic approach to targeting COX-2-mediated inflammatory response in IBC.

Potentially, the RANK and COX-2 pathways can converge to induce an inflammatory response in IBC and TNBC. We found several stem cell genes modulated by the suppression of RANK in the TNBC cells that are linked with inflammatory signaling pathways activated in breast cancer cells. The RANKL/RANK can activate NFkB transcriptional activity, leading to the induction of COX-2 gene expression. In turn, activation of the COX-2 pathway can stimulate the production and secretion of $PGE_{2,}$ leading to an upregulation of RANKL and RANK gene expression (117). In addition to NF-kB, the AP-1 transcription factor, which activates the expression of the COX-2 gene, PTGS2, can be upregulated by the JNK pathway downstream of RANKL/RANK (117). While it is not clear which downstream pathway is involved in the regulation of RANKL/RANK activity of TNBC cells, however, it can be speculated that the inflammatory signaling pathways mediate the transformation and aggressive phenotype of IBC and TNBC

Collectively, RANKL and EGFR are promising targets for the development of novel strategies to prevent or inhibit TNBC and IBC progression. Therapeutic targeting of RANKL and EGFR using humanized monoclonal antibodies, denosumab and panitumumab, may lead to the suppression of the inflammatory mediators produced by RANKL/RANK and EGFR/COX-2 signaling. Abrogated signaling through these receptors is concomitant with the downregulation of the tumor-promoting activity of CSCs in IBC and TNBC. Measurement of the efficacy of these antibodies to target the CSC population will occur through the detection of circulating tumor cells (CTCs) in the peripheral blood, described as $EPCAM^{+}/CD45^{-}$ (118), and disseminated tumor cells (DTCs) or epithelial cells expressing $CD326^{+}CD45^{low}$ localized to the bone can be evaluated based on multiparameter flow cytometry analysis of $CD44^{+}CD24^{-}$ and ALDH

activity (119). On the basis of our data, we expect that TNBC and IBC patients treated with denosumab or panitumumab will reduce COX-2, EGFR and Nodal activity in primary breast tumors, and reduce the number of CTCs in peripheral blood and DTCs in bone marrow. We envision that such a therapy may prevent patient morbidity through the elimination of *de novo* metastasis and improved long-term survival.

Appendix A) TNBC and non-TNBC cell line APC-RANK median

TNBC	Median difference	Non-TNBC	Median difference
HCC70	26321	SUM190	7378
MDA-MB-468	8279	HCC1954	5994
SUM159	6664	SKBR3	3651
BT20	5908	BT474	949
MDA-MB-231	5421	KPL4	515
HCC38	5013	MCF7	410
SUM149	653		
Average	8323	Average	3150

Appendix B) TNBC and non-TNBC cell line APC-RANK median

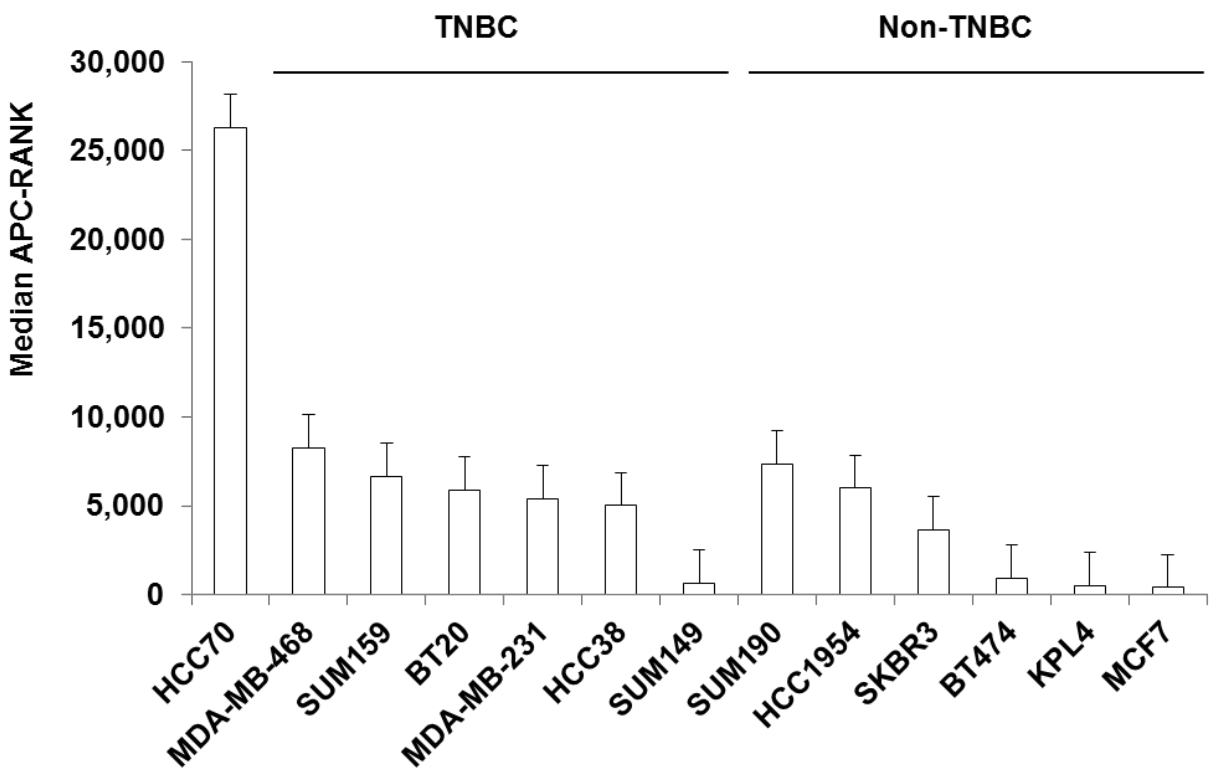

CHAPTER 5: REFERENCES

1. American Cancer Society. Cancer Facts & Figures 2014. Atlanta: American Cancer Society: American Cancer Society, Inc.; 2014. p. 18.

2. Vargo-Gogola T, Rosen JM. Modelling breast cancer: one size does not fit all. Nature reviews Cancer. 2007;7:659-72.

3. Kalluri KPaR. The Role of the Microenvironment in Mammary Gland Development and Cancer. In: Bissell MJ, editor. The Mammary Gland as an Experimental Model. Cold Spring Harbor: Cold Spring Harbor Laboratory Press; 2011. p. 166.

4. Eric A. Strom AUB, and Kelly K. Hunt. Multidisciplinary care of the breast cancer patient: Overview and Implementation. In: Kelly K. Hunt GLR, Erica A. Stom, and Naoto T. Ueno, editor. Breast Cancer. New York, NY: Springer; 2001. p. 9-12.

5. Huang EH, Tucker SL, Strom EA, McNeese MD, Kuerer HM, Buzdar AU, Valero V, Perkins GH, Schechter NR, Hunt KK, Sahin AA, Hortobagyi GN, Buchholz TA. Postmastectomy radiation improves local-regional control and survival for selected patients with locally advanced breast cancer treated with neoadjuvant chemotherapy and mastectomy. Journal of clinical oncology : official journal of the American Society of Clinical Oncology. 2004;22:4691-9.

6. Francisco J. Esteva aHAF, Jr. Serum and Tissue Markers for Breast Cancer. In: Kelly K. Hunt GLR, Erica A. Stom, and Naoto T. Ueno, editor. Breast Cancer. New York, NY: Springer; 2001. p. 294.

7. Anderson WF, Rosenberg PS, Prat A, Perou CM, Sherman ME. How many etiological subtypes of breast cancer: two, three, four, or more? Journal of the National Cancer Institute. 2014;106.

8. Hynes NE, Watson CJ. Mammary gland growth factors: roles in normal development and in cancer. Cold Spring Harbor perspectives in biology. 2010;2:a003186.

9. Masuda H, Zhang D, Bartholomeusz C, Doihara H, Hortobagyi GN, Ueno NT. Role of epidermal growth factor receptor in breast cancer. Breast cancer research and treatment. 2012;136:331-45.

10. Del Vecchio CA, Jensen KC, Nitta RT, Shain AH, Giacomini CP, Wong AJ. Epidermal growth factor receptor variant III contributes to cancer stem cell phenotypes in invasive breast carcinoma. Cancer research. 2012;72:2657-71.

11. Arun B, Bayraktar S, Liu DD, Gutierrez Barrera AM, Atchley D, Pusztai L, Litton JK, Valero V, Meric-Bernstam F, Hortobagyi GN, Albarracin C. Response to neoadjuvant systemic therapy for breast cancer in BRCA mutation carriers and noncarriers: a single-institution experience. Journal of clinical oncology : official journal of the American Society of Clinical Oncology. 2011;29:3739-46.

12. Lehmann BD, Bauer JA, Chen X, Sanders ME, Chakravarthy AB, Shyr Y, Pietenpol JA. Identification of human triple-negative breast cancer subtypes and preclinical models for selection of targeted therapies. The Journal of clinical investigation. 2011;121:2750-67.

13. Cha YI, DuBois RN. NSAIDs and cancer prevention: targets downstream of COX-2. Annual review of medicine. 2007;58:239-52.

14. Dent R, Hanna WM, Trudeau M, Rawlinson E, Sun P, Narod SA. Pattern of metastatic spread in triple-negative breast cancer. Breast cancer research and treatment. 2009;115:423-8.

15. Bertucci F, Finetti P, Cervera N, Esterni B, Hermitte F, Viens P, Birnbaum D. How basal are triple-negative breast cancers? International journal of cancer Journal international du cancer. 2008;123:236-40.

16. Mayer IA, Abramson VG, Lehmann BD, Pietenpol JA. New strategies for triple-negative breast cancer--deciphering the heterogeneity. Clinical cancer research : an official journal of the American Association for Cancer Research. 2014;20:782-90.

17. Masuda H, Baggerly KA, Wang Y, Iwamoto T, Brewer T, Pusztai L, Kai K, Kogawa T, Finetti P, Birnbaum D, Dirix L, Woodward WA, Reuben JM, Krishnamurthy S, Symmans W, Van Laere SJ, Bertucci F, Hortobagyi GN, Ueno NT. Comparison of molecular subtype distribution in triple-negative inflammatory and non-inflammatory breast cancers. Breast cancer research : BCR. 2013;15:R112.

18. Dent R, Trudeau M, Pritchard KI, Hanna WM, Kahn HK, Sawka CA, Lickley LA, Rawlinson E, Sun P, Narod SA. Triple-negative breast cancer: clinical features and patterns of recurrence. Clinical cancer research : an official journal of the American Association for Cancer Research. 2007;13:4429-34.

19. Nogi H, Kobayashi T, Suzuki M, Tabei I, Kawase K, Toriumi Y, Fukushima H, Uchida K. EGFR as paradoxical predictor of chemosensitivity and outcome among triple-negative breast cancer. Oncology reports. 2009;21:413-7.

20. Ferraro DA, Gaborit N, Maron R, Cohen-Dvashi H, Porat Z, Pareja F, Lavi S, Lindzen M, Ben-Chetrit N, Sela M, Yarden Y. Inhibition of triple-negative breast cancer models by combinations of antibodies to EGFR. Proceedings of the National Academy of Sciences of the United States of America. 2013;110:1815-20.

21. Carey LA. Targeted chemotherapy? Platinum in BRCA1-dysfunctional breast cancer. Journal of clinical oncology : official journal of the American Society of Clinical Oncology. 2010;28:361-3.

22. Baselga J, Gomez P, Greil R, Braga S, Climent MA, Wardley AM, Kaufman B, Stemmer SM, Pego A, Chan A, Goeminne JC, Graas MP, Kennedy MJ, Ciruelos Gil EM, Schneeweiss A, Zubel A, Groos J, Melezinkova H, Awada A. Randomized phase II study of the anti-epidermal growth factor receptor monoclonal antibody cetuximab with cisplatin versus cisplatin alone in patients with metastatic triple-negative breast cancer. Journal of clinical oncology : official journal of the American Society of Clinical Oncology. 2013;31:2586-92.

23. Nabholtz JM, Abrial C, Mouret-Reynier MA, Dauplat MM, Weber B, Gligorov J, Forest AM, Tredan O, Vanlemmens L, Petit T, Guiu S, Van Praagh I, Jouannaud C, Dubray-Longeras P, Tubiana-Mathieu N, Benmammar KE, Kullab S, Bahadoor MR, Radosevic-Robin N, Kwiatkowski F, Desrichard A, Cayre A, Uhrhammer N, Chalabi N, Chollet P, Penault-Llorca F. Multicentric neoadjuvant phase II study of panitumumab combined with an anthracycline/taxane-based chemotherapy in operable triple-negative breast cancer: identification of biologically defined signatures predicting treatment impact. Annals of oncology : official journal of the European Society for Medical Oncology / ESMO. 2014;25:1570-7.

24. Anderson WF, Schairer C, Chen BE, Hance KW, Levine PH. Epidemiology of inflammatory breast cancer (IBC). Breast disease. 2005;22:9-23.

25. Hance KW, Anderson WF, Devesa SS, Young HA, Levine PH. Trends in inflammatory breast carcinoma incidence and survival: the surveillance, epidemiology,

and end results program at the National Cancer Institute. Journal of the National Cancer Institute. 2005;97:966-75.

26. Gonzalez-Angulo AM, Hennessy BT, Broglio K, Meric-Bernstam F, Cristofanilli M, Giordano SH, Buchholz TA, Sahin A, Singletary SE, Buzdar AU, Hortobagyi GN. Trends for inflammatory breast cancer: is survival improving? The oncologist. 2007;12:904-12.

27. Ueno NT, Buzdar AU, Singletary SE, Ames FC, McNeese MD, Holmes FA, Theriault RL, Strom EA, Wasaff BJ, Asmar L, Frye D, Hortobagyi GN. Combined-modality treatment of inflammatory breast carcinoma: twenty years of experience at M. D. Anderson Cancer Center. Cancer chemotherapy and pharmacology. 1997;40:321-9.

28. Yang WT, Le-Petross HT, Macapinlac H, Carkaci S, Gonzalez-Angulo AM, Dawood S, Resetkova E, Hortobagyi GN, Cristofanilli M. Inflammatory breast cancer: PET/CT, MRI, mammography, and sonography findings. Breast cancer research and treatment. 2008;109:417-26.

29. Yamauchi H, Woodward WA, Valero V, Alvarez RH, Lucci A, Buchholz TA, Iwamoto T, Krishnamurthy S, Yang W, Reuben JM, Hortobagyi GN, Ueno NT. Inflammatory breast cancer: what we know and what we need to learn. The oncologist. 2012;17:891-9.

30. Lacerda L, Reddy JP, Liu D, Larson R, Li L, Masuda H, Brewer T, Debeb BG, Xu W, Hortobagyi GN, Buchholz TA, Ueno NT, Woodward WA. Simvastatin radiosensitizes differentiated and stem-like breast cancer cell lines and is associated with improved local control in inflammatory breast cancer patients treated with postmastectomy radiation. Stem cells translational medicine. 2014;3:849-56.

31. Cabioglu N, Gong Y, Islam R, Broglio KR, Sneige N, Sahin A, Gonzalez-Angulo AM, Morandi P, Bucana C, Hortobagyi GN, Cristofanilli M. Expression of growth factor and chemokine receptors: new insights in the biology of inflammatory breast cancer. Annals of oncology : official journal of the European Society for Medical Oncology / ESMO. 2007;18:1021-9.

32. Lee J, Bartholomeusz C, Mansour O, Humphries J, Hortobagyi GN, Ordentlich P, Ueno NT. A class I histone deacetylase inhibitor, entinostat, enhances lapatinib efficacy in HER2-overexpressing breast cancer cells through FOXO3-mediated Bim1 expression. Breast cancer research and treatment. 2014;146:259-72.

33. Finn RS, Press MF, Dering J, Arbushites M, Koehler M, Oliva C, Williams LS, Di Leo A. Estrogen receptor, progesterone receptor, human epidermal growth factor receptor 2 (HER2), and epidermal growth factor receptor expression and benefit from lapatinib in a randomized trial of paclitaxel with lapatinib or placebo as first-line treatment in HER2-negative or unknown metastatic breast cancer. Journal of clinical oncology : official journal of the American Society of Clinical Oncology. 2009;27:3908-15.

34. Zhang D, LaFortune TA, Krishnamurthy S, Esteva FJ, Cristofanilli M, Liu P, Lucci A, Singh B, Hung MC, Hortobagyi GN, Ueno NT. Epidermal growth factor receptor tyrosine kinase inhibitor reverses mesenchymal to epithelial phenotype and inhibits metastasis in inflammatory breast cancer. Clinical cancer research : an official journal of the American Association for Cancer Research. 2009;15:6639-48.

35. Chang JT, Mani SA. Sheep, wolf, or werewolf: cancer stem cells and the epithelial-to-mesenchymal transition. Cancer letters. 2013;341:16-23.

36. Kang Y, Massague J. Epithelial-mesenchymal transitions: twist in development and metastasis. Cell. 2004;118:277-9.

37. Pattabiraman DR, Weinberg RA. Tackling the cancer stem cells - what challenges do they pose? Nature reviews Drug discovery. 2014;13:497-512.

38. Fan F, Samuel S, Evans KW, Lu J, Xia L, Zhou Y, Sceusi E, Tozzi F, Ye XC, Mani SA, Ellis LM. Overexpression of snail induces epithelial-mesenchymal transition and a cancer stem cell-like phenotype in human colorectal cancer cells. Cancer medicine. 2012;1:5-16.

39. Benton G, Arnaoutova I, George J, Kleinman HK, Koblinski J. Matrigel: From discovery and ECM mimicry to assays and models for cancer research. Advanced drug delivery reviews. 2014.

40. May CD, Sphyris N, Evans KW, Werden SJ, Guo W, Mani SA. Epithelial-mesenchymal transition and cancer stem cells: a dangerously dynamic duo in breast cancer progression. Breast cancer research : BCR. 2011;13:202.

41. Shipitsin M, Campbell LL, Argani P, Weremowicz S, Bloushtain-Qimron N, Yao J, Nikolskaya T, Serebryiskaya T, Beroukhim R, Hu M, Halushka MK, Sukumar S, Parker LM, Anderson KS, Harris LN, Garber JE, Richardson AL, Schnitt SJ, Nikolsky Y, Gelman RS, Polyak K. Molecular definition of breast tumor heterogeneity. Cancer cell. 2007;11:259-73.

42. Gong Y, Wang J, Huo L, Wei W, Ueno NT, Woodward WA. Aldehyde dehydrogenase 1 expression in inflammatory breast cancer as measured by immunohistochemical staining. Clinical breast cancer. 2014;14:e81-8.

43. Wang R, Lv Q, Meng W, Tan Q, Zhang S, Mo X, Yang X. Comparison of mammosphere formation from breast cancer cell lines and primary breast tumors. Journal of thoracic disease. 2014;6:829-37.

44. Al-Hajj M, Wicha MS, Benito-Hernandez A, Morrison SJ, Clarke MF. Prospective identification of tumorigenic breast cancer cells. Proceedings of the National Academy of Sciences of the United States of America. 2003;100:3983-8.

45. Sarrio D, Franklin CK, Mackay A, Reis-Filho JS, Isacke CM. Epithelial and mesenchymal subpopulations within normal basal breast cell lines exhibit distinct stem cell/progenitor properties. Stem cells. 2012;30:292-303.

46. Zhou J, Wulfkuhle J, Zhang H, Gu P, Yang Y, Deng J, Margolick JB, Liotta LA, Petricoin E, 3rd, Zhang Y. Activation of the PTEN/mTOR/STAT3 pathway in breast cancer stem-like cells is required for viability and maintenance. Proceedings of the National Academy of Sciences of the United States of America. 2007;104:16158-63.

47. Battula VL, Shi Y, Evans KW, Wang RY, Spaeth EL, Jacamo RO, Guerra R, Sahin AA, Marini FC, Hortobagyi G, Mani SA, Andreeff M. Ganglioside GD2 identifies breast cancer stem cells and promotes tumorigenesis. The Journal of clinical investigation. 2012;122:2066-78.

48. Watson NEHaCJ. Mammary Gland Growth Factors: Roles in Normal Development and Cancer. In: Bissell MJ, editor. Cold Spring Harbor Perspectives in Biology The Mammary Gland as an Experimental Model. Cold Spring Harbor, NY: CSHL Press; 2011. p. 87.

49. Wei H, Wang S, Zhang D, Hou S, Qian W, Li B, Guo H, Kou G, He J, Wang H, Guo Y. Targeted delivery of tumor antigens to activated dendritic cells via CD11c

molecules induces potent antitumor immunity in mice. Clinical cancer research : an official journal of the American Association for Cancer Research. 2009;15:4612-21.

50. Yoshida K, Fujino H, Otake S, Seira N, Regan JW, Murayama T. Induction of cyclooxygenase-2 expression by prostaglandin E2 stimulation of the prostanoid EP4 receptor via coupling to Galphai and transactivation of the epidermal growth factor receptor in HCA-7 human colon cancer cells. European journal of pharmacology. 2013;718:408-17.

51. Fouad TM, Kogawa T, Reuben JM, Ueno NT. The role of inflammation in inflammatory breast cancer. Advances in experimental medicine and biology. 2014;816:53-73.

52. Shostak K, Chariot A. NF-kappaB, stem cells and breast cancer: the links get stronger. Breast cancer research : BCR. 2011;13:214.

53. Lerebours F, Vacher S, Andrieu C, Espie M, Marty M, Lidereau R, Bieche I. NF-kappa B genes have a major role in inflammatory breast cancer. BMC cancer. 2008;8:41.

54. Goldenberg MM. Celecoxib, a selective cyclooxygenase-2 inhibitor for the treatment of rheumatoid arthritis and osteoarthritis. Clinical therapeutics. 1999;21:1497-513; discussion 27-8.

55. Blake ML, Tometsko M, Miller R, Jones JC, Dougall WC. RANK expression on breast cancer cells promotes skeletal metastasis. Clinical & experimental metastasis. 2014;31:233-45.

56. Mukherjee D, Nissen SE, Topol EJ. Risk of cardiovascular events associated with selective COX-2 inhibitors. Jama. 2001;286:954-9.

57. Wu WK, Sung JJ, Lee CW, Yu J, Cho CH. Cyclooxygenase-2 in tumorigenesis of gastrointestinal cancers: an update on the molecular mechanisms. Cancer letters. 2010;295:7-16.

58. Singh B, Irving LR, Tai K, Lucci A. Overexpression of COX-2 in celecoxib-resistant breast cancer cell lines. The Journal of surgical research. 2010;163:235-43.

59. Singh B, Cook KR, Vincent L, Hall CS, Martin C, Lucci A. Role of COX-2 in tumorospheres derived from a breast cancer cell line. The Journal of surgical research. 2011;168:e39-49.

60. Bocca C, Ievolella M, Autelli R, Motta M, Mosso L, Torchio B, Bozzo F, Cannito S, Paternostro C, Colombatto S, Parola M, Miglietta A. Expression of Cox-2 in human breast cancer cells as a critical determinant of epithelial-to-mesenchymal transition and invasiveness. Expert opinion on therapeutic targets. 2014;18:121-35.

61. Takahashi Y, Kawahara F, Noguchi M, Miwa K, Sato H, Seiki M, Inoue H, Tanabe T, Yoshimoto T. Activation of matrix metalloproteinase-2 in human breast cancer cells overexpressing cyclooxygenase-1 or -2. FEBS letters. 1999;460:145-8.

62. Huang M, Sharma S, Mao JT, Dubinett SM. Non-small cell lung cancer-derived soluble mediators and prostaglandin E2 enhance peripheral blood lymphocyte IL-10 transcription and protein production. Journal of immunology. 1996;157:5512-20.

63. Li Q, Liu L, Zhang Q, Liu S, Ge D, You Z. Interleukin-17 Indirectly Promotes M2 Macrophage Differentiation through Stimulation of COX-2/PGE2 Pathway in the Cancer Cells. Cancer research and treatment : official journal of Korean Cancer Association. 2014;46:297-306.

64. Zhu ZH, Yang P, Tang ZN, Zeng YG, Dong J, Zheng LP, Wang ZT. [Pharmacological actions of "8204" on the cardiovascular system and bronchial smooth muscle]. Yao xue xue bao = Acta pharmaceutica Sinica. 1985;20:886-90.

65. Quail DF, Siegers GM, Jewer M, Postovit LM. Nodal signalling in embryogenesis and tumourigenesis. The international journal of biochemistry & cell biology. 2013;45:885-98.

66. Quail DF, Zhang G, Findlay SD, Hess DA, Postovit LM. Nodal promotes invasive phenotypes via a mitogen-activated protein kinase-dependent pathway. Oncogene. 2014;33:461-73.

67. Schier AF. Nodal morphogens. Cold Spring Harbor perspectives in biology. 2009;1:a003459.

68. Strizzi L, Postovit LM, Margaryan NV, Seftor EA, Abbott DE, Seftor RE, Salomon DS, Hendrix MJ. Emerging roles of nodal and Cripto-1: from embryogenesis to breast cancer progression. Breast disease. 2008;29:91-103.

69. Quail DF, Taylor MJ, Walsh LA, Dieters-Castator D, Das P, Jewer M, Zhang G, Postovit LM. Low oxygen levels induce the expression of the embryonic morphogen Nodal. Molecular biology of the cell. 2011;22:4809-21.

70. Campbell JP, Karolak MR, Ma Y, Perrien DS, Masood-Campbell SK, Penner NL, Munoz SA, Zijlstra A, Yang X, Sterling JA, Elefteriou F. Stimulation of host bone marrow stromal cells by sympathetic nerves promotes breast cancer bone metastasis in mice. PLoS biology. 2012;10:e1001363.

71. Onishi T, Hayashi N, Theriault RL, Hortobagyi GN, Ueno NT. Future directions of bone-targeted therapy for metastatic breast cancer. Nature reviews Clinical oncology. 2010;7:641-51.

72. Fata JE, Kong YY, Li J, Sasaki T, Irie-Sasaki J, Moorehead RA, Elliott R, Scully S, Voura EB, Lacey DL, Boyle WJ, Khokha R, Penninger JM. The osteoclast differentiation factor osteoprotegerin-ligand is essential for mammary gland development. Cell. 2000;103:41-50.

73. Wittrant Y, Theoleyre S, Chipoy C, Padrines M, Blanchard F, Heymann D, Redini F. RANKL/RANK/OPG: new therapeutic targets in bone tumours and associated osteolysis. Biochimica et biophysica acta. 2004;1704:49-57.

74. Casimiro S, Mohammad KS, Pires R, Tato-Costa J, Alho I, Teixeira R, Carvalho A, Ribeiro S, Lipton A, Guise TA, Costa L. RANKL/RANK/MMP-1 molecular triad contributes to the metastatic phenotype of breast and prostate cancer cells in vitro. PloS one. 2013;8:e63153.

75. Canon JR, Roudier M, Bryant R, Morony S, Stolina M, Kostenuik PJ, Dougall WC. Inhibition of RANKL blocks skeletal tumor progression and improves survival in a mouse model of breast cancer bone metastasis. Clinical & experimental metastasis. 2008;25:119-29.

76. Dougall WC. Molecular pathways: osteoclast-dependent and osteoclast-independent roles of the RANKL/RANK/OPG pathway in tumorigenesis and metastasis. Clinical cancer research : an official journal of the American Association for Cancer Research. 2012;18:326-35.

77. Clark IM, Swingler TE, Sampieri CL, Edwards DR. The regulation of matrix metalloproteinases and their inhibitors. The international journal of biochemistry & cell biology. 2008;40:1362-78.

78. Lu X, Wang Q, Hu G, Van Poznak C, Fleisher M, Reiss M, Massague J, Kang Y. ADAMTS1 and MMP1 proteolytically engage EGF-like ligands in an osteolytic signaling cascade for bone metastasis. Genes & development. 2009;23:1882-94.

79. Buijs JT, van der Horst G, van den Hoogen C, Cheung H, de Rooij B, Kroon J, Petersen M, van Overveld PG, Pelger RC, van der Pluijm G. The BMP2/7 heterodimer inhibits the human breast cancer stem cell subpopulation and bone metastases formation. Oncogene. 2012;31:2164-74.

80. Mundy GR. Metastasis to bone: causes, consequences and therapeutic opportunities. Nature reviews Cancer. 2002;2:584-93.

81. Palafox M, Ferrer I, Pellegrini P, Vila S, Hernandez-Ortega S, Urruticoechea A, Climent F, Soler MT, Munoz P, Vinals F, Tometsko M, Branstetter D, Dougall WC, Gonzalez-Suarez E. RANK induces epithelial-mesenchymal transition and stemness in human mammary epithelial cells and promotes tumorigenesis and metastasis. Cancer research. 2012;72:2879-88.

82. Schramek D, Leibbrandt A, Sigl V, Kenner L, Pospisilik JA, Lee HJ, Hanada R, Joshi PA, Aliprantis A, Glimcher L, Pasparakis M, Khokha R, Ormandy CJ, Widschwendter M, Schett G, Penninger JM. Osteoclast differentiation factor RANKL controls development of progestin-driven mammary cancer. Nature. 2010;468:98-102.

83. Body JJ, Greipp P, Coleman RE, Facon T, Geurs F, Fermand JP, Harousseau JL, Lipton A, Mariette X, Williams CD, Nakanishi A, Holloway D, Martin SW, Dunstan CR, Bekker PJ. A phase I study of AMGN-0007, a recombinant osteoprotegerin construct, in patients with multiple myeloma or breast carcinoma related bone metastases. Cancer. 2003;97:887-92.

84. Garraway IP. Targeting the RANKL pathway: putting the brakes on prostate cancer progression in bone. Journal of clinical oncology : official journal of the American Society of Clinical Oncology. 2013;31:3838-40.

85. Gelmon K, Dent R, Mackey JR, Laing K, McLeod D, Verma S. Targeting triple-negative breast cancer: optimising therapeutic outcomes. Annals of oncology : official journal of the European Society for Medical Oncology / ESMO. 2012;23:2223-34.

86. Elsamany S, Abdullah S. Triple-negative breast cancer: future prospects in diagnosis and management. Med Oncol. 2014;31:834.

87. Gonzalez-Suarez E, Jacob AP, Jones J, Miller R, Roudier-Meyer MP, Erwert R, Pinkas J, Branstetter D, Dougall WC. RANK ligand mediates progestin-induced mammary epithelial proliferation and carcinogenesis. Nature. 2010;468:103-7.

88. Parinyanitikul N, Blumenschein GR, Wu Y, Lei X, Chavez-Macgregor M, Smart M, Gonzalez-Angulo AM. Mesothelin expression and survival outcomes in triple receptor negative breast cancer. Clinical breast cancer. 2013;13:378-84.

89. Wood CE, Branstetter D, Jacob AP, Cline JM, Register TC, Rohrbach K, Huang LY, Borgerink H, Dougall WC. Progestin effects on cell proliferation pathways in the postmenopausal mammary gland. Breast cancer research : BCR. 2013;15:R62.

90. Bayraktar S, Gutierrez-Barrera AM, Liu D, Tasbas T, Akar U, Litton JK, Lin E, Albarracin CT, Meric-Bernstam F, Gonzalez-Angulo AM, Hortobagyi GN, Arun BK. Outcome of triple-negative breast cancer in patients with or without deleterious BRCA mutations. Breast cancer research and treatment. 2011;130:145-53.

91. Tang ZN, Zhang F, Tang P, Qi XW, Jiang J. RANKL-induced migration of MDA-MB-231 human breast cancer cells via Src and MAPK activation. Oncology reports. 2011;26:1243-50.

92. Yamada T, Tsuda M, Takahashi T, Totsuka Y, Shindoh M, Ohba Y. RANKL expression specifically observed in vivo promotes epithelial mesenchymal transition and tumor progression. The American journal of pathology. 2011;178:2845-56.

93. Santini D, Schiavon G, Vincenzi B, Gaeta L, Pantano F, Russo A, Ortega C, Porta C, Galluzzo S, Armento G, La Verde N, Caroti C, Treilleux I, Ruggiero A, Perrone G, Addeo R, Clezardin P, Muda AO, Tonini G. Receptor activator of NF-kB (RANK) expression in primary tumors associates with bone metastasis occurrence in breast cancer patients. PloS one. 2011;6:e19234.

94. Pfitzner BM, Branstetter D, Loibl S, Denkert C, Lederer B, Schmitt WD, Dombrowski F, Werner M, Rudiger T, Dougall WC, von Minckwitz G. RANK expression as a prognostic and predictive marker in breast cancer. Breast cancer research and treatment. 2014;145:307-15.

95. Owen S, Ye L, Sanders AJ, Mason MD, Jiang WG. Expression profile of receptor activator of nuclear-kappaB (RANK), RANK ligand (RANKL) and osteoprotegerin (OPG) in breast cancer. Anticancer research. 2013;33:199-206.

96. Park HS, Lee A, Chae BJ, Bae JS, Song BJ, Jung SS. Expression of receptor activator of nuclear factor kappa-B as a poor prognostic marker in breast cancer. Journal of surgical oncology. 2014;110:807-12.

97. Jones DH, Nakashima T, Sanchez OH, Kozieradzki I, Komarova SV, Sarosi I, Morony S, Rubin E, Sarao R, Hojilla CV, Komnenovic V, Kong YY, Schreiber M, Dixon SJ, Sims SM, Khokha R, Wada T, Penninger JM. Regulation of cancer cell migration and bone metastasis by RANKL. Nature. 2006;440:692-6.

98. Pellegrini P, Cordero A, Gallego MI, Dougall WC, Purificacion M, Pujana MA, Gonzalez-Suarez E. Constitutive activation of RANK disrupts mammary cell fate leading to tumorigenesis. Stem cells. 2013;31:1954-65.

99. Rosen V. BMP and BMP inhibitors in bone. Annals of the New York Academy of Sciences. 2006;1068:19-25.

100. Oktem G, Bilir A, Uslu R, Inan SV, Demiray SB, Atmaca H, Ayla S, Sercan O, Uysal A. Expression profiling of stem cell signaling alters with spheroid formation in CD133/CD44 prostate cancer stem cells. Oncology letters. 2014;7:2103-9.

101. Kang Y, Siegel PM, Shu W, Drobnjak M, Kakonen SM, Cordon-Cardo C, Guise TA, Massague J. A multigenic program mediating breast cancer metastasis to bone. Cancer cell. 2003;3:537-49.

102. Tavazoie SF, Alarcon C, Oskarsson T, Padua D, Wang Q, Bos PD, Gerald WL, Massague J. Endogenous human microRNAs that suppress breast cancer metastasis. Nature. 2008;451:147-52.

103. Leis O, Eguiara A, Lopez-Arribillaga E, Alberdi MJ, Hernandez-Garcia S, Elorriaga K, Pandiella A, Rezola R, Martin AG. Sox2 expression in breast tumours and activation in breast cancer stem cells. Oncogene. 2012;31:1354-65.

104. Kurebayashi J, Otsuki T, Tang CK, Kurosumi M, Yamamoto S, Tanaka K, Mochizuki M, Nakamura H, Sonoo H. Isolation and characterization of a new human breast cancer cell line, KPL-4, expressing the Erb B family receptors and interleukin-6. British journal of cancer. 1999;79:707-17.

105. Zhang D, Pal A, Bornmann WG, Yamasaki F, Esteva FJ, Hortobagyi GN, Bartholomeusz C, Ueno NT. Activity of lapatinib is independent of EGFR expression

level in HER2-overexpressing breast cancer cells. Molecular cancer therapeutics. 2008;7:1846-50.

106. Tome Y, Uehara F, Mii S, Yano S, Zhang L, Sugimoto N, Maehara H, Bouvet M, Tsuchiya H, Kanaya F, Hoffman RM. 3-dimensional tissue is formed from cancer cells in vitro on Gelfoam(R), but not on Matrigel. Journal of cellular biochemistry. 2014;115:1362-7.

107. Subbaramaiah K, Norton L, Gerald W, Dannenberg AJ. Cyclooxygenase-2 is overexpressed in HER-2/neu-positive breast cancer: evidence for involvement of AP-1 and PEA3. The Journal of biological chemistry. 2002;277:18649-57.

108. Subbaramaiah K, Howe LR, Port ER, Brogi E, Fishman J, Liu CH, Hla T, Hudis C, Dannenberg AJ. HER-2/neu status is a determinant of mammary aromatase activity in vivo: evidence for a cyclooxygenase-2-dependent mechanism. Cancer research. 2006;66:5504-11.

109. Masuda H, Brewer TM, Liu DD, Iwamoto T, Shen Y, Hsu L, Willey JS, Gonzalez-Angulo AM, Chavez-MacGregor M, Fouad TM, Woodward WA, Reuben JM, Valero V, Alvarez RH, Hortobagyi GN, Ueno NT. Long-term treatment efficacy in primary inflammatory breast cancer by hormonal receptor- and HER2-defined subtypes. Annals of oncology : official journal of the European Society for Medical Oncology / ESMO. 2014;25:384-91.

110. Li W, Zhang B, Li H, Zhao C, Zhong Y, Sun J, Lv S. TGF beta1 mediates epithelial mesenchymal transition via beta6 integrin signaling pathway in breast cancer. Cancer investigation. 2014;32:409-15.

111. Wang X, Wang G, Zhao Y, Liu X, Ding Q, Shi J, Ding Y, Wang S. STAT3 mediates resistance of CD44(+)CD24(-/low) breast cancer stem cells to tamoxifen in vitro. J Biomed Res. 2012;26:325-35.

112. Debeb BG, Cohen EN, Boley K, Freiter EM, Li L, Robertson FM, Reuben JM, Cristofanilli M, Buchholz TA, Woodward WA. Pre-clinical studies of Notch signaling inhibitor RO4929097 in inflammatory breast cancer cells. Breast Cancer Res Treat. 2012;134:495-510.

113. Quail DF, Zhang G, Findlay SD, Hess DA, Postovit LM. Nodal promotes invasive phenotypes via a mitogen-activated protein kinase-dependent pathway. Oncogene. 2013.

114. Van Poznak C, Cross SS, Saggese M, Hudis C, Panageas KS, Norton L, Coleman RE, Holen I. Expression of osteoprotegerin (OPG), TNF related apoptosis inducing ligand (TRAIL), and receptor activator of nuclear factor kappaB ligand (RANKL) in human breast tumours. Journal of clinical pathology. 2006;59:56-63.

115. Jin H, Pi J, Huang X, Huang F, Shao W, Li S, Chen Y, Cai J. BMP2 promotes migration and invasion of breast cancer cells via cytoskeletal reorganization and adhesion decrease: an AFM investigation. Applied microbiology and biotechnology. 2012;93:1715-23.

116. Hess KR, Pusztai L, Buzdar AU, Hortobagyi GN. Estrogen receptors and distinct patterns of breast cancer relapse. Breast cancer research and treatment. 2003;78:105-18.

117. Leibbrandt A, Penninger JM. RANK/RANKL: regulators of immune responses and bone physiology. Annals of the New York Academy of Sciences. 2008;1143:123-50.

118. Cristofanilli M, Hayes DF, Budd GT, Ellis MJ, Stopeck A, Reuben JM, Doyle GV, Matera J, Allard WJ, Miller MC, Fritsche HA, Hortobagyi GN, Terstappen LW. Circulating tumor cells: a novel prognostic factor for newly diagnosed metastatic breast cancer. Journal of clinical oncology : official journal of the American Society of Clinical Oncology. 2005;23:1420-30.

119. Reuben JM, Lee BN, Gao H, Cohen EN, Mego M, Giordano A, Wang X, Lodhi A, Krishnamurthy S, Hortobagyi GN, Cristofanilli M, Lucci A, Woodward WA. Primary breast cancer patients with high risk clinicopathologic features have high percentages of bone marrow epithelial cells with ALDH activity and CD44(+)CD24lo cancer stem cell phenotype. European journal of cancer. 2011;47:1527-36.

CHAPTER 6: VITA

Monica Elizabeth Reyes was born on January 23, 1982 in Saint Petersburg, FL. She was raised in Orlando, Florida by her parents Eduardo and Linda L. Linan. While growing up she had always loved science. It wasn't until she attended the University of South Florida in Tampa, FL to pursue a degree in marine biology that she discovered a passion for cancer biology. She earned her Bachelor in Science degree in Biomedical Sciences and minored in Biomedical Physics at the University of South Florida. Prior to entering the Graduate School of Biomedical Sciences at The University of Texas at Houston, Monica completed a post-baccalaureate program at Baylor College of Medicine. Monica lives in Houston with her husband Jorge Reyes and two children, Hugo Alejandro Reyes and Ainhoa Isabelle Reyes.

Permanent Address:

13702 Drakeford Court

Houston, TX 77047